COMPARATIVE STUDY OF DIFFERENT TYPE OF SUPERSTRUCTURES UNDER HIGH-SPEED TRAIN LOADING

Thesis Submitted
in Partial Fulfillment of the Requirements
for the Degree of

MASTER OF TECHNOLOGY

in
Structural Engineering
By

UMASHANKAR MISHRA

(Roll No. 2K21/STE/504)

Under the Supervision of

DR. NIRENDRA DEV

Professor, Civil Engineering Department

Delhi Technological University

To the Department of Civil Engineering

DELHI TECHNOLOGICAL UNIVERSITY

(Formerly Delhi College of Engineering)

Shahba Daulatpur, Main Bawana Road, Delhi-110042, India

May 2024

DELHI TECHNOLOGICAL UNIVERSITY

(Formerly Delhi College of Engineering)

Shahbad Daulatpur, Main Bawana Road, Delhi-110042, India

CANDIDATE'S DECLARATION

I **Umashankar Mishra** hereby certify that the work which is being presented in the thesis entitled "**COMPARATIVE STUDY OF DIFFERENT TYPE OF SUPERSTRUCTURES UNDER HIGH-SPEED TRAIN LOADING**" in partial fulfilment of the requirements for the award of the degree of Master of Technology, submitted in the **Department Civil Engineering**, Delhi Technological University is an authentic record of own work carried out during the period from **January 2024 to May 2024** under the supervision of **Dr. Nirendra Dev.**

The matter presented in the thesis has not been submitted by me for the award of any other degree of this or any other Institute.

Candidate's Signature

This is to certify that the student has incorporated all the corrections suggested by the examiners in the thesis and the statement made by the candidate is correct to the best of our knowledge.

Signature of Supervisor **Signature of External Examiner**

DELHI TECHNOLOGICAL UNIVERSITY

(Formerly Delhi College of Engineering)

Shahbad Daulatpur, Main Bawana Road, Delhi-110042, India

CERTIFICATE BY THE SUPERVSOR

Certified that **Umashankar Mishra (2K21/STE/504)** has carried out their research work presented in this thesis entitled **"Comparative Study of Different type of superstructures Under High-Speed Train Loading"** for the award of **Master of Technology in Structural Engineering** from the Department of Civil Engineering, Delhi Technological University, Delhi, Under my supervision. The thesis embodies results of original work, and studies are carried out by the student himself and the contents of the thesis do not form the basis for the award of any other degree to the candidate or to anybody else from this or any other University/Institution.

Signature

Dr. Nirendra Dev

Professor, Civil Engineering Department

DELHI TECHNOLOGICAL UNIVERSITY

Shahba Daulatpur, Main Bawana Road, Delhi-110042, India

Date:

Comparative Study of Different type of superstructures Under High-Speed Train Loading

Umashankar Mishra

ABSTRACT

This thesis presents a comprehensive comparative study on the impact of high-speed train loading on two types of superstructures: U-Girder and Box Girder, specifically within the context of the Regional Rapid Transit System (RRTS) in India. The research delves into the structural behaviour, dynamic response, economic considerations, and construction benefits under high-speed rail loading conditions.

The study employs a detailed dynamic analysis of U-Girder and Box Girder bridges using finite element models created with SOFISTIK software. The analysis methodology includes modal superposition for dynamic analysis, considering various loading scenarios such as dead load, superimposed dead load, and live load. The numerical modelling process, parameter variations, and validation steps are meticulously outlined, ensuring accurate and reliable results.

Key aspects analysed include maximum acceleration, deflection under different speed, span configurations, and the feasibility of these sections under high-speed loading. The results indicate that U-Girder tend to exhibit higher deflection due to their lower torsional rigidity, whereas Box Girder demonstrate greater torsional rigidity, resulting in reduced deflection and enhanced suitability for longer spans and higher loads. Box Girder also shows lower vertical acceleration and deflection compared to U-Girder, attributed to their closed cross-section which provides greater stiffness and stability. However, both types maintain acceptable levels of vertical acceleration and displacement according to BS EN 1991-2:2003 and BS EN 1990 Standards.

The analysis reveals that U-Girder require less concrete compared to Box-Girders, leading to potential cost savings and reduced environmental impact. Despite their smaller

volumes, U-Girder maintain sufficient structural integrity and load-carrying capacity, making them a cost-effective option for elevated construction projects. The simpler and faster construction process of U-Girder results in lower energy consumption and emissions, further reducing their carbon footprint. Additionally, the benefits of U-Girder extend to the reduction in the longitudinal profile of the rail line, lowering stations levels, and minimizing earthwork, all contributing to cost savings and environmental benefits.

The study's findings suggest that U-Girder are a viable and advantageous choice for high-speed rail infrastructure, balancing performance, cost efficiency, and environmental sustainability. The conclusions drawn provide valuable insights into ensuring safe operational conditions for both U-Girder and Box Girder viaducts/Bridges under dynamic loading, facilitating the standardization of cross-section for various span lengths, and ultimately reducing economic and environmental impacts. This research lays a strong foundation for future studies, including understanding the behaviour under continuous span configurations, shell modelling of superstructure to understand the lateral distribution, and comprehensive life cycle assessments to further evaluate the environmental impact of elevated construction projects involving U-Girder and Box Girder.

ACKNOWLEDGEMENTS

I, **Umashankar Mishra** would like to express my sincere appreciation and gratitude to everyone who has contributed to the successful completion of this project. Although it may not be possible to name everyone who has helped me along the way, I would like to recognize some individuals for their exceptional support and guidance.

First and foremost, I would like to express my sincere gratitude to my project supervisor, **Dr. Nirendra Dev**, for their unwavering support and guidance throughout my project. Their expertise, feedback, and insightful comments have been invaluable in shaping the direction and scope of this study. I am grateful for their patience, dedication, and mentorship throughout my research journey.

Furthermore, I would like to extend my gratitude to the faculty and staff of the department for providing me with access to necessary resources and facilities. I am thankful for their support and encouragement.

Finally, I would like to express my heartfelt appreciation to my family, friends, and colleagues for their constant encouragement and motivation. Their unwavering support has been instrumental in helping me achieve my academic goals.

I am grateful to everyone who has contributed to the successful completion of this project. I am humbled and honored by their support and guidance, and I will cherish these experiences for a lifetime.

Signature

Umashankar Mishra

Table of Contents

LIST OF TABLES

LIST OF FIGURES

LIST OF SYMBOLS, ABBREVIATIONS AND NOMENCLATURE

RRTS - Regional Rapid Transport System

FEA - Finite Element Analysis

Fck - Characteristic Strength of Concrete

Ec - Young's Modulus of Concrete

f_y - Yield Strength of Reinforcement

BS - British Standard

α - Mass Damping Coefficients

β - Stiffness Damping Coefficients

CHAPTER 1: INTRODUCTION

1.1. GENERAL

In the wake of rapid urbanization and burgeoning populations, the demand for efficient transportation systems has become paramount, particularly in countries like India where urban centers are experiencing unprecedented growth. Among the various modes of transportation, the development of high-speed train networks has emerged as a promising solution to alleviate congestion, reduce travel times, and promote sustainable urban mobility. The implementation of regional rapid transit systems (RRTS) in India represents a significant step towards modernizing transportation infrastructure and fostering economic development.

Figure 1.1-1: Viaduct of RRTS corridor crossing over Metro Blue Line

The success and safety of high-speed train operations crucially depend on the performance and resilience of their superstructures, which encompass bridges, viaducts, and other elevated structures. These superstructures must withstand dynamic loads imposed by

high-speed trains while ensuring passenger safety and operational efficiency. As India embarks on the ambitious task of expanding its high-speed rail network through the introduction of RRTS, it becomes imperative to conduct a comparative study of different types of superstructures under high-speed train loading conditions.

This thesis aims to address this critical gap in research by undertaking a systematic analysis of various superstructure (i.e. U-Girder & Box Girder) designs employed in high-speed rail projects, with a focus on their applicability to the unique operational requirements and environmental conditions prevalent in the Indian context. By evaluating the performance, cost-effectiveness of different superstructure types, this study seeks to provide valuable insights for the standardizing the superstructure for various span lengths for undergoing RRTS loading.

1.2. SCOPE OF RESEARCH

Despite the rapid advancement in high-speed rail technology and the increasing emphasis on developing regional rapid transit systems (RRTS) in India, there exists a significant research gap regarding the optimal choice of superstructure section between U girder and Box girder configurations, particularly concerning their structural performance under high-speed loading conditions and their economic feasibility.

Structural Performance under High-Speed Loading: While both U girder and Box girder configurations are commonly used in elevated rail infrastructure, there is a lack of comprehensive studies specifically evaluating their structural behavior and performance under high-speed train loading in the context of RRTS projects. Existing research often focuses on static loading scenarios or lower-speed rail systems, failing to capture the dynamic effects and fatigue considerations inherent in high-speed operations. Therefore, there is a need for empirical investigations and numerical simulations to assess the dynamic response, fatigue life, and overall structural integrity of U girder and Box girder superstructures subjected to high-speed train loads.

Standardization of Section Based on Economy: The selection of superstructure sections significantly influences the cost and economic viability of RRTS projects. However, there is a dearth of comprehensive research addressing the standardization of section based on economy between U girder and Box girder configurations for RRTS projects. While U girders may offer potential cost advantages in terms of material usage, Box girders may provide enhanced structural efficiency requirements over the lifecycle of the infrastructure. Therefore, there is a critical need for comparative studies considering factors such as initial construction costs, robustness and speed of construction to inform the standardization of superstructure sections in RRTS projects.

Construction Benefits and Efficiency: While both U girder and Box girder configurations offer distinct advantages during construction, there is limited research addressing their comparative construction benefits, particularly concerning speed of construction, ease of assembly, and overall project timeline. Understanding the construction benefits associated with each superstructure section is crucial for optimizing construction methodologies, minimizing project durations, and enhancing overall project efficiency. Therefore, there is a need for empirical studies and case analyses to identify and quantify the construction advantages of U girder and Box girder configurations in the context of RRTS projects in India.

1.3. OBJECTIVE OF RESEARCH

i. To check the feasibility of different type (i.e., U- Shaped & Box Girder) of PSC super-structures under high-speed loading.
ii. Maximum design speed evaluation for various span configurations.
iii. Comparison and cost optimization of different type of structures i.e., U- Shaped, Box Girder for various span configurations.
iv. Based on Dynamic Analysis, evaluation of most optimum type of superstructures for a particular span.

1.4. LITERATURE REVIEW

This chapter provides a thorough exploration of the current body of literature centered on the dynamic analysis of superstructures through the application of Finite Element Method (FEM) modeling. The review is organized into distinct sections that offer a comprehensive understanding of the dynamic behavior of structures, with a specific focus on superstructure such as Box Girders and U-girders as employed in Rapid Transit systems.

Nallasivam et al. (2023) undertook a study to analyze the dynamic behavior of box-girder bridges using finite element analysis. This investigation aimed to comprehend how these bridges respond to dynamic loading, a crucial aspect for assessing structural integrity and security across varying load conditions. Box-girder bridges, renowned for their structural efficiency, stiffness, and aesthetic appeal, form a common design in modern civil engineering. A paramount requirement for their enduring safe performance is an in-depth understanding of their dynamic behavior. This research delves into the dynamic analysis of bridges, a pivotal field in structural engineering. Numerous studies exploring diverse loading scenarios, encompassing traffic, wind, earthquakes, and trains, have been documented. Employing finite element analysis (FEA), a robust numerical tool, the study models and analyzes the dynamic behavior of bridge structures. FEA comprehensively simulates intricate structural systems, considering material characteristics, geometry, and loading conditions, providing insights into dynamic attributes such as natural frequencies, mode shapes, and amplification factors. Dynamic loading effects on box-girder bridges have been a focal point in various investigations. The literature highlights the influence of factors like moving loads, wind-induced vehicular vibrations, and earthquake resonances on the dynamic response of these bridges. The aim of such exploration is to ensure the prolonged structural integrity of bridges by examining resonance phenomena, fatigue efficiency, and failure mechanisms under dynamic loading conditions. To ensure the fidelity of dynamic analyses, the validation and calibration of finite element models are critical. Experimental tests, including modal tests and vibration measurements, validate numerical models and enhance result reliability through model calibration aligning material properties, boundary conditions, and parameters with known bridge behavior.

Furthermore, the paper extensively investigates design strategies for optimal dynamic responses in box-girder bridges. These measures incorporate supplementary damping devices, material advancements, and vibration control systems to minimize vibrations, static amplification, and enhance overall bridge performance under dynamic loads.

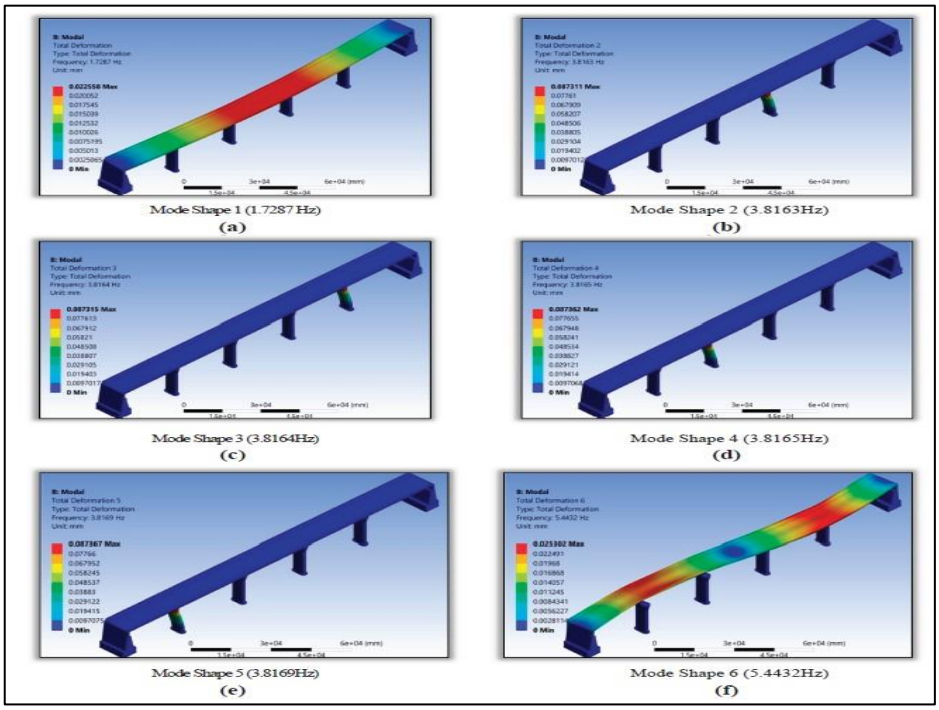

Figure 1.4-1:Mode shapes of bridge without sub-track system.

In conclusion the research augments existing knowledge by investigating the dynamic behavior of box-girder bridges through finite element analysis. The study underscores the significance of understanding bridge dynamics under diverse loading scenarios, advocating for design interventions that ensure structural integrity and safety. While the specific paper's details will only be accessible in 2023, the anticipation is that it will advance previous research by integrating contemporary finite element analysis techniques and exploring innovative strategies for dynamic enhancement.

Menon et al. (2018) simulated two U-girder decks have been using Structural Analysis Program software, employing shell elements. The outcomes of three-dimensional finite-

element analysis validate the applicability of the thin-walled beam theory. It's important to note that this study's scope is confined to a straight U-girder bridge deck with uniform section and thin-walled characteristics. Furthermore, the impact of load position variations has also been explored, establishing that the thin-walled beam theory is well-suited for accurately estimating and designing U-girder bridges to withstand longitudinal stresses. In contemporary railway and highway projects, the utilization of simply supported U-shaped pre-stressed concrete bridge decks is on the rise. Design practices often rely on simplified analysis methods. In the case of longitudinal considerations, the U-girder is typically treated as a beam. However, when subjected to eccentric loading, basic beam analysis tends to provide overly optimistic assessments of longitudinal forces due to torsional warping. To gain insights into the behavior of U-girder bridge decks under torsional loads, the application of Vlasov's thin-walled beam theory proves beneficial. This theory can be seamlessly employed as an alternative to conventional beam analysis, leading to significantly enhanced projections of longitudinal stresses.

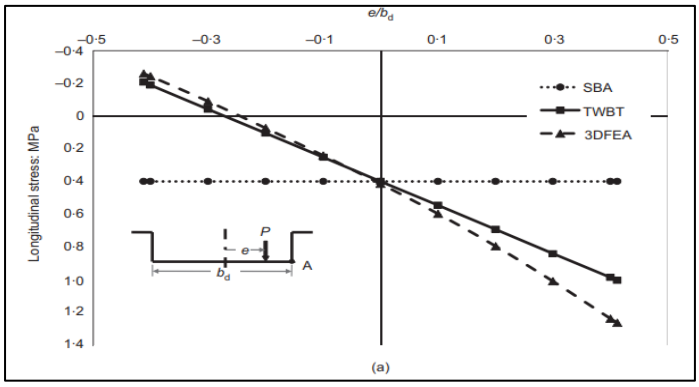

Figure 1.4-2:Variations in maximum longitudinal stress (MPa) at web–deck slab junction 'A': (a) at mid-span with varying transverse eccentricity (e/bd)

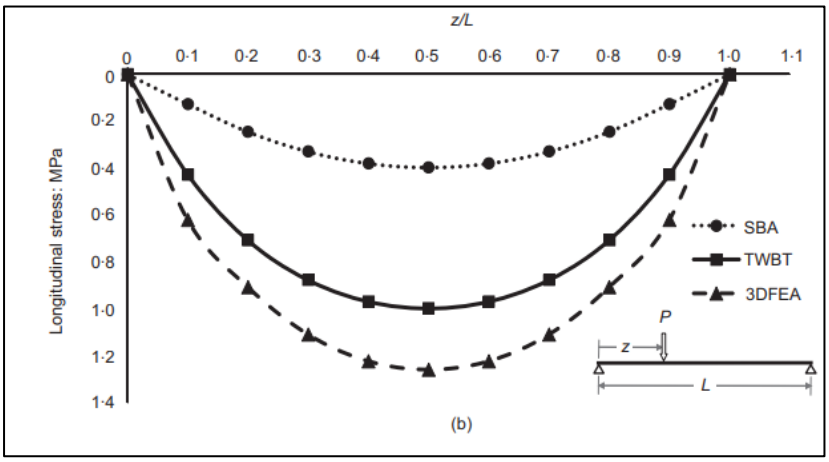

Figure 1.4-3: Variations in maximum longitudinal stress (MPa) at web–deck slab junction 'A' at section matching load location, which varies longitudinally (z/L) with maximum eccentricity (e/bd 5 +0.41)

The conventional and widely used simplified beam analysis (SBA) method, applied for longitudinally analyzing U-girder bridge decks, is proven to yield overly optimistic outcomes when faced with eccentric loading. In a bid to enhance SBA, the Thin-Walled Beam Theory (TWBT), originally attributed to Vlasov in 1961, is embraced as a means to accurately estimate the longitudinal stresses endured by simply supported U-girder bridge decks subjected to eccentric vehicle loads.

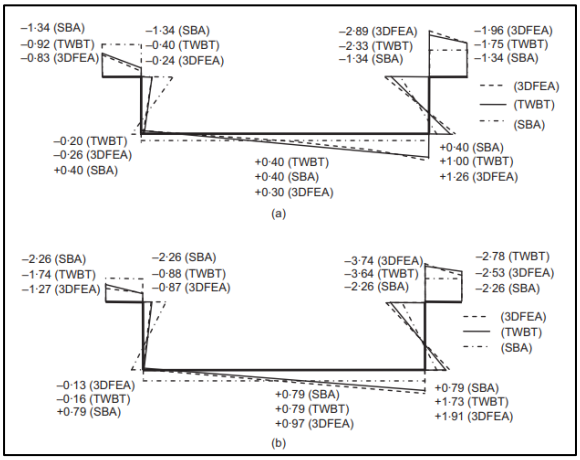

Figure 1.4-4: Comparison of longitudinal stress (MPa) distribution by SBA, TWBT and 3DFEA: (a) example 1, eccentric, concentrated (wheel) load at mid-span; (b) example 2, eccentric, uniformly distributed (line) load over the entire span

To showcase the effectiveness of this approach, two scenarios are examined: (a) the effect of an eccentric wheel load on a highway bridge deck, and (b) the influence of a metro rail line load on a double track. A comprehensive comparison is made between the results obtained through conventional SBA, TWBT, and more intricate three-dimensional finite element analysis (3DFEA). The findings reveal that SBA significantly underestimates the peak stresses at the web-deck slab junction (located near the applied load) by up to 68% and 59% in examples 1 and 2, respectively. On the other hand, TWBT only underestimates these stresses by 21% and 9% for examples 1 and 2, respectively. The notable errors observed in SBA stem from its inherent inability to capture the torsional effects triggered by eccentric loading. While TWBT accounts for these torsional effects, there remains a slight margin of error attributed to distortion, shear lag, and the degradation of concrete stiffness.

Ayoub el al. (2015) the 2.7 kilometers double track elevated viaducts for the Doha metro green line involves a mix of cast-in-situ and precast segmental simply supported spans, with lengths ranging from 20 to 35 meters. Additionally, continuous cast-in-situ U-trough decks are utilized, with non-standard span arrangements including two and three spans ranging from 30 to 68 meters. These configurations were necessitated by the presence of existing utilities and infrastructure underneath.

To ensure passenger comfort and traffic safety, a comprehensive dynamic analysis was indispensable. This analysis focused on assessing vertical accelerations, vertical displacements, and lateral frequencies of vibration across all spans, including simply supported and continuous spans. The analysis utilized data from the real train of the project, comprising 6 vehicles with a total length of 120 meters and actual axle loads.

Various train speeds, ranging from 60 km/hr to the maximum permissible speed of 160 km/hr, were considered in the dynamic analysis. Both direct time integration of the equation of motion and modal time history analysis methods were employed. Results were compared against allowable values outlined in EN 1991-2 and EN 1990-Annex 2, and it was found that all segments of the elevated viaduct met the relevant Euro norm

requirements for vertical accelerations and vertical deflections.

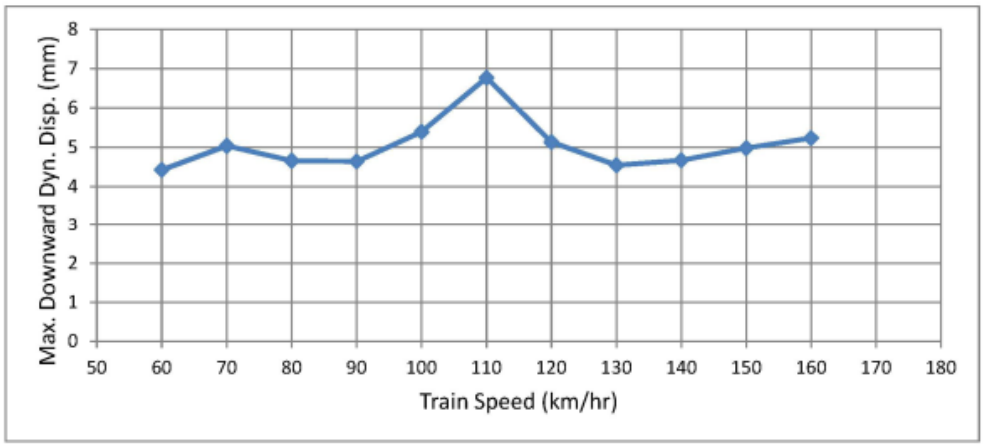

Figure 1.4-5:Maximum downward dynamic Displacement for 32m SS span.

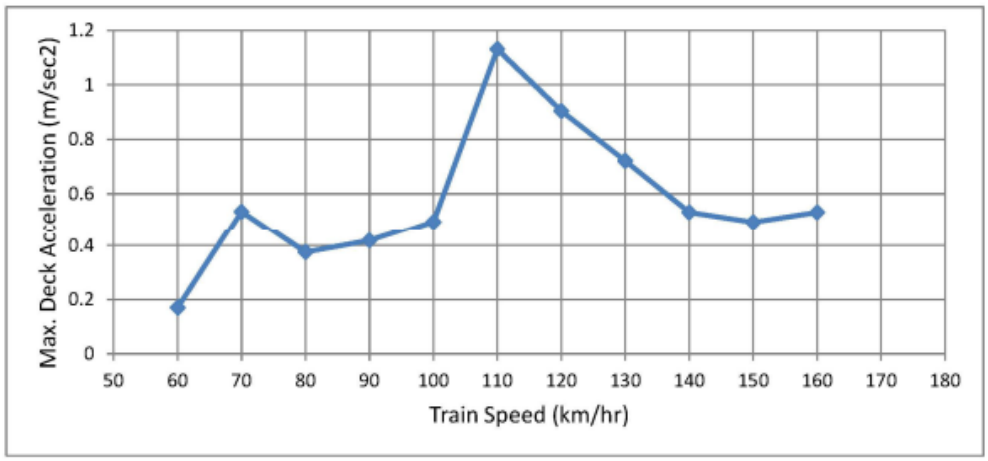

Figure 1.4-6: Maximum Deck Vertical Acceleration for 32m SS span.

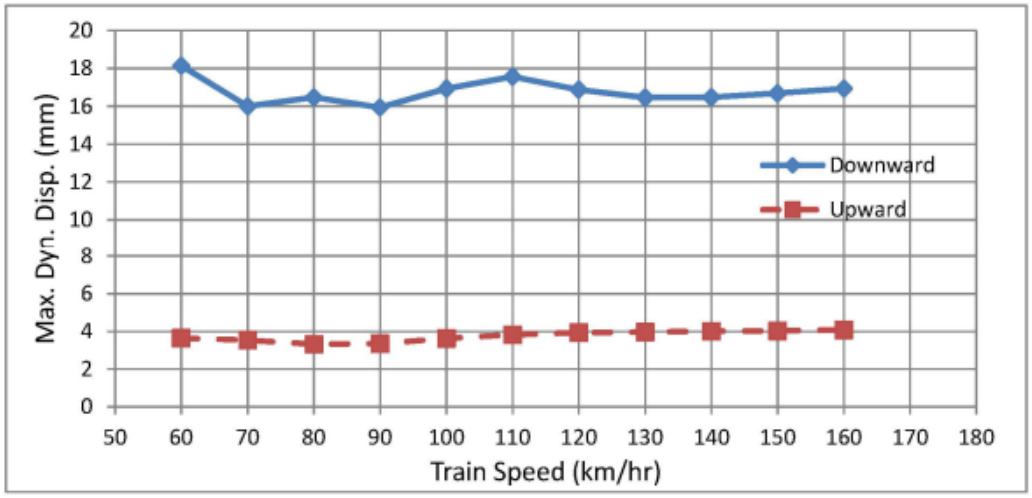

Figure 1.4-7:Maximum Dynamic Displacement for 57m two span continuous span

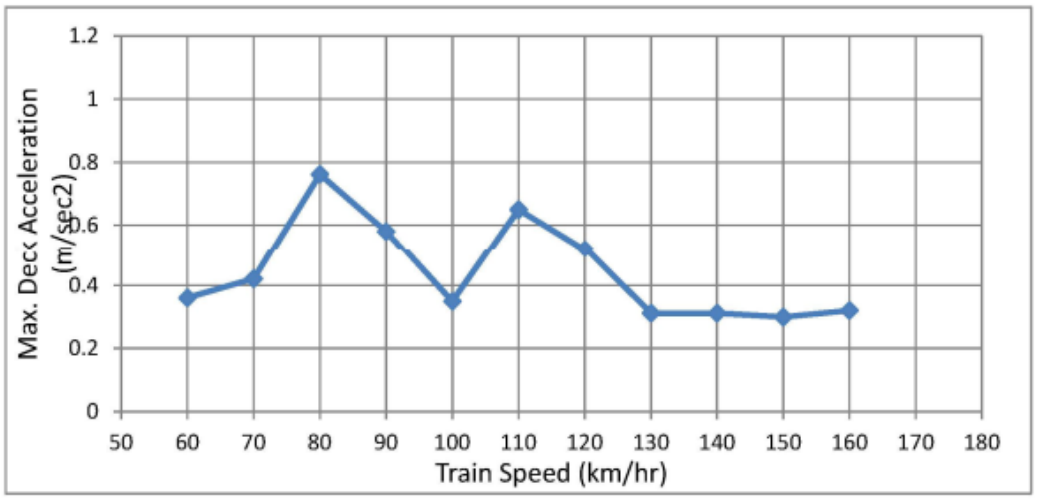

Figure 1.4-8: Maximum Deck Vertical Acceleration for 57m two span continuous span

In conclusion, the dynamic analysis of the elevated viaducts for the Doha metro green line, accommodating double tracks with actual trains carrying maximum axle loads, ensures compliance with EN standards for passenger comfort under real train moving loads. The analysis encompassed a range of train speeds and focused on vertical deflections, vertical accelerations, and fundamental lateral and vertical frequencies. Both direct time integration and modal time history analysis yielded consistent results, demonstrating compliance with EN requirements across all segments of the project.

H. Xia et al (2002). investigated the dynamic interaction between articulated high-speed trains and bridges. A dynamic interaction model for the bridge-articulated train system is developed, comprising an articulated vehicle element model and a finite element bridge model. The vehicle model is tailored to the structure and suspension properties of articulated trains, and a computer simulation program is developed accordingly. As a case study, the paper analyzes the passage of a Thalys articulated train over the Antoing Bridge on the Paris–Brussels high-speed railway line. The dynamic responses of both the bridge and the vehicles are computed, and the proposed analysis model and solution method are validated through a comparison within situ measured data. The paper also delves into the vibration behavior exhibited by articulated trains.

A Thalys high-speed train consists of a locomotive, followed by one transition carriage, six normal articulated cars, another transition carriage, and a rear locomotive. Each locomotive has two independent bogies and can be modeled traditionally as three rigid bodies, each with 15 degrees of freedom (DOFs). The transition carriage has an independent bogie at the locomotive end and shares an articulated bogie with the adjacent passenger car. The normal passenger cars share bogies with adjacent cars or the transition carriage. In total, a Thalys train comprises 10 vehicles, 13 bogies, and 26 wheel-sets. As the second to the ninth vehicles are articulated with each other, they are collectively treated as a group, modeled with 17 rigid bodies and 85 DOFs. Including the 30 DOFs of the two locomotives, the entire train model has 115 DOFs.

In modeling, the articulated train group is represented as a series of articulated vehicle elements consisting of car bodies, bogies, and wheel sets. Each articulated vehicle element connects the car body to the front bogie with transverse and vertical springs and dampers and to the following car body with a central elastic hinge. This arrangement ensures geometric stability, with the car body connected to adjacent rigid bodies through three elastic or damping points. The four dampers between adjacent car bodies also reduce nodding and yawing movements, simulated as viscous damping. Notably, this modeling

approach allows for uniform representation of different vehicle types, simplifying programming.

An articulated vehicle comprises two suspension systems. In the primary suspension, wheels are elastically connected to the bogie frame via lateral positioning rubber blocks and vertical axle-box springs and dampers. The secondary suspension, between the car body and bogies, utilizes flexible air springs with minimal vertical damping. Lateral springs and dampers in the secondary suspension system are positioned between the car body and the bogies.

In the step-by-step integration of the combined vehicle and bridge system, the Newmark-b algorithm is employed. This method, known for its unconditional convergence, eliminates the need for a specific step length. Within each time step, the program calculates the generalized displacement, velocity, and acceleration of both the vehicle and the bridge system. Ensuring convergence of the generalized displacement for each degree of freedom (DOF) in both systems is imperative within each step.

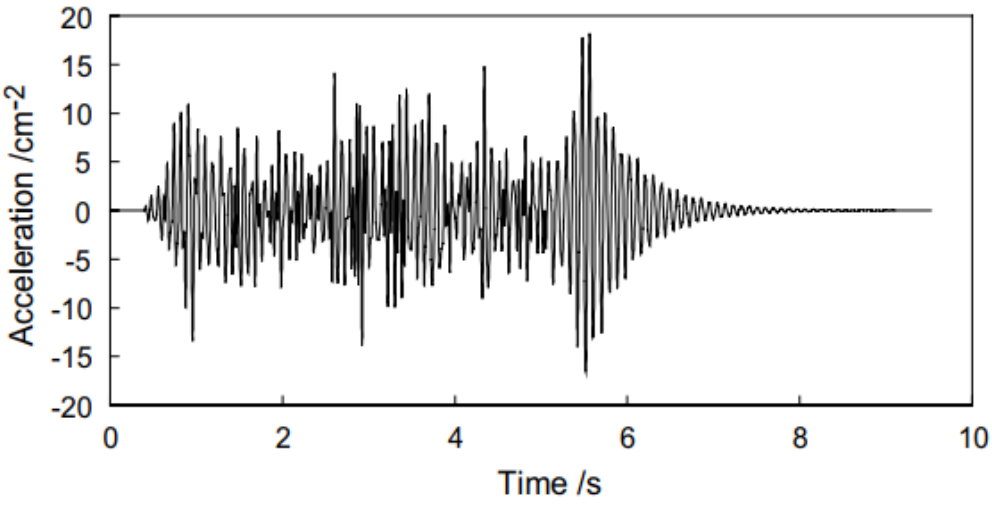

Figure 1.4-9: Calculated lateral acceleration history of girder.

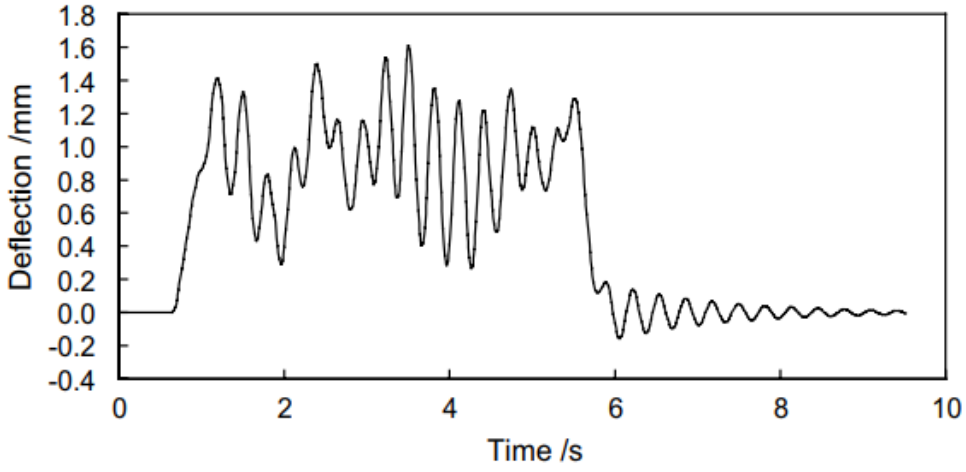

Figure 1.4-10: Calculated deflection history of the girder.

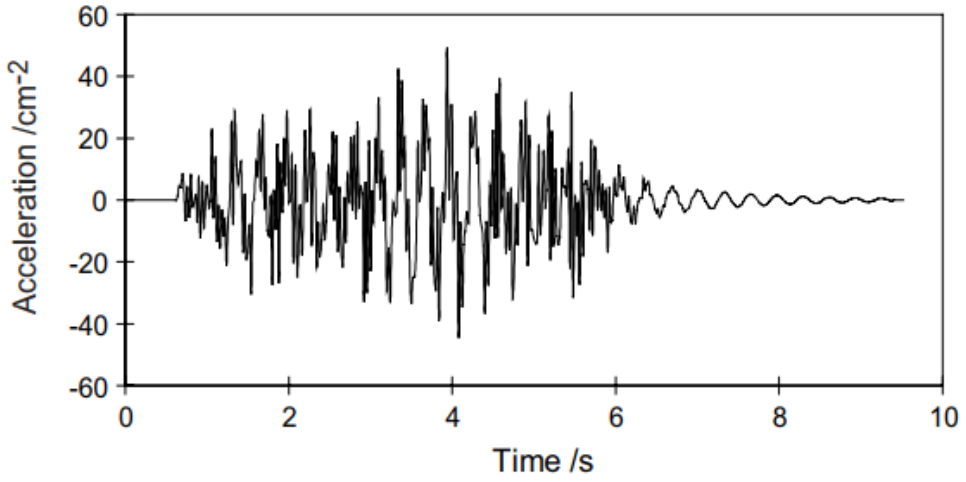

Figure 1.4-11: Calculated vertical acceleration history of girder.

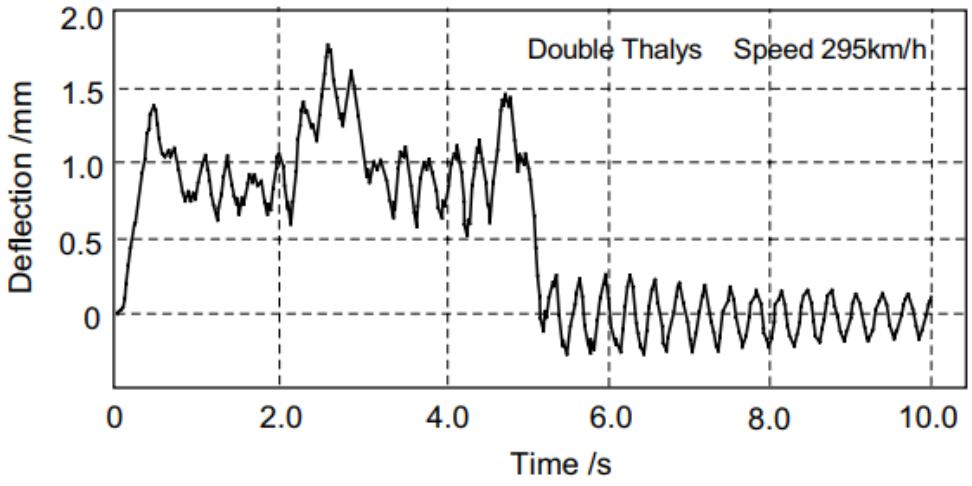

Figure 1.4-12: Measured deflection history of girder

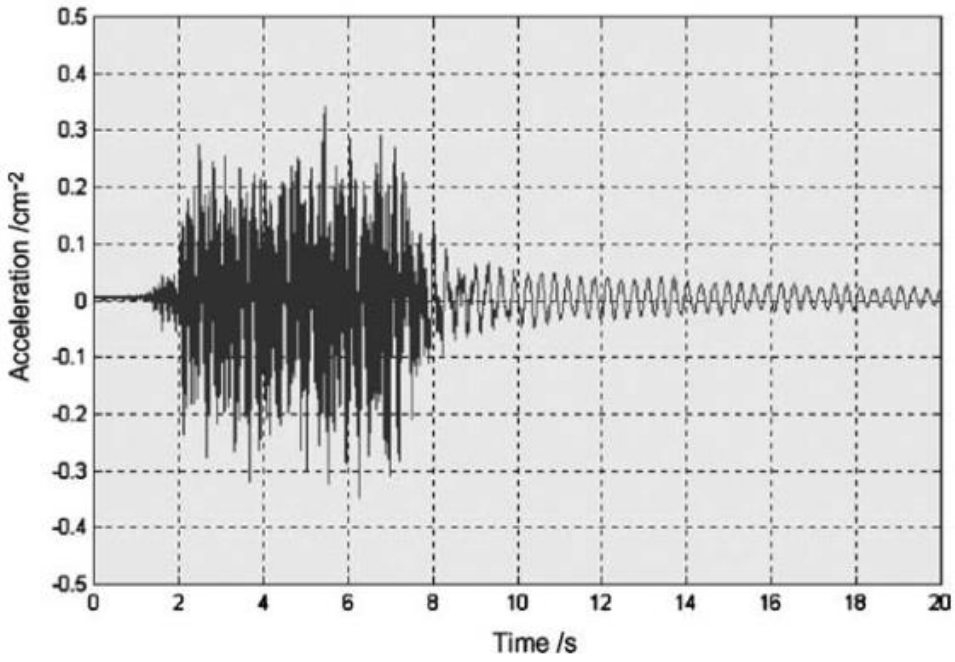

Figure 1.4-13: Measured vertical acceleration history of girder

The dynamic analytical model proposed in this paper for the bridge-articulated-train system, along with the accompanying computer simulation method, effectively captures the principal vibration characteristics of both the bridge and the articulated train vehicle.

Through comparison within situ measured data, the calculated results exhibit strong alignment in response curves, amplitudes, and distribution tendencies, affirming the reliability of the analytical model and simulation method.

Furthermore, the Antoing Bridge demonstrates excellent dynamic characteristics, boasting a deflection-to-span ratio smaller than similar bridges in China. The deflections of the girder and the lateral and vertical accelerations of both the girder and the car body adhere to established safety and comfort standards for bridges and running train vehicles.

Moreover, articulated train vehicles exhibit favorable running properties at high speeds, contributing to the reduction of impact on bridge structures. This favorable running behavior further enhances the overall operational efficiency and safety of the railway system.

Ko et al. (2022) focused on the dynamic analysis of high-speed trains operating on perforated beams based on the theory of Timoshenko and Euler Bernoulli. The purpose of this study is to investigate the dynamics of beams and their interaction with tracks in order to determine the effects of perforations on track structure. These findings provide insight into the vibration characteristics and structural behavior of the beams under high speed train loading conditions. The literature recognizes that, considering their interaction with the underlying track and supported structure, high-speed train dynamics have a significant role to play. In order to ensure comfort for passengers, track stability and the structural integrity of support columns, it is important to know how high-speed trains behave. The study aims to examine the kinetic effects caused by train movements on perforation beams. Perforated beams, composed of structural components that are periodically fitted with holes or openings which may have a significant influence on their dynamic behavior. The literature is filled with the distinct characteristics of perforated beams, such as their change in mass distribution, stiffness, and damping properties. In order to assess structural integrity and evaluate its performance under different loading conditions, the dynamic response of perforated beams shall be analyzed.

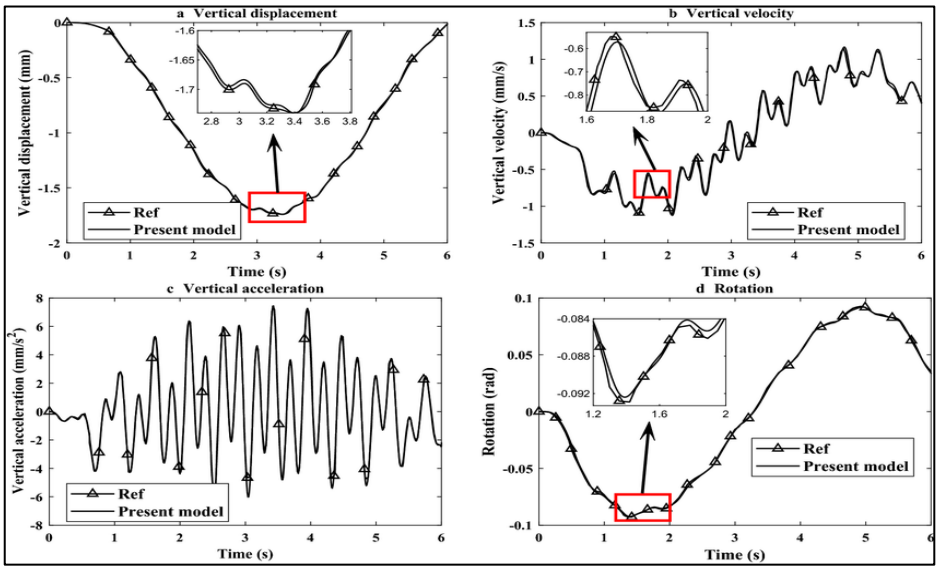

Figure 1.4-14 : Comparisons of dynamic responses of the train body

A comparison of the dynamic analysis results on perforated beams using two well-known beam theory methods: Timoshenko and Eulerucci, is made in this research paper. An overview of this theory is set out in the literature, with an emphasis on assumptions and applicability. Timoshenko theory considers deformation effects, whereas the EulerBulli beam theory does not take into account deformations caused by shears. Understanding the impact of shears deformations on the dynamic response of a perforated beam is facilitated by comparing results from both theories. The interaction of a high velocity train with the rails and perforation beams is investigated in this study. In order to accurately model the dynamic response of the perforated beams, the literature emphasizes the importance of considering the interaction between the train tracks and the structure. The analysis shall take account of dynamics that have been created by the train's journey, e.g. wheel rail interactions and aerodynamic effects. This is capable of providing a complete view of the beam's response in real loading conditions. The vibration properties and structure characteristics of the perforated beams are investigated in this research paper. The literature reviews the findings related to the natural frequencies, mode shapes, and dynamic response of the beams during high-speed train loading.

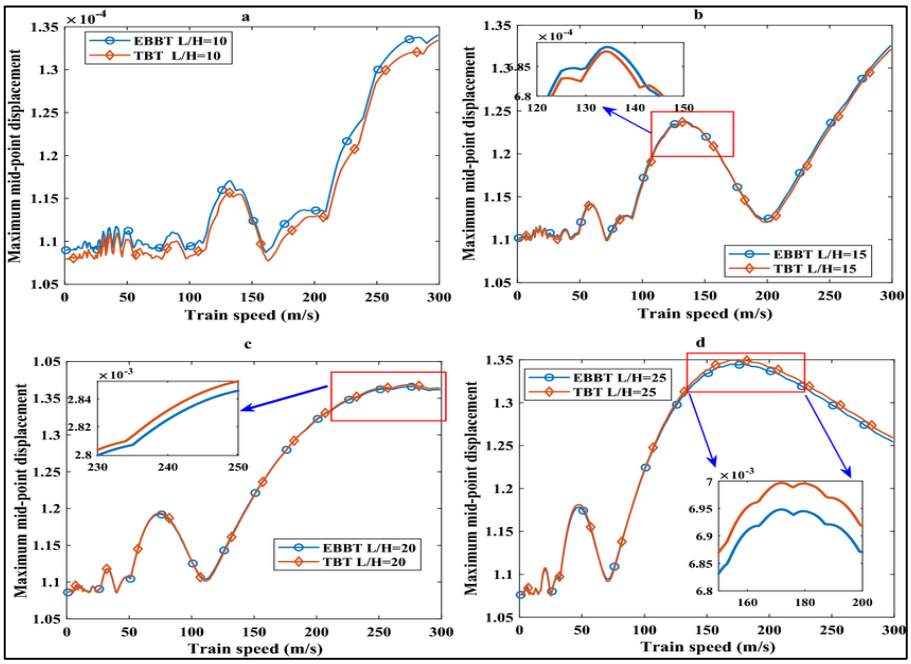

Figure 1.4-15: Dynamic response of the perforated beams for the mid-point transverse deflection considering different L/H ratios and filling ratio α = 1 with EBBT and TBT.

The study will investigate the influence of perforation parameters, for example hole size, arrangement, and density, on beam dynamics. These findings are essential for assessing structural performance and optimizing the structure of perforated beams. Practical implications for the design and maintenance of railway infrastructure are found in dynamic analyses of high-speed trains fitted with perforated beams. The literature makes it clear that when designing beams to be fitted with High-Speed trains, consideration should be given to the effect of perforation. The report also reviews possible vibration control measures, such as deflection treatments or modifications to the perforation design, with a view to reducing excessively strong vibrations and ensuring longer lifetime performance and safety of beams. This research paper has contributed to the understanding of dynamically responding or behaving perforated beams when they are transported by high-speed trains. The literature review emphasizes the importance of looking at structural interaction between train tracks and choosing a beam theory in Dynamic Analysis. For engineers and researchers involved in the design and assessment of railroad structures that have been subjected to heavy train loads, these results will give an invaluable insight.

Further investigation should be carried out on other aspects, such as the effects of varying perforation parameters and development of a more detailed model in order to analyze the dynamic response of perforated beam.

Erduran et al. (2022) performed a numerical study that aims to explore the dynamic behavior of railway bridges under vibrations induced by heavy-haul traffic. For this purpose, a finite element code that can conduct moving load and moving mass analysis of single span bridges was developed. The software was validated by comparing the numerical response to the analytical solution for various speeds. The numerical analysis of the benchmark bridge under the benchmark train showed the interplay between the natural frequency of the bridge, the mass of the train and the loading frequency. A comprehensive parametric study to investigate the impact of different parameters on the dynamic behavior of railway bridges is also provided. The bridge span length, normalized train length, normalized mass of the train, bridge deck stiffness, and train speed are the variables considered in the parametric study. The results of the extensive numerical analyses improve the understanding of railway bridge behavior.

Under heavy haul trains, and highlight the impact of the inertial effect of the trains on bridges, especially for varying span length and deck stiffness. It is also demonstrated that, when the train-to-bridge mass ratio exceeds 40%, the inertial effects of the train mass needs to be included in the analysis in order to obtain a reliable estimate of the bridge behavior under different train speeds. rowing demands on railway bridges have led to an imperative for their assessment to accommodate higher train speeds and axle loads. This study addresses the dearth of research on the dynamic behavior of railway bridges under vibrations induced by heavy-haul trains and the role of critical model parameters.

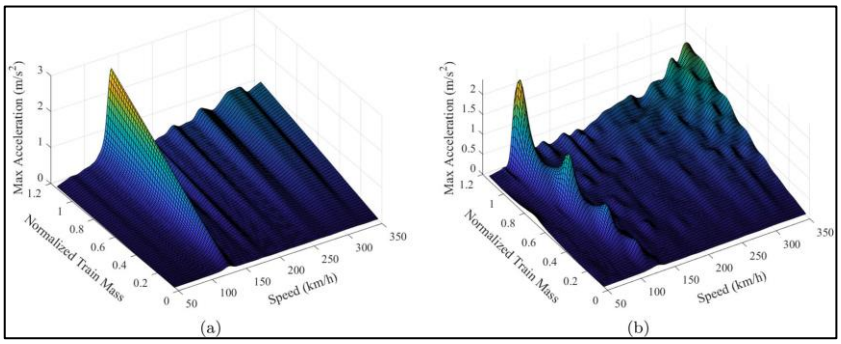

Figure 1.4-16: Variation of maximum acceleration with train mass and train speed for (a) moving load model (b) moving mass model.

A Finite Element code that incorporates train mass inertial effects is developed to analyze the behavior of simply-supported railway bridges. Validation is conducted using existing literature. The Norddals Bridge in Norway, which supports heavy-haul iron ore trains, and a typical freight train form the benchmark cases. A parameter study explores the effects of bridge span length, train length and mass, and deck stiffness on dynamic behavior. This involves dynamic analyses under varying train speeds using moving load and mass models. An acceleration amplification factor (AAF) is introduced to gauge the train's inertia impact on bridge response at different speeds. Key findings include the impact of train mass on vibration frequency, the influence of bridge span length and deck stiffness, and the role of train length in acceleration. The two-fold influence of train mass on dynamic behavior is also highlighted. AAF is highest when loading frequency matches natural frequency

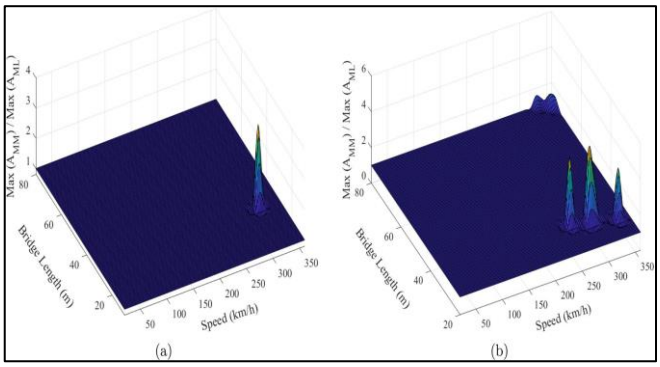

Figure 1.4-17: Variation of AAF with bridge length and train speed for a normalized train mass of (a) 0.25 and (b) 0.5.

The study underscores the necessity of accounting for train mass, especially when it's substantial compared to the bridge's mass. This research contributes to comprehending dynamic railway bridge behavior under heavy-haul trains. While limited to simply-supported bridges and a single train geometry, further research is recommended to extend observations to multi-span bridges and diverse train geometries. Future studies should also incorporate a moving system model with train stiffness and damping properties to quantify their impact on dynamic behavior under heavy axle loads.

Verma et al. (2021) elaborate on modal analysis of narrow walled box girder bridges and an associated rail track based on a finite element framework. The study is intended to explore the Dynamic Characteristics of Bridges and Rail Systems, including Naturally Occurred Frequency and Mode. These results provide valuable information on structural behavior and vibration characteristics, which will assist in the design and assessment of such systems. A basic method for studying the dynamics of structures, by determining their natural frequency and form characteristics, is to use a mode analysis technique. The literature notes the importance of modal analysis for understanding the vibration characteristics and structural response of a box girding bridge or railway track. This will serve as the basis for assessment of dynamic performance, Structural Inside less Assessment and identification of possible resonance issues. In view of their high strength-to-weight ratio aesthetic appeal, walled box-girder bridges are often used in railway and rail infrastructure. The literature is devoted to the specific characteristics of box-girder bridges, such as their complexity in geometry, materials properties and supportive conditions. In order for these structures to operate effectively and safely, it is important to understand the dynamics of their behavior by means of modal analysis.

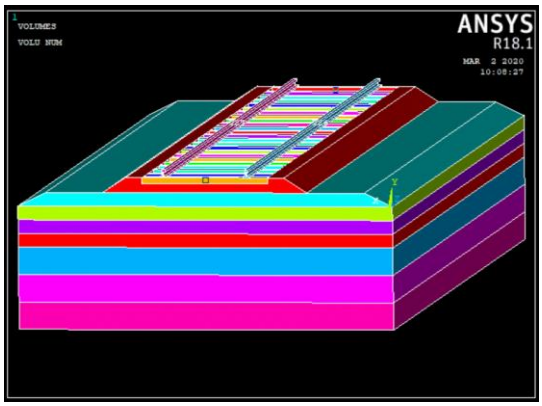

Figure 1.4-18- Railway track model.

The research paper also deals with modal analysis for the related railway network in addition to the bridge structure. The literature reviewed the relevance of analyzing track dynamics, e.g. rail, sleepers and ballast when they are in close proximity to a bridge. The modal analysis of a track allows us to gain insight into its response to dynamic forces, influences on the bridge behavior and potential interactions between tracks. The finite element method (FEM) is widely used for modal analysis due to its ability to model complex structures and accurately capture their dynamic behavior. The literature discusses the use of the FEM in the research paper to develop numerical models of the thin-walled box-girder bridge and railway track. It highlights the advantages of the FEM in simulating the structural response and conducting modal analysis to obtain accurate mode shapes and natural frequencies.

Dynamic properties and mode shapes of the box-girder Bridge and train track are investigated in this research paper. The literature reviews the findings related to the first few mode shapes, their corresponding natural frequencies, and the factors influencing mode participation. These results have provided us with information on vibrational behaviour, potential resonance issues and the fundamental structure components of the bridge and track system. In order to design and assess box girdle bridges as well as rail tracks, it is vital that we understand their structural characteristics. The literature provides insight into the consequences of modal analysis findings in terms of structural stability,

vibration control measures, fatigue life estimation and maintenance practices. In order to optimize the design, guarantee structural security and improve system performance in terms of bridges and tracks, technical knowledge gained from transport analysis will be helpful.

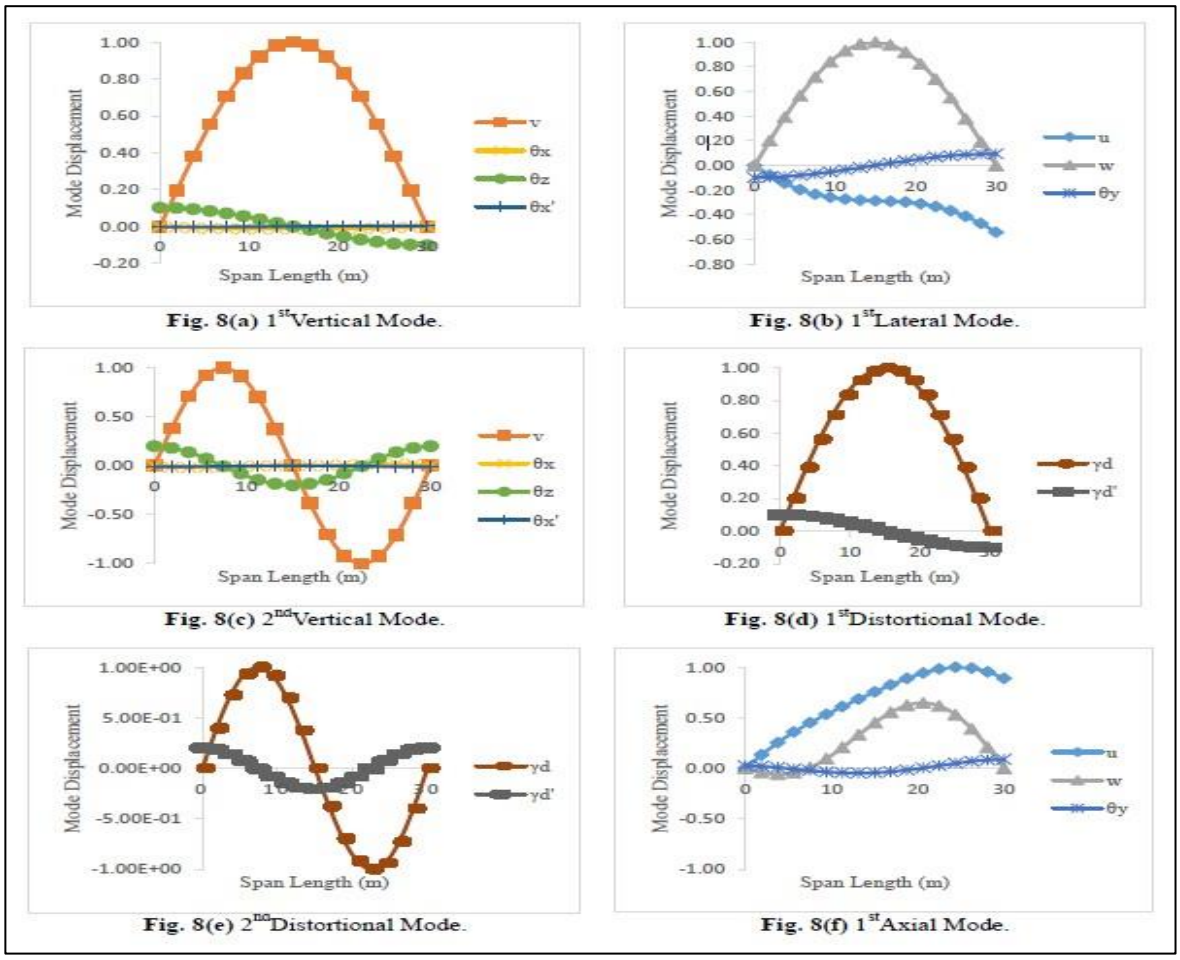

Figure 1.4-19 – Mode Displacement Results.

CHAPTER 2: FINITE ELEMENT MODELLING

2.1. INTRODUCTION

This chapter outlines the methodology employed for the thorough examination of U-girders and Box Girder subjected to RRTS loading dynamics. It delves into the research framework, numerical modeling approach, parameter variations, data analysis methods, and the validation process of the numerical models in comprehensive detail. These concerted efforts were aimed at achieving the research objectives effectively.

2.2. STRUCTURAL SPECIFICATIONS OF SUPERSTRUCTURE

The type of superstructure considered for this research are U-Gider and Box Girder which serves as a prestressed precast architectural elements. It consists of a single upper framework, pre-cast and prestressed, spanning 28 meters with a center-to-center distance of 26.6 meters between bearings. Below are the specific structural characteristics:

U-Girder:

- Area: - 3259250.0000
- Perimeter: - 19015.3318
- Centroid: - X: 0.0000, Y: 0.0000
- Moments of inertia: - X: 1.5659E+12, Y: 1.2177E+13
- Product of inertia: - XY: -3.6546E+11
- Radii of gyration: - X: 693.1541, Y: 1932.8799
- Principal moments and X-Y directions about centroid: - I: 1.5534E+12 along [0.9994 0.0344], J: 1.2189E+13 along [-0.0344 0.9994]

Box Girder:

- Area: - 5495344.2805
- Perimeter: - 33302.4346
- Centroid: - X: 0.0000, Y: 0.0000
- Moments of inertia: - X: 2.8277E+12, Y: 3.4738E+13
- Product of inertia: XY: -174388068.5625
- Radii of gyration: - X: 717.3282, Y: 2514.2353
- Principal moments and X-Y directions about centroid: - I: 2.8277E+12 along [1.0000 0.0000], J: 3.4738E+13 along [0.0000 1.0000]

The boundary condition, elevation view, plan view and cross-sectional view are as shown below:

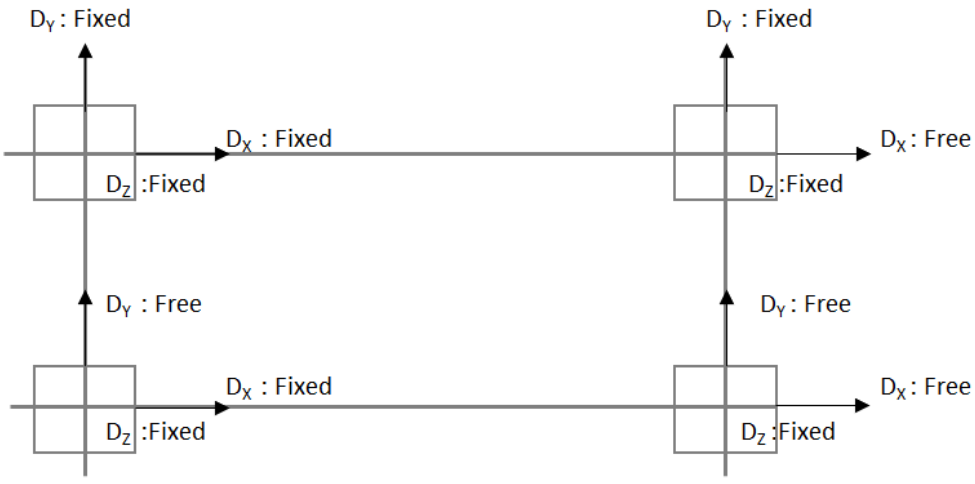

Figure 2.2-1: Boundary Condition

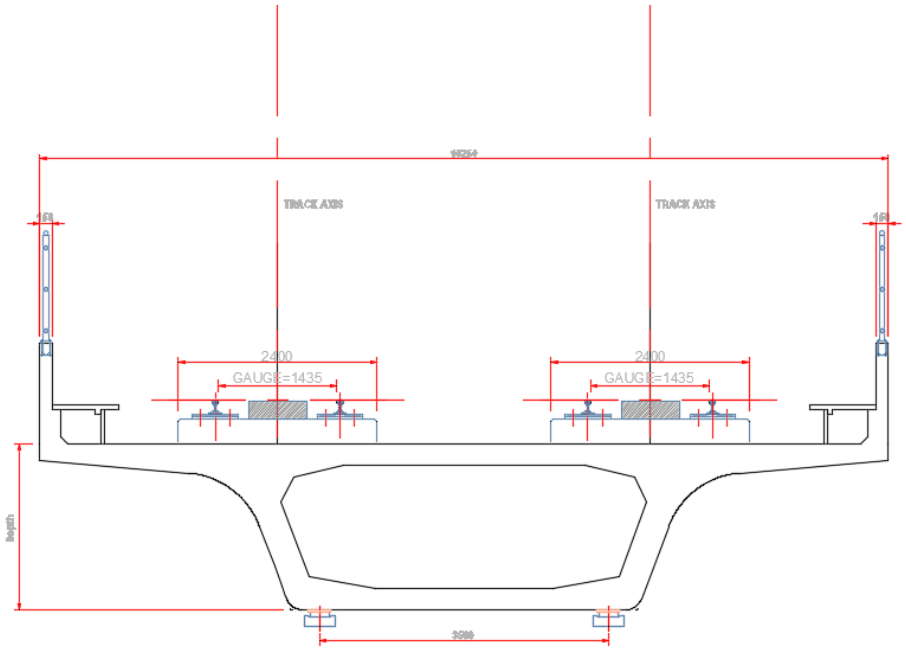

Figure 2.2-2: Box Gider Cross section.

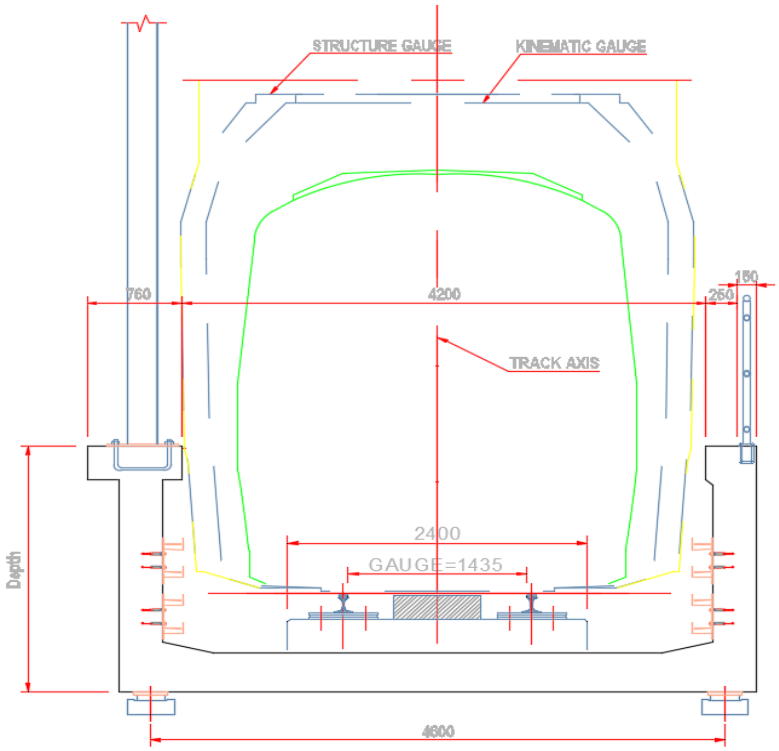

Figure 2.2-3: U-Gider Cross Section

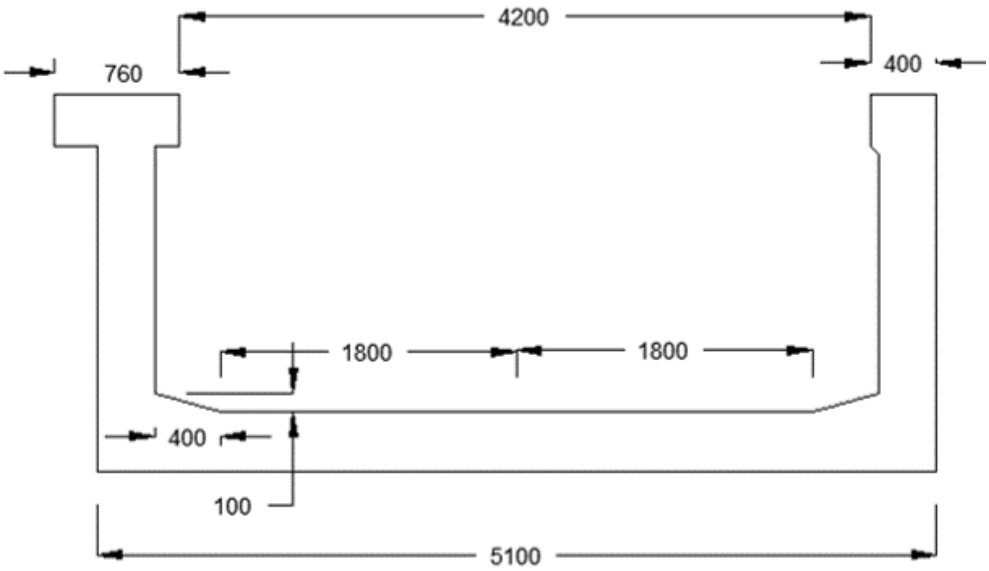

Figure 2.2-4: Cross sectional of U- Girder.

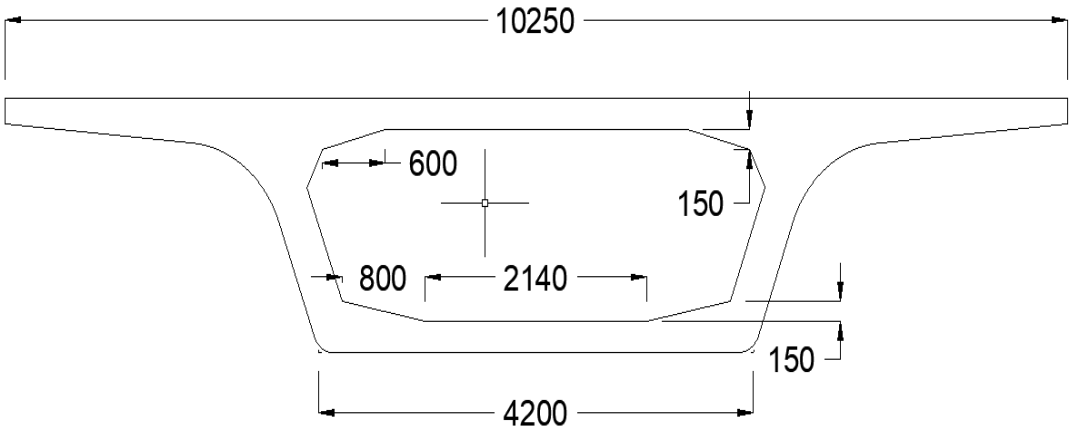

Figure 2.2-5: Cross sectional of Box Girder.

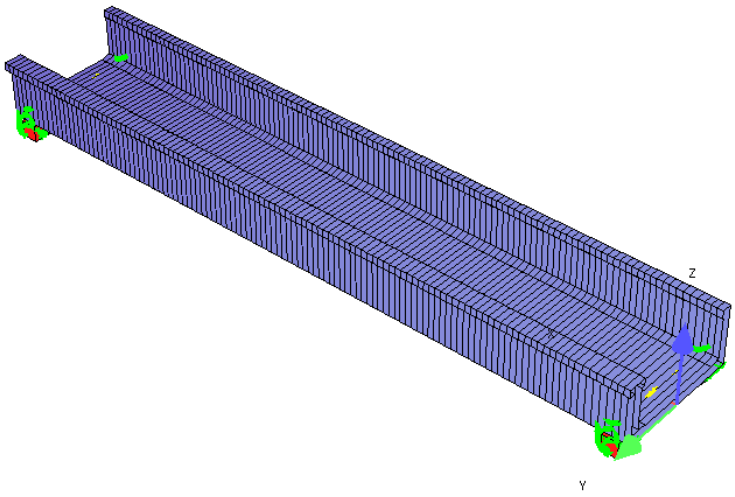

Figure 2.2-6: Isometric View U- Girder

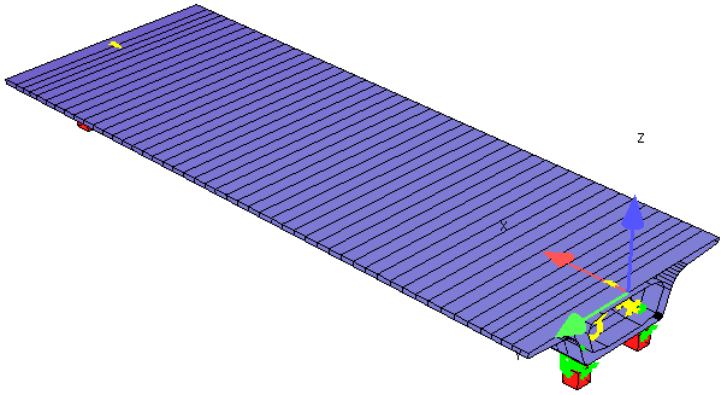

Figure 2.2-7:Isometric View Box Girder

2.3. MATERIAL PARAMETERS

2.3.1. CONCRETE CHARACTERISTICS

- Characteristic Strength: fck = 55 MPa (on Cube), 45 MPa (on Cylinder)
- Young's Modulus of Concrete: Ec = 35,000 MPa
- Poisson's ratio of Concrete: $\nu = 0.2$
- Volumetric Weight: $\gamma = 25$ kN/m^3 or 2.55 t/m^3

2.3.2. REINFORCEMENT

- Grade of Reinforcement f_y = 500Mpa
- Young's Modulus of Reinforcement E_s = 200,000 Mpa
- Cover = 50mm

2.3.3. PRESTRESSING STEEL CHARACTERISTICS

- Nominal Area of Strand : $A_s = 140mm^2$
- ULS Strength of Strand : $f_{pk} = 1860$ Mpa
- Maximum Jacking Stress : $0.75\ f_{pu} = 1395$ Mpa
- Modulus of Elasticity : $E_p = 195000$ Mpa
- Anchorage Set-in : 6mm

2.4. RESEARCH DESIGN AND APROACH

This section details the comprehensive plan and approach employed in the parametric investigation. Additionally, it discusses the sequential methodology developed for conducting dynamic analysis and subsequent parametric exploration.

2.4.1. METHODOLOGY

The geometric configuration of the analysis model was established using the SOFISTIK platform, incorporating a comprehensive layout representation. Both the U-girder and Box Girder structures were modelled as finite elements, utilizing the capabilities of the SOFISTIK Software.

The dynamic analysis was conducted employing the modal superposition approach, enabling efficient exploration of various high-speed train models and velocities. The analysis comprised the following steps:

A 2D finite element (FE) model was developed using SOFISTIK to accurately capture the structural and dynamic characteristics of both the U-girder and Box Girder. This model

underwent modal analysis to determine crucial modal features such as vibration modes, natural frequencies, and overall mass distribution.

The results obtained from the SOFISTIK model were utilized to investigate the dynamic behaviour of both structures.

Figures 2.2-2 to 2.2-7 provide a detailed representation of the geometry within the SOFISTIK Model, aimed at encapsulating the dynamic behaviour of both structures. Boundary constraints are depicted in Figure 2.2-1.

2.4.2. ABOUT SOFTWARE

SOFISTIK software is a powerful and specialized tool used in structural engineering for analysis, design, and simulation of complex structures. It provides capabilities for finite element analysis and modelling of various types of structures, including bridges, buildings, and other civil engineering projects. SOFISTIK offers a range of features such as generating finite element models, conducting structural analysis (static, dynamic, and nonlinear), simulating real-world behaviours, and assessing structural integrity. It is known for its capabilities in addressing intricate geometries, material behaviours, and boundary conditions, making it a popular choice in the field of structural engineering.

SOFISTIK software specializes in plate analysis, enabling engineers to model, simulate, and analyse the behaviour of two-dimensional structural plates commonly found in buildings and bridges. It calculates deflections, stresses, and natural frequencies under different loads, aiding in optimizing designs and ensuring structural integrity.

The equation of dynamics is as follows:

$$M\ddot{a} + C\dot{a} + K a = F(t) \qquad (2.1)$$

where,

M represents the mass matrix, C stands for the damping matrix, and K denotes the stiffness matrix. The variables (ä, ȧ, a) correspond to acceleration, velocity, and nodal displacement respectively. Additionally, F (t) signifies the time-dependent load function applied to each node.

The inherent frequencies solely rely on the initial condition of the U-girder, specifically in the absence of dynamic loads, and are computed using:

$$M\ddot{a} + K a = 0 \tag{2.2}$$

With solutions for a harmonic function of time:

$$a = Ø * \sin \omega(T - t0) \tag{2.3}$$

So,

$$K Ø - \omega^2 M * Ø = 0 \tag{2.4}$$

In conjunction with mechanical properties, the dynamic analysis necessitates the incorporation of mass inertia. (Polar inertia * density).

The dynamic response will be computed for a user-specified critical velocity. The user provides the analysis speed as well as the start and end times for the analysis. The software introduces a mobile load along the beam, incorporating changes in train speed. The solution for "a" is as follows:

$$a = Ø * Q \tag{2.5}$$

where,

Ø is Eigen vector

Q is Vector depending on time

The time step integration interval is determined to ensure sufficient accuracy in generating functions for each calculated speed (approximately 0.001 seconds in our scenario).

Main Input Data:

- Geometry of structure
- Density of materials
- Young modulus
- Modulus of inertia
- Train Speed
- Time integration step

Main Output Data:

- Acceleration
- Deflection

2.4.3. LOADS

This section provides detailed insights into the selection process of loading scenarios for the parametric investigation. The aim is to carefully choose relevant loading conditions that cover a wide range of real-world scenarios, while ensuring the analysis remains practical and informative.

The study focuses on dynamic loading scenarios induced by RRTS trains, with particular emphasis on the train's velocity and axle loads. These loading scenarios are derived from actual metro rail networks. A range of train speeds, ranging from 140 to 300 kmph, has been chosen to assess their impact on the dynamic behaviour of both structures.

2.4.3.1 DEAD LOAD

For the calculation of dead load the density of concrete was taken as 2.55 T/m^3.

2.4.3.2 SUPERIMPOSED DEAD LOAD

S.No.	Element	Unfactored Load (t/m)
1	Railing 1m high – 3 Nos (50Kg each - both side & Central)	0.150
2	Both Track structure	6.240
3	Rail Guards between Rails (both tracks)	0.606
4	Rail + Pads (both tracks)	0.300
5	Cables	0.070
6	Cable trays/Hanger	0.100
7	Parapet (Excluding Integral Part of Box)	0.574
8	Walk way cum Cable Trough + Pedestal for Central Railing + Pedestal for OHE Mast	0.920
9	Miscellaneous (OHE Mast, Signaling etc.)	0.400
		9.36 t/m

say	**9.40 t/m**
Fixed	**1.65 t/m** (railing/walkway/Parapet)
Variable	**7.75 t/m**

Table 2.4-1: Super Imposed Dead Load

2.4.3.3 LIVE LOAD

The RRTS Live load will have the following axle configuration.

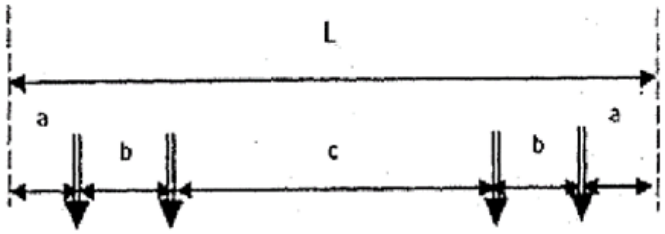

All axle loads = 17 tons

Maximum number of successive cars = 12

Where,

L = 21.340m / 22.340m (Length of a car)

a = 1.920m (overhang)

b = 2.500m (Wheelbase in a bogie)

c = 12.500m / 13.500m (Distance between Axle-2 and Axle-3 in the car)

Maximum Service speed of the Train: 250 kmph

In analysing the RRTS train load model, various speeds up to the highest specified design speed are considered. This maximum design speed is determined to be 1.2 times the maximum permissible speed on the structure. Consequently, the maximum design speed under consideration is calculated as 1.20 multiplied by 250 kmph, resulting in 300 kmph.

It's crucial to emphasize that calculations must be performed for a series of speeds, starting from 140 kmph and progressing up to 300 kmph, with intervals of 5 kmph.

2.4.4. DYNAMIC ANALYSIS

According to Clause 2.4.1.1 of the IRS Bridge Rules, the impact factor is applicable for speeds up to 160 km/h on Broad Gauge. Therefore, a separate dynamic analysis is necessary for vehicles traveling at speeds exceeding 160 km/h.

Clause 6.4 of the BS EN 1991-2 lays out the criteria to carry out dynamic analysis including resonance. The criteria for determining whether a static or dynamic analysis is required are illustrated in Figure 6.9 of BS EN 1991-2, which has been shown below.

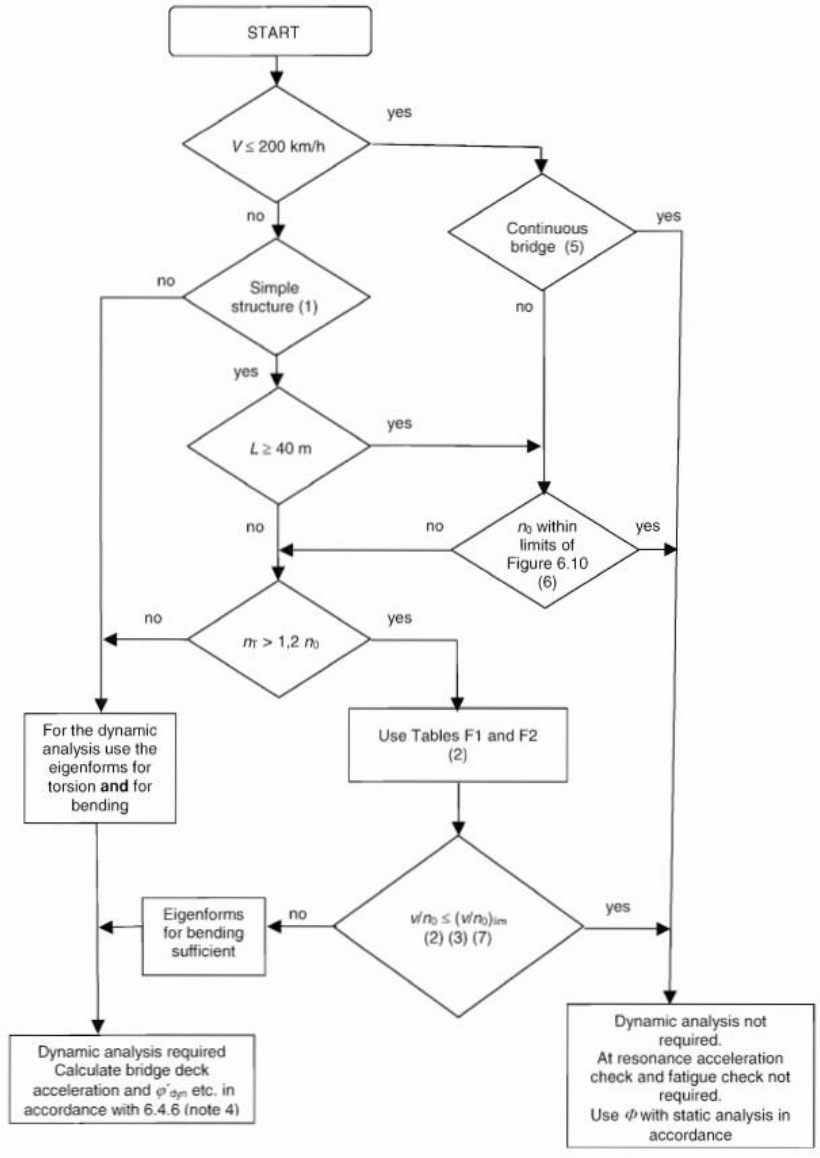

As per note 7 of Cl 6.4.4, BS EN 1991-2, natural frequency limits are calculated.

NOTE 6 For bridges with a first natural frequency n_0 within the limits given by Figure 6.10 and a Maximum Line Speed at the Site not exceeding 200km/h, a dynamic analysis is not required.

NOTE 7 For bridges with a first natural frequency n_0 exceeding the upper limit (1) in Figure 6.10 a dynamic analysis is required. Also see 6.4.6.1.1(7).

The upper limit of n_0 is governed by dynamic enhancements due to track irregularities and is given by :

$$n_0 = 94{,}76L^{-0{,}748} \qquad (6.1)$$

The lower limit of n_0 is governed by dynamic impact criteria and is given by :

$$n_0 = 80/L \quad \text{for } 4\text{m} \le L \le 20\text{m}$$
$$n_0 = 23{,}58L^{-0{,}592} \quad \text{for } 20\text{m} < L \le 100\text{m} \qquad (6.2)$$

where:

n_0 is the first natural frequency of the bridge taking account of mass due to permanent actions,
L is the span length for simply supported bridges or L_Φ for other bridge types.

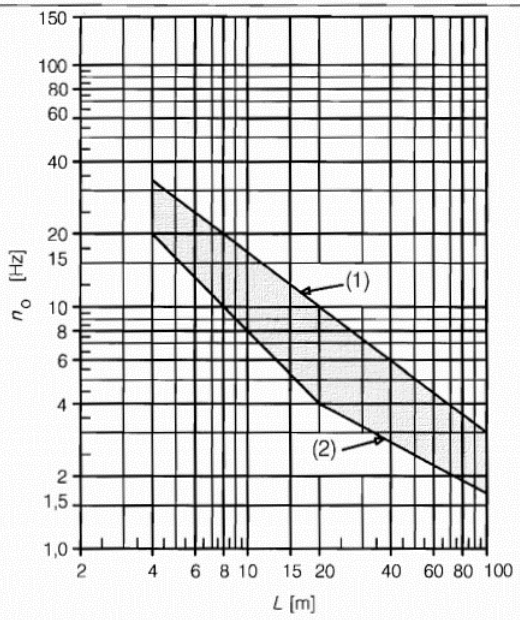

Key
(1) Upper limit of natural frequency
(2) Lower limit of natural frequency

Figure 6.10 - Limits of bridge natural frequency n_0 [Hz] as a function of L [m]

As per Note 8 of Cl 6.4.4, BS EN 1991-2, natural frequency for a simply supported bridge subjected to bending only is shown below.

NOTE 8 For a simply supported bridge subjected to bending only, the natural frequency may be estimated using the formula :

$$n_0\,[\text{Hz}] = \frac{17{,}75}{\sqrt{\delta_0}} \qquad (6.3)$$

where:

δ_0 is the deflection at mid span due to permanent actions [mm] and is calculated, using a short term modulus for concrete bridges, in accordance with a loading period appropriate to the natural frequency of the bridge.

2.4.4.1 TYPE OF ANALYSIS

A time history analysis involving the direct integration of the equation of motion is performed within the SOFISTIK software.

The procedure for time history varies based on the train speed, where each progression involves shifting the train load model forward in increments of 0.001 (Time Step) seconds.

2.4.4.2 STRUCTURAL DAMPING

The table below provides the prescribed damping values to be employed in the dynamic analysis.

Bridge Type	ζ Lower limit of percentage of critical damping [%]	
	Span L < 20m	Span $L \geq$ 20m
Steel and composite	$\zeta = 0{,}5 + 0{,}125\ (20 - L)$	$\zeta = 0{,}5$
Prestressed concrete	$\zeta = 1{,}0 + 0{,}07\ (20 - L)$	$\zeta = 1{,}0$
Filler beam and reinforced concrete	$\zeta = 1{,}5 + 0{,}07\ (20 - L)$	$\zeta = 1{,}5$

Figure 2.4-1: Structural Damping Calculation.

The span length of the structure is more than 20m, thus damping of 1.0% will be used for pre-stressed concrete. Additional damping is calculated according to EN1991-2 art 6.4.6.4.the damping can be increased for spans shorter than 30 m by:

$$\Delta\zeta = \frac{0.0187L - 0.00064L^2}{1 - 0.0441L - 0.0044L^2 + 0.000255L^3}\,[\%] \tag{2.6}$$

$$\zeta + \Delta\zeta = D\% \tag{2.7}$$

In the Time History Analysis, the Rayleigh damping coefficients are computed for both the initial vertical Eigen frequency and the maximum value between 30 Hz, 1.5 times the first Eigen frequency (f1), and the third Eigen frequency (f3) = 30 Hz.

$$\alpha = \frac{\zeta 4\pi f_1 f_2}{f_1 + f_2} \tag{2.8}$$

$$\beta = \frac{\zeta}{\pi(f_1 + f_2)} \tag{2.9}$$

2.4.5. HIGH SPEED TRAIN MODEL

2.4.5.1 TRAIN MODEL

The Dynamic analysis is caried out using characteristic value of the loading from RRTS train having 12 number of bogies. The selection of rail trains considers each train formation for the highest permitted or planned speeds up to 250 km/h (Design Speed = 1.2 x 250 = 300 kmph)

The Characteristic of the Train loads are given below:

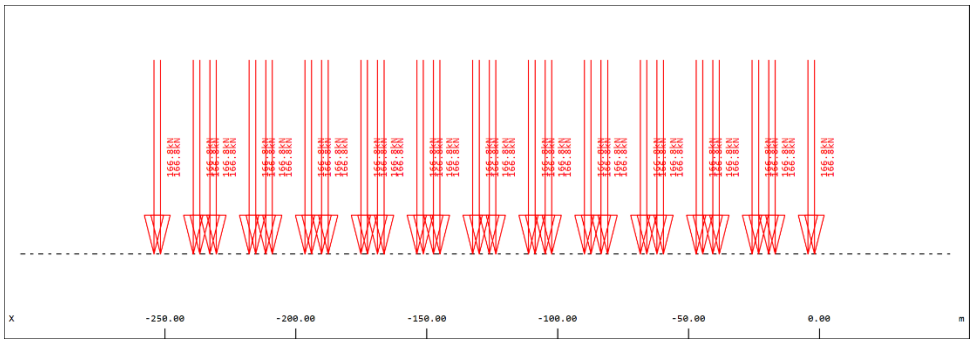

Figure 2.4-2: RRTS Train for 21.34m Bogie Length

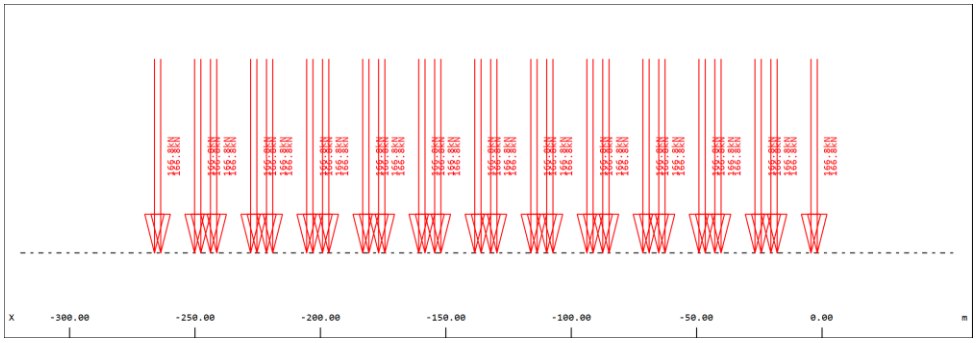

Figure 2.4-3: RRTS Train for 22.34m Bogie Length

2.4.5.2 SPEED TO BE CONSIDERED

For each train model of specified bogie, maximum design speed is considered.

Maximum Design Speed for RRTS = 300 [kmph] = 83.33 [m/s]

The dynamic analysis is done with speed increment of 5 kmph.

As per Note 5 of Clause no. 6.4.6.2 of EN 1991-2-2003, Maximum design speed shall be 1.2 times of the maximum commissioning speed.

NOTE 5 It is recommended that the individual project specify additional requirements for checking structures where there is a requirement for a section of line to be suitable for commissioning tests of a Real Train. The Maximum Design Speed used for the Real Train should be at least 1,2 × Maximum Train Commissioning Speed. Calculations are required to demonstrate that safety considerations (maximum deck accelerations, maximum load effects, etc.) are satisfactory for structures at speeds in excess of 200 km/h. Fatigue and passenger comfort criteria need not be checked at 1,2 × Maximum Train Commissioning Speeds.

2.4.6. VERIFICATION

The dynamic analysis allows performing the following verifications.

2.4.6.1 ACCELERATION CHECKING:

According to Cl. A2.4.4.2.1(4), BS EN 1990+A1, the maximum acceleration allowed is 5.0 m/s^2 (for direct fastened tracks with track and structural elements designed for high-speed traffic)

2.4.6.2 DEFLECTION CHECKING:

According to Cl. A2.4.4.3.2(3), BS EN 1990+A1, a specific dynamic calculation should be carried out to verify the deflection criterion for passenger comfort.

According to Cl. A2.4.4.3.2(5), BS EN 1990+A1, for a bridge comprising of either a single span or a succession of two simply-

supported span, the values of $\frac{L}{\delta}$ shall be multiplied by a factor of 0.7.

$$d_{max} = \frac{L}{0.7\ x\ \delta}$$

2.4.7. VALIDATION

2.4.7.1 INTRODUCTION

This chapter is centred around the validation of the methodology employed to conduct dynamic analysis on U-girders and Box Girder experiencing RRTS loading. The chapter's outset entails an overview of the validation procedure, elaborating on the juxtaposition between numerical findings extracted from the work by Shaikh et al. (2021) and outcomes derived from accessible software. The contrasts and parallels between numerical results and empirical data are visually illustrated through graphical representations. An in-depth scrutiny of the concurrences or disparities within these comparisons ensues, culminating in an evaluation of the method's precision and dependability in terms of accuracy and reliability.

2.4.7.2 MODEL SPECIFICATION

To verify the accuracy of the transient analysis technique employed, a study was conducted on a plate that was simply supported at its ends and exposed to a moving force acting on two opposing edges, as depicted in Figure 2.4-4. The validation process involved the utilization of the SOFISTIK Workbench for modelling and assessment. The ensuing details provide an overview of the material properties and attributes of the dynamic force being applied:

- Force = 4.4482 N,
- Speed of force=96.56 km/h.
- Density=2400 kg/m3.
- Young’s Modulus of Elasticity (E) =20,684.4 MPa.
- Poisson’s ratio=0.15.

- Plate thickness=0.4572 m.
- Plate (length x width) =6.096 m.

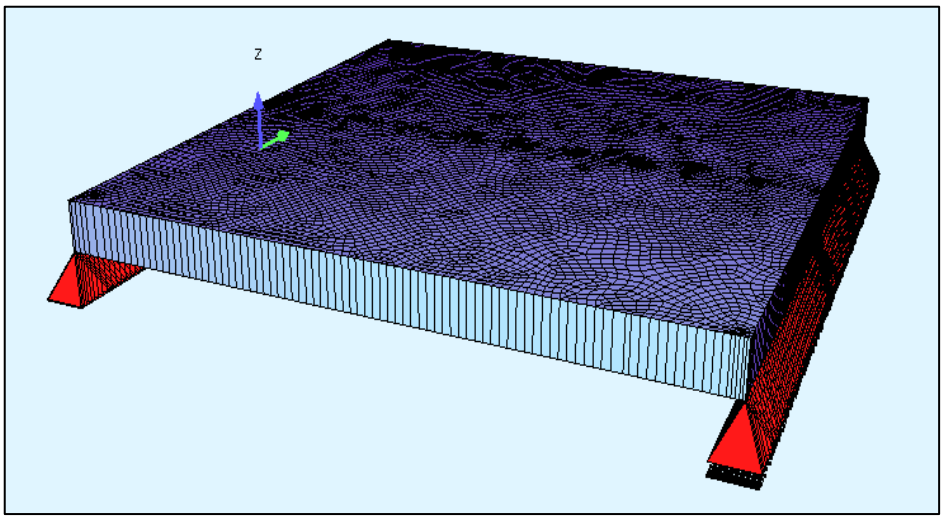

Figure 2.4-4: FEM model of a simply supported plate.

2.4.7.3 ANALYSIS OF VALIDATION RESULTS

The validation outcomes of the technique employed for dynamic analysis of the U-girder under metro rail loading hold utmost significance in gauging the precision and dependability of the model. Illustrated in Figure 25 is the dynamic response of the plate when subjected to an operational force, portrayed through normalized mid-span displacements. The normalized mid-span displacement signifies “the ratio of the dynamic displacement at mid span to the greatest static displacement at mid span when the load is applied at any point along the span”. The present findings are juxtaposed with the research by *Mohammad Farhan Shaikh* and *K. Nallasivam (2023)*, who employed the finite element method to analyse the model the connection between the normalized mid-span displacement and the normalized vehicle position across the plate's span is delineated in Figure 2.4-5. The graphical representation distinctly reveals the substantial alignment between the numerical outcomes and the previous research. The data displayed in the

graph effectively validate the precision and applicability of the finite element method.

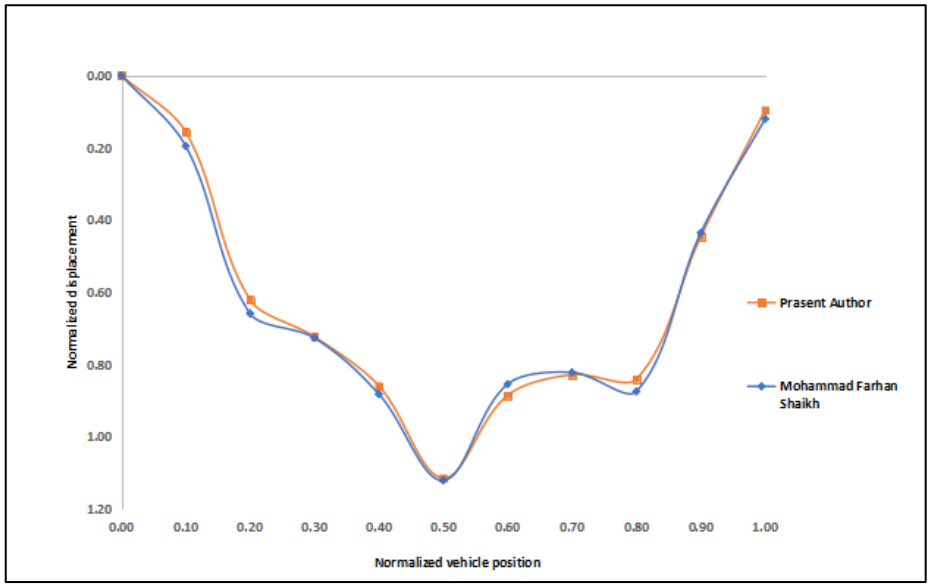

Figure 2.4-5: Normalized displacement at the centre of simply supported plate

2.4.7.4 CONCLUSION

The graph visibly demonstrates a notable alignment with the reference research (*Shaikh et al.),* exhibiting a mere 0.54% error rate. The thorough assessment of the method validation outcomes affirms with confidence that the technique utilized for the dynamic analysis of the U-girder and Box Girder stands as valid and proficient in accurately anticipating its dynamic response under RRTS loading conditions. The insights garnered from this verified model establish a robust groundwork for the extensive exploration of diverse parameters and their impact on the structure's dynamic behaviour. This validated approach forms the core for delving into various parameters in the parametric investigation, as expounded upon in Chapter 3.

CHAPTER 3: ANALYSIS, RESULTS & INTERPRETATION

3.1. RESULTS

This section presents the outcomes of a detailed dynamic analysis of U-girder and Box Girder under RRTS loading. The investigation systematically varied key factors such as cross-sectional geometry, span arrangement and Live load. To ensure the accuracy and reliability of the research, the methodology underwent rigorous validation. The findings from the parametric study are assessed with respect to their implications for structural design and safety.

Iterations for various cross sections, live load for different spans i.e. 28m, 26m, 23m, 20m have been done to ascertain the behavior of U-Girder and Box Gider.

3.1.1. CONTROL POINTS

The results for accelerations and deflections are studied at the mid span.

3.1.2. STRUCTURAL DAMPING.

The Peak response of the structure at traffic speeds corresponding to resonant loading is highly dependent upon damping. The Structural and additional damping for spans less than 30m has been shown below, following which the total damping has been considered.

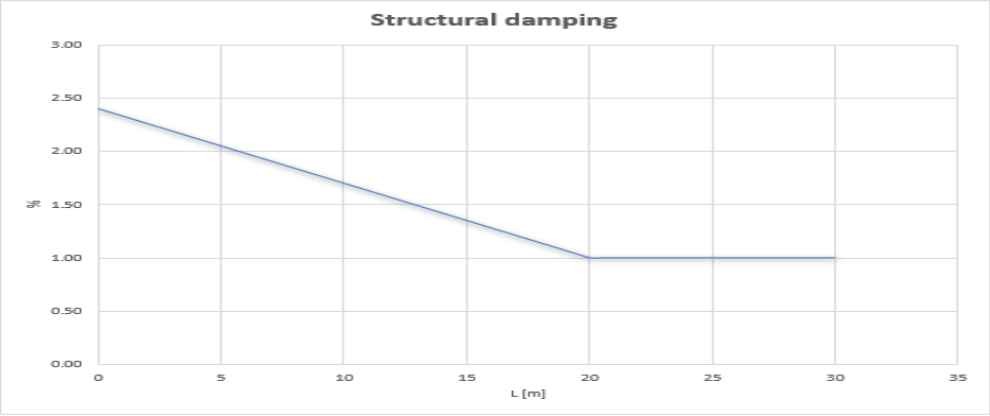

Figure 3.1-1: Structural Damping

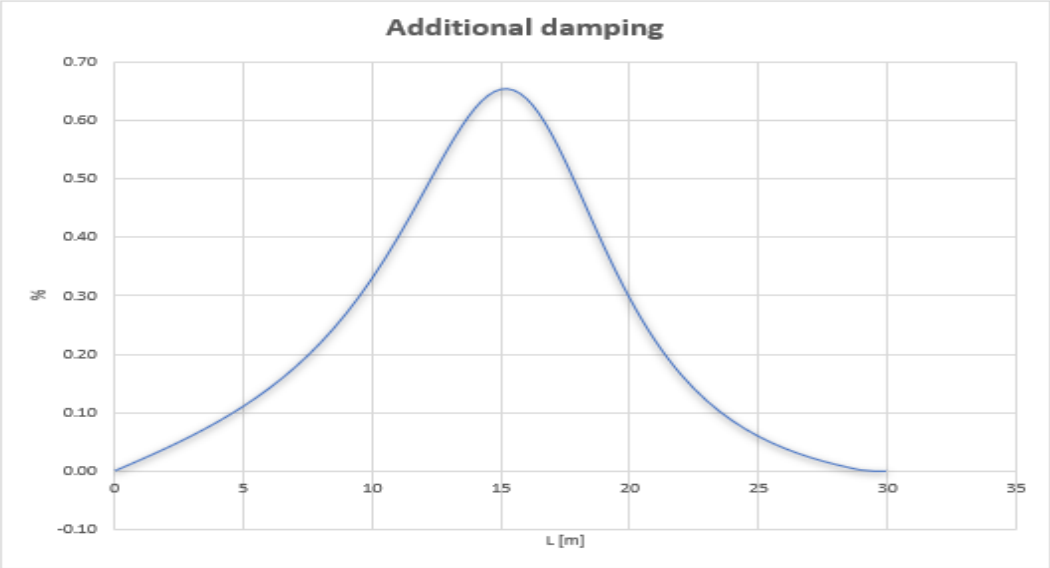

Figure 3.1-2: Additional Damping

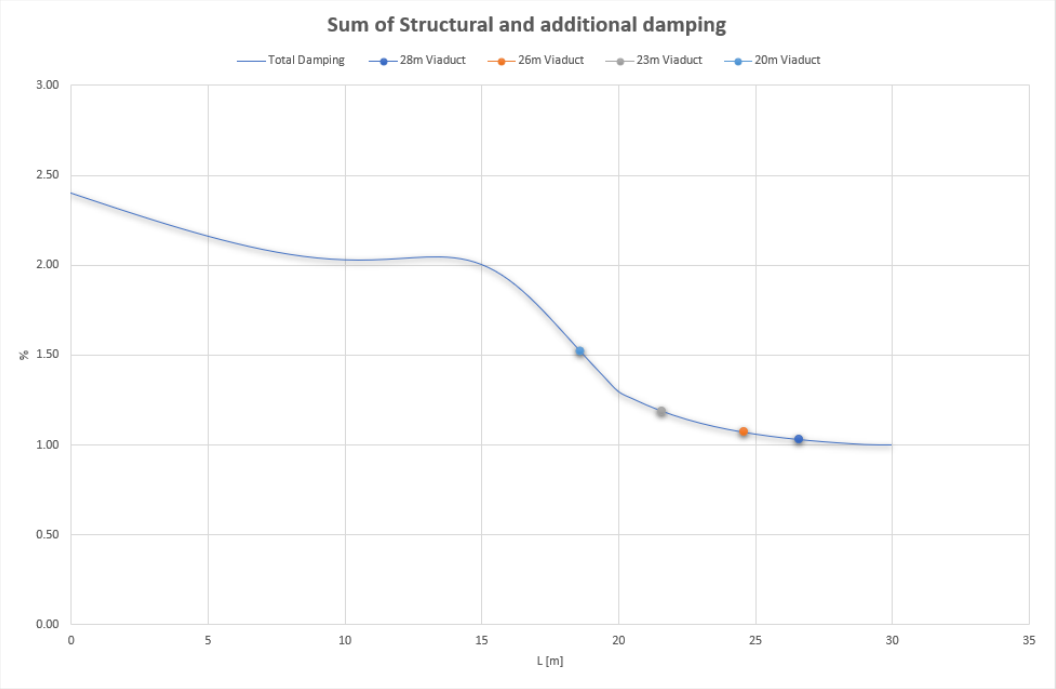

Figure 3.1-3: Damping Considered

3.1.3. DYNAMIC ANALYSIS REQUIREMENT

The table below presents the requirements for dynamic analysis as outlined in Section 2.4.4 of this report.

Details	**U-Girder**				**Box Girder**			
Span	28m	26m	23m	20m	28m	26m	23m	20m
Deflection due to Permanent loads	16.9	16.22	14.11	12.21	14.34	13.26	10.53	8.01
First natural bending frequency as per code n_0	4.32	4.41	4.73	5.08	4.69	4.87	5.47	6.27
First natural frequency from SOFISTIK	4.33	4.59	4.66	5.02	4.55	4.74	5.30	6.06
First Torsional frequency from SOFISTIK	14.39	16.09	18.86	22.83	14.55	15.53	16.99	18.37
n_0 upper limit $= 94.76*L^{-0.748}$	7.84	8.28	9.08	10.08	7.84	8.28	9.08	10.08
n_0 lower limit $= 80/L$ for $4m \leq L \leq 20m$ $= 23.58*L^{-0.592}$ for $20m < L \leq 100m$	3.28	3.43	3.68	4.00	3.28	3.43	3.68	4.00
	Dynamic Analysis Required.	Dynamic Analysis Required.	Dynamic Analysis Required.	Dynamic Analysis Required.	Dynamic Analysis Required.	Dynamic Analysis Required.	Dynamic Analysis Required.	Dynamic Analysis Required.
1.2 x n_0	5.20	5.51	5.59	6.02	5.46	5.69	6.36	7.27
	Dynamic Analysis Required.	Dynamic Analysis Required.	Dynamic Analysis Required.	Dynamic Analysis Required.	Dynamic Analysis Required.	Dynamic Analysis Required.	Dynamic Analysis Required.	Dynamic Analysis Required.
v/n0	19.25	18.15	17.90	16.60	18.30	17.59	15.71	13.75
$v/(n_0)_{lim}$	10.20	10.20	7.08	7.08	10.63	10.63	7.50	7.50
	Dynamic Analysis Required.	Dynamic Analysis Required.	Dynamic Analysis Required.	Dynamic Analysis Required.	Dynamic Analysis Required.	Dynamic Analysis Required.	Dynamic Analysis Required.	Dynamic Analysis Required.

Table 3.1-1: Dynamic Analysis Requirement

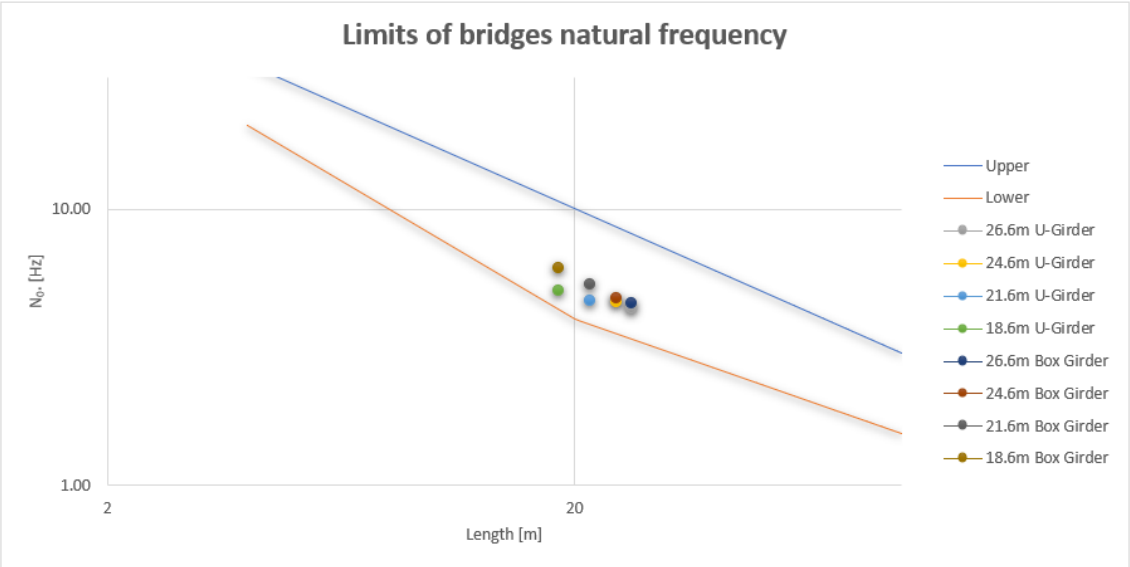

It can be inferred from the above table and section 2.2 that the boundary conditions are considered to be Simply Supported and the length of the span is less than 40m following which the First Torsional frequency is less than 1.2 time of natural frequency obtained.

Therefore, Dynamic analysis is required for given structural configuration.

3.1.4. ANALYSIS: U-GIRDER

The Analysis results such as acceleration and deformation for various spans are shown below:

3.1.4.1 28m SPAN: EXPLORING DEPTH OF SECTION REQUIRED.

The section considered for 28m span is shown below where the depth of the U-Girder is considered to be 2.35m.

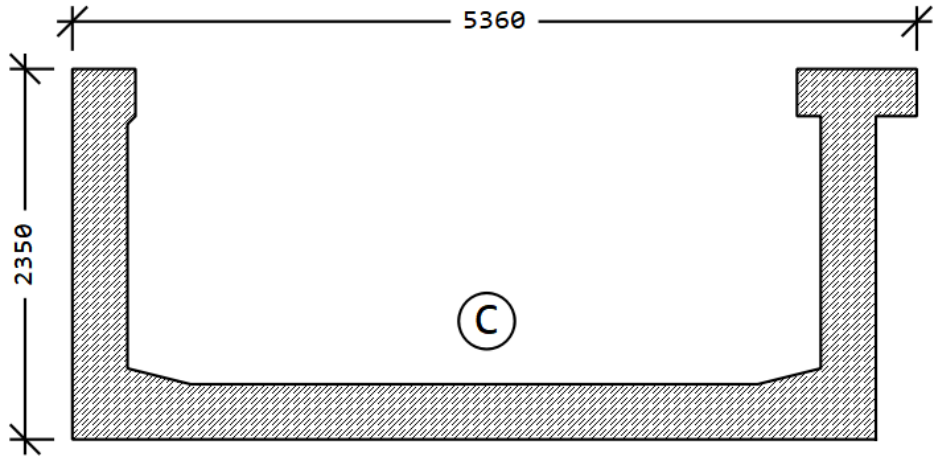

Figure 3.1-4: Cross Section-2.35m

Cross Section Properties:

Static properties of cross section

SNo	Mat MRf	A[m2] It[m4]	Ay[m2] Az[m2] Ayz[m2]	Iy[m4] Iz[m4] Iyz[m4]	yc[mm] zc[mm]	ysc[mm] zsc[mm]	E[N/mm2] G[N/mm2]	g[kg/m]	I-1[m4] I-2[m4] α[°]
1	10	3.3643E+00	1.493E+00	1.878E+00	2.6	-116.0	35000	8410.6	1.278E+01
	20[1]	1.461E-01	1.092E+00	1.277E+01	-750.2	645.2	15217	(BEAM)	1.864E+00
				3.909E-01					-87.95

= U-Girder

[1] No valid reinforcements are defined

SNo	section number	yc[mm],zc[mm]	ordinate of elastic centroid
Mat	material number	ysc[mm],zsc[mm]	ordinate of shear centre
A[m2]	sectional area	E[N/mm2]	Young's modulus
Ay[m2],Az[m2],Ayz[m2]	transverse shear deformation area	g[kg/m]	mass per length
Iy[m4],Iz[m4],Iyz[m4]	bending moment of inertia		
I-1[m4],I-2[m4],α[°]	principal moments of inertia and angle of the principal axes		
MRf	reinforcement material number		
It[m4]	torsional moment of inertia		
G[N/mm2]	Shear modulus		

Acceleration:

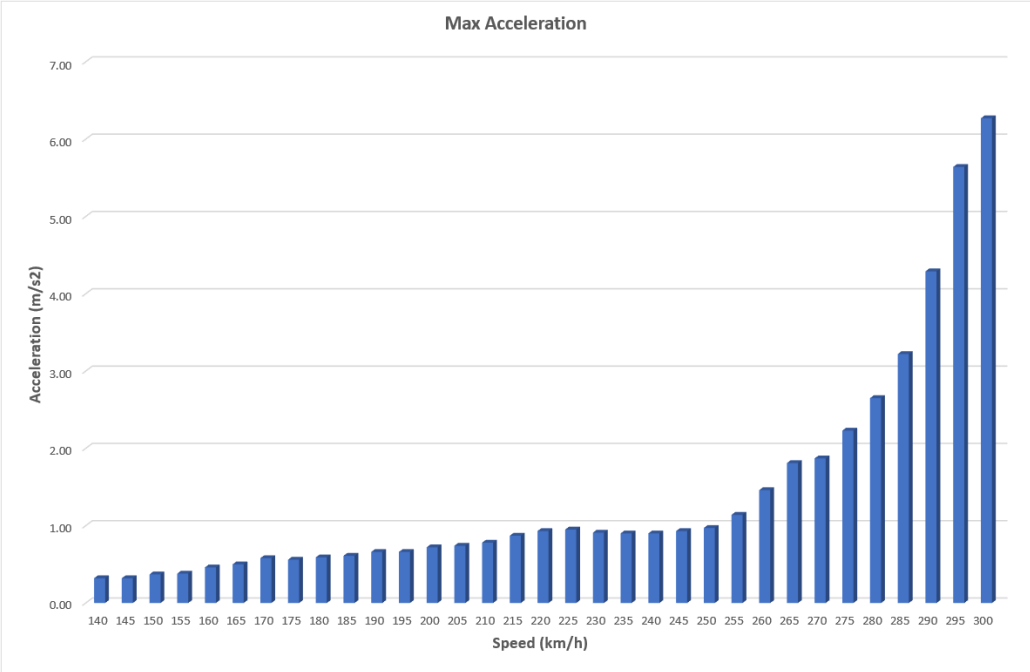

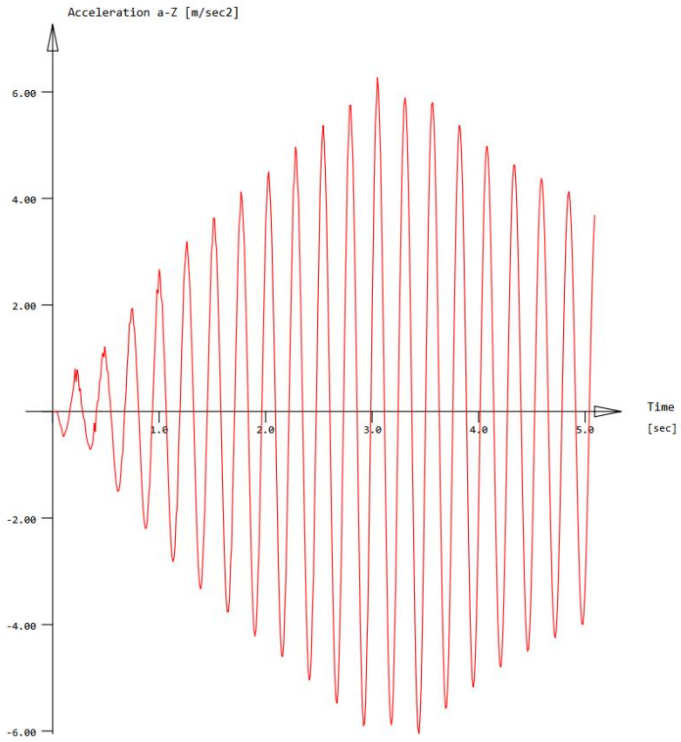

Figure 3.1-5: Maximum acceleration 28m span.

Deformation:

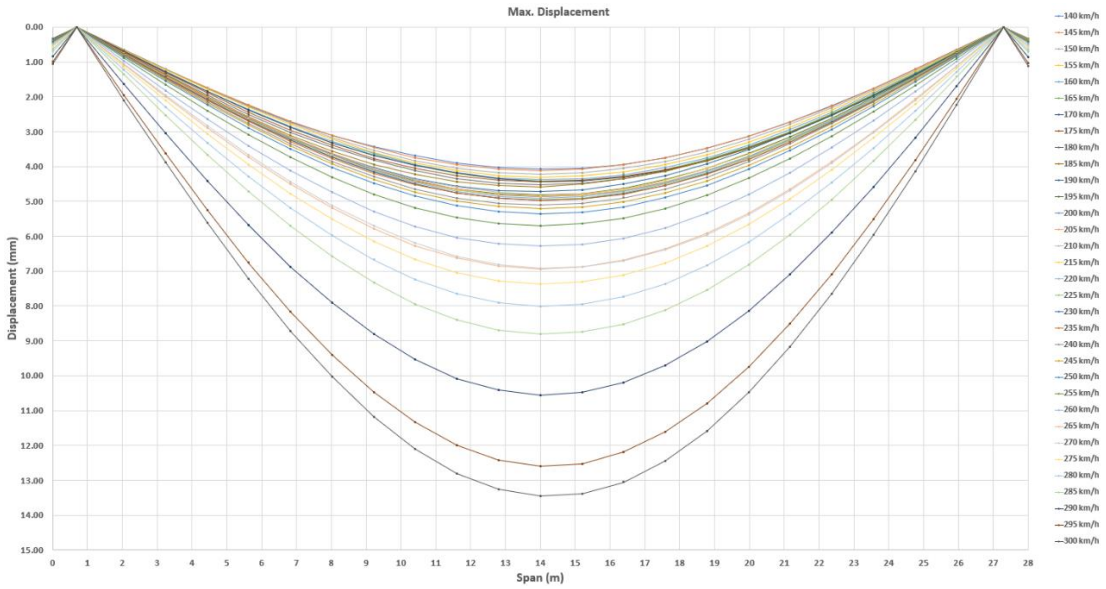

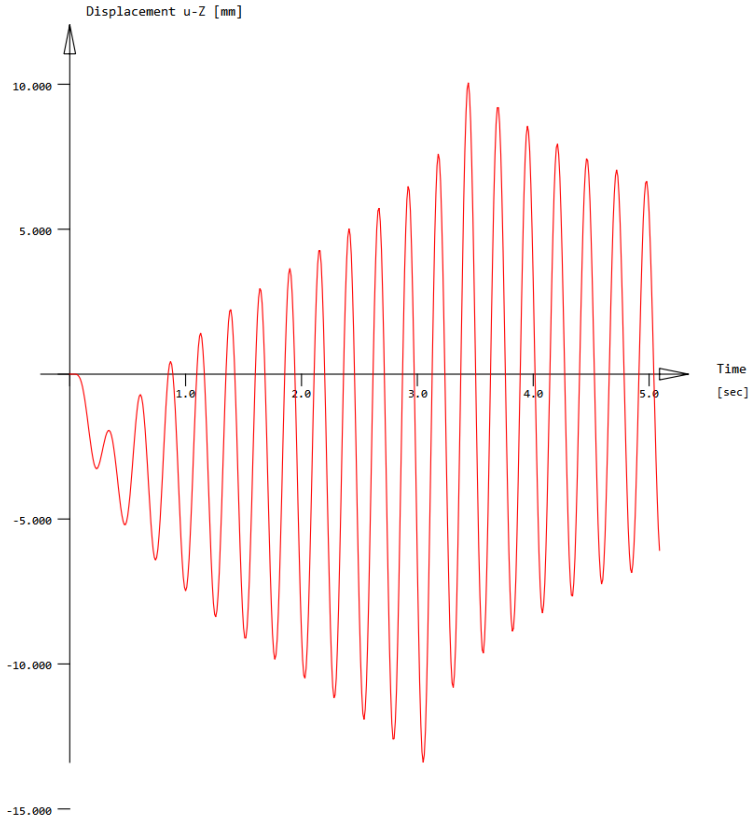

Figure 3.1-6: Maximum deformation 28m span.

3.1.4.2 28m SPAN

Analysis performed for RRTS Bogie Length – 21.34m

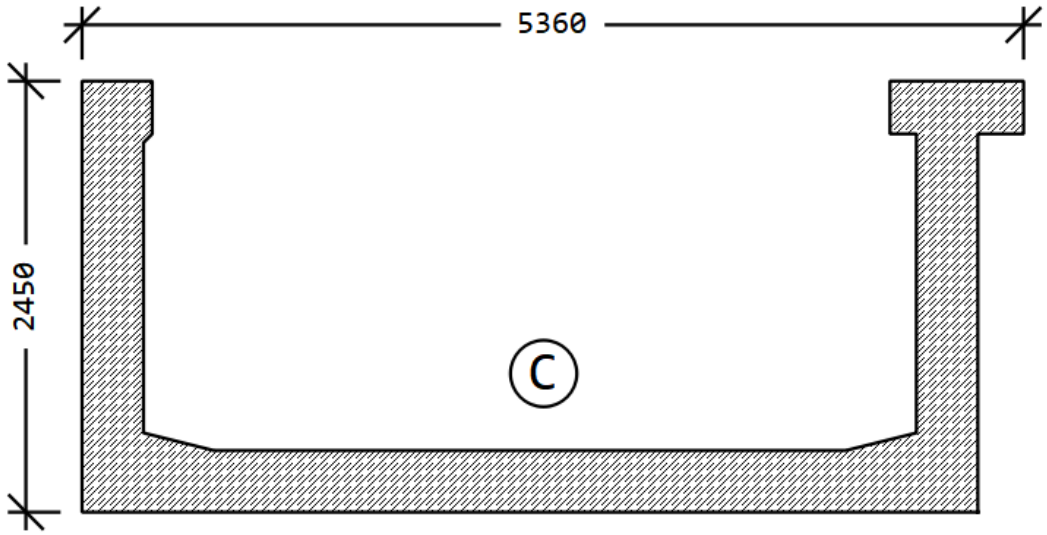

Figure 3.1-7: Cross Section-2.45m

Cross Section Properties:

Static properties of cross section

SNo	Mat	A[m2]	Ay[m2]	Iy[m4]	yc[mm]	ysc[mm]	E[N/mm2]	g[kg/m]	I-1[m4]
	MRf	It[m4]	Az[m2]	Iz[m4]	zc[mm]	zsc[mm]	G[N/mm2]		I-2[m4]
			Ayz[m2]	Iyz[m4]					α[°]
1	10	3.4343E+00	1.480E+00	2.105E+00	4.2	-110.2	35000	8585.6	1.318E+01
	20[1]	1.490E-01	1.155E+00	1.317E+01	-787.9	692.0	15217	(BEAM)	2.090E+00
				4.077E-01					-87.89
= U-Girder									

[1] No valid reinforcements are defined

SNo	section number	yc[mm],zc[mm]	ordinate of elastic centroid
Mat	material number	ysc[mm],zsc[mm]	ordinate of shear centre
A[m2]	sectional area	E[N/mm2]	Young's modulus
Ay[m2],Az[m2],Ayz[m2]	transverse shear deformation area	g[kg/m]	mass per length
Iy[m4],Iz[m4],Iyz[m4]	bending moment of inertia		
I-1[m4],I-2[m4],α[°]	principal moments of inertia and angle of the principal axes		
MRf	reinforcement material number		
It[m4]	torsional moment of inertia		
G[N/mm2]	Shear modulus		

Acceleration:

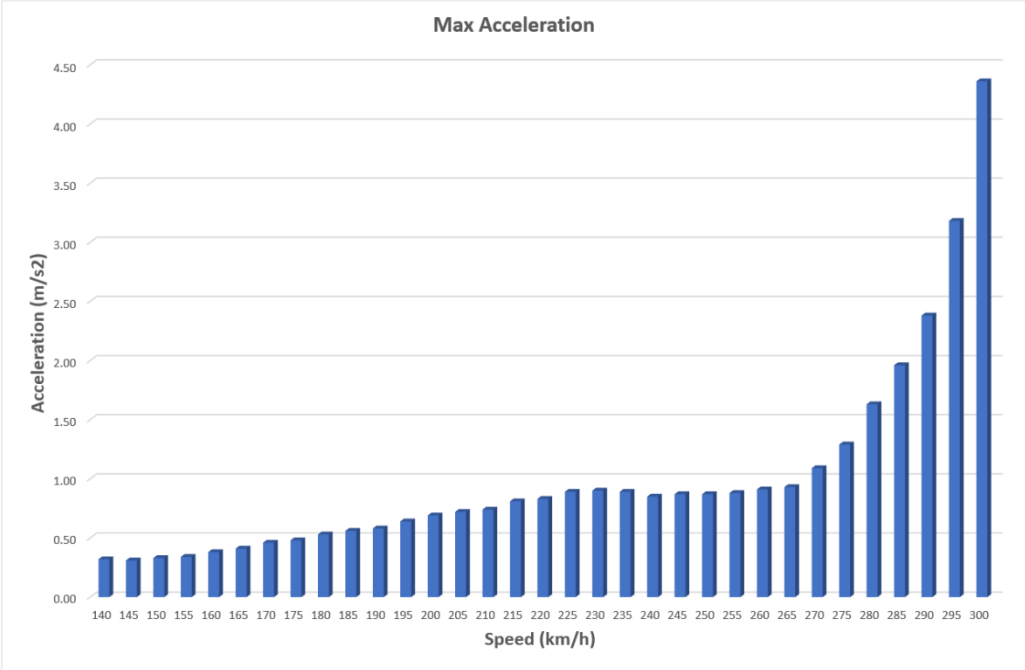

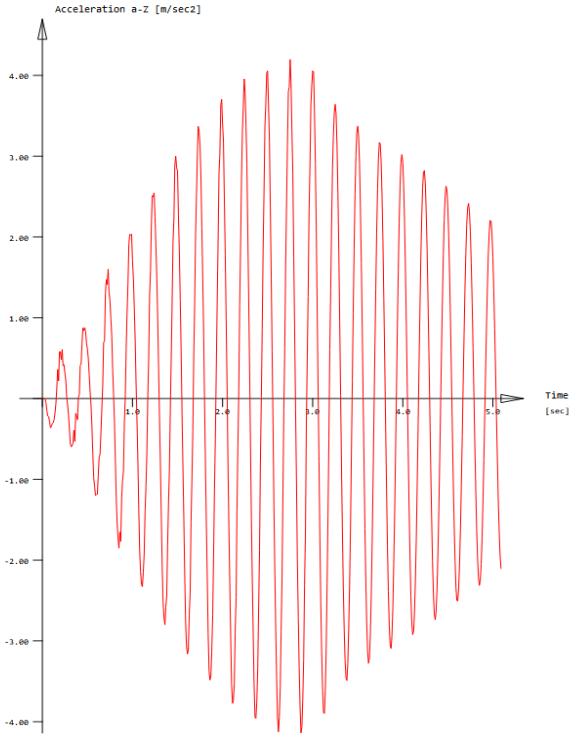

Figure 3.1-8: Maximum acceleration 28m span.

Deformation:

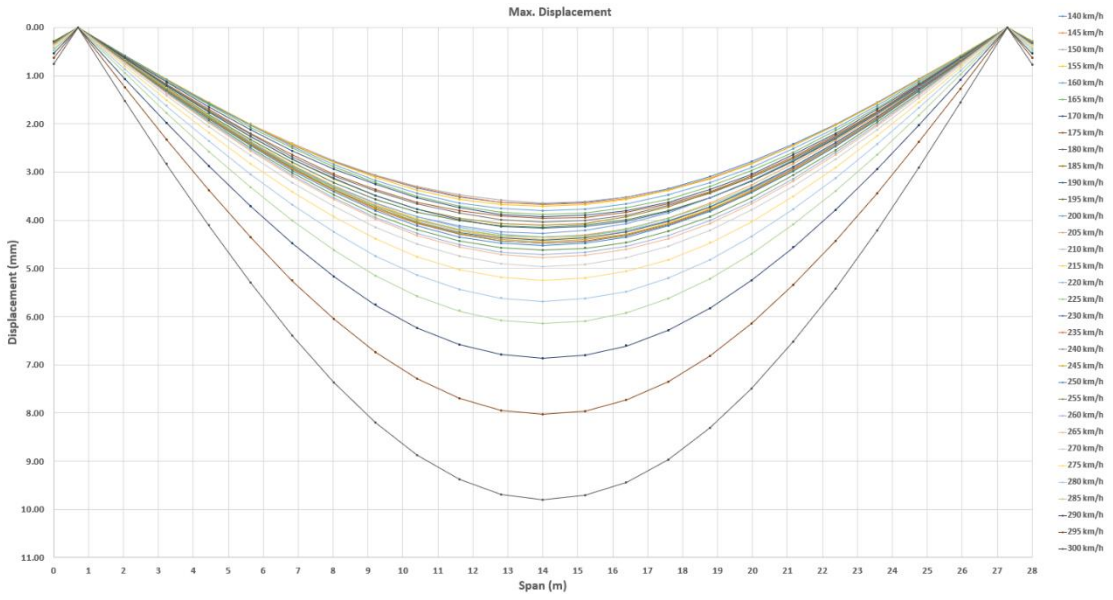

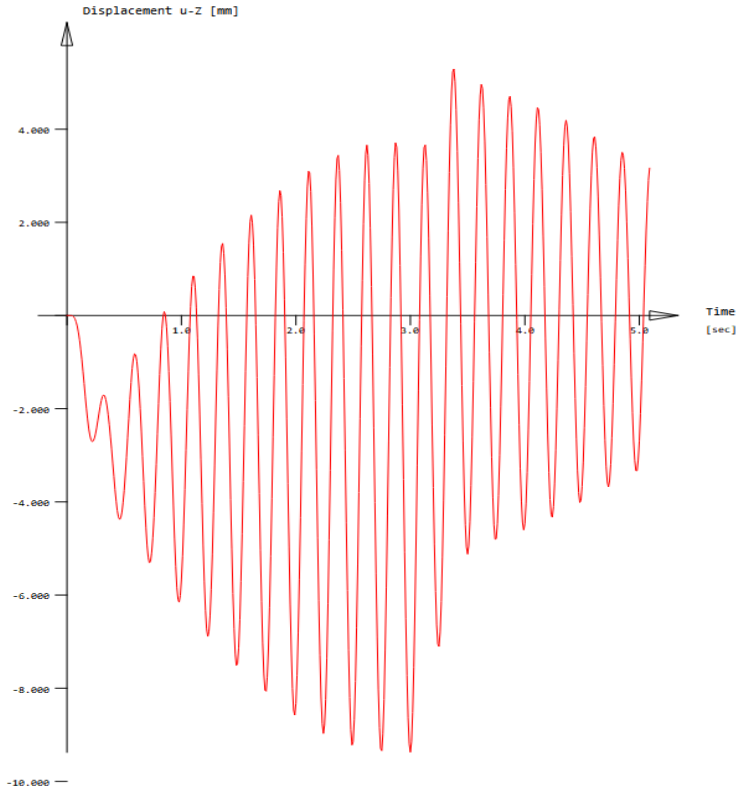

Figure 3.1-9: Maximum deformation 28m span.

Analysis performed for RRTS Bogie Length – 22.34m

Acceleration:

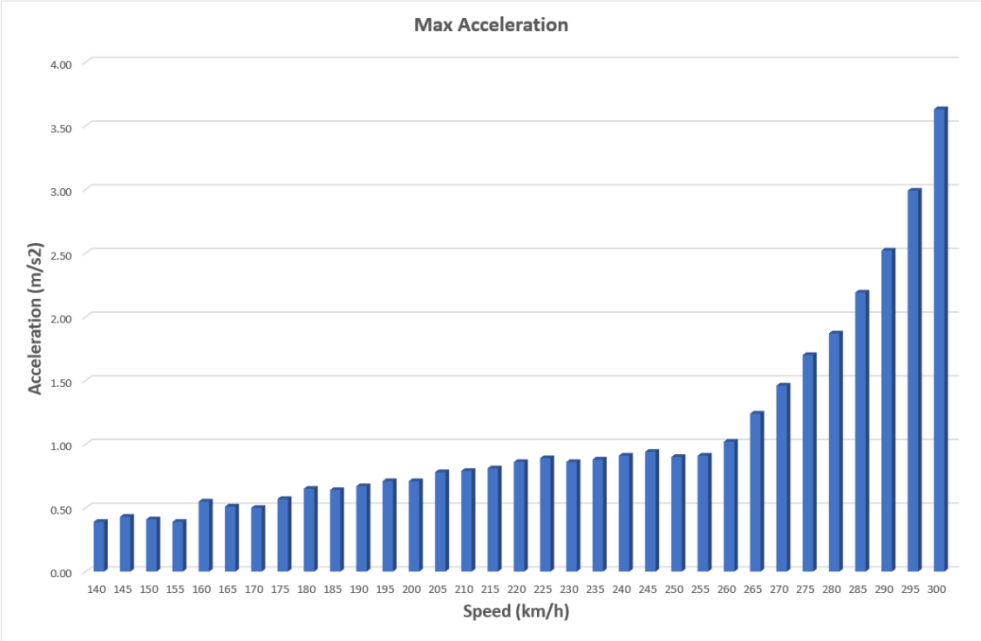

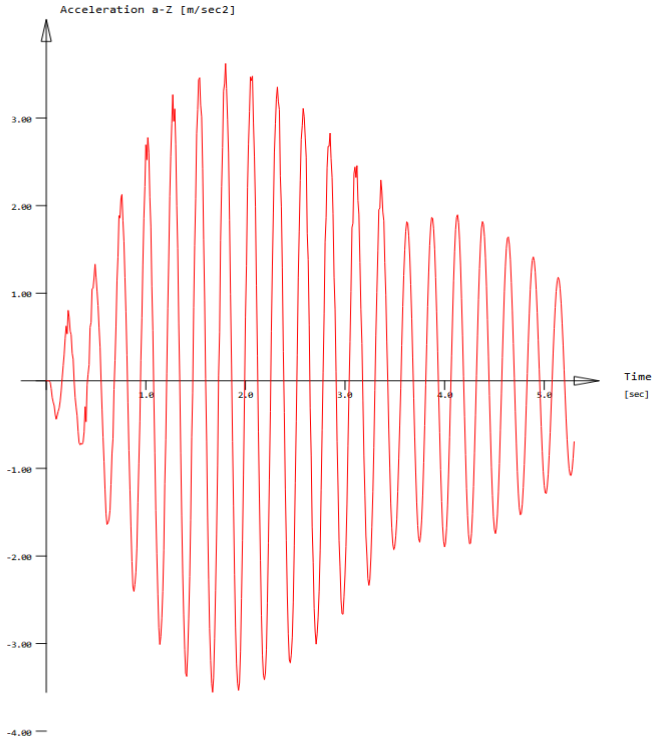

Figure 3.1-10: Maximum acceleration 28m span.

Deformation:

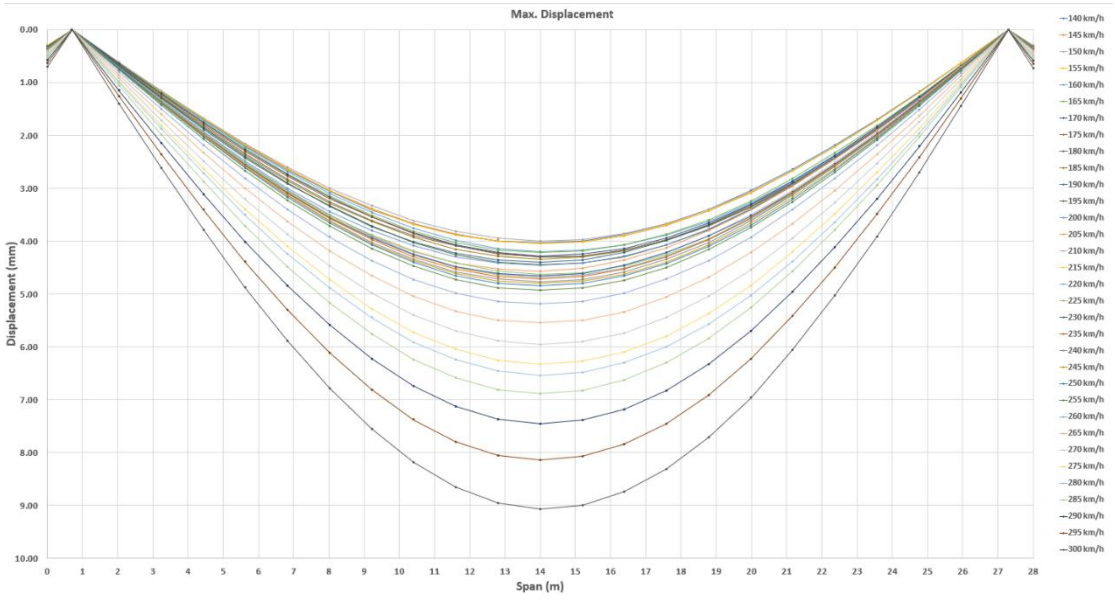

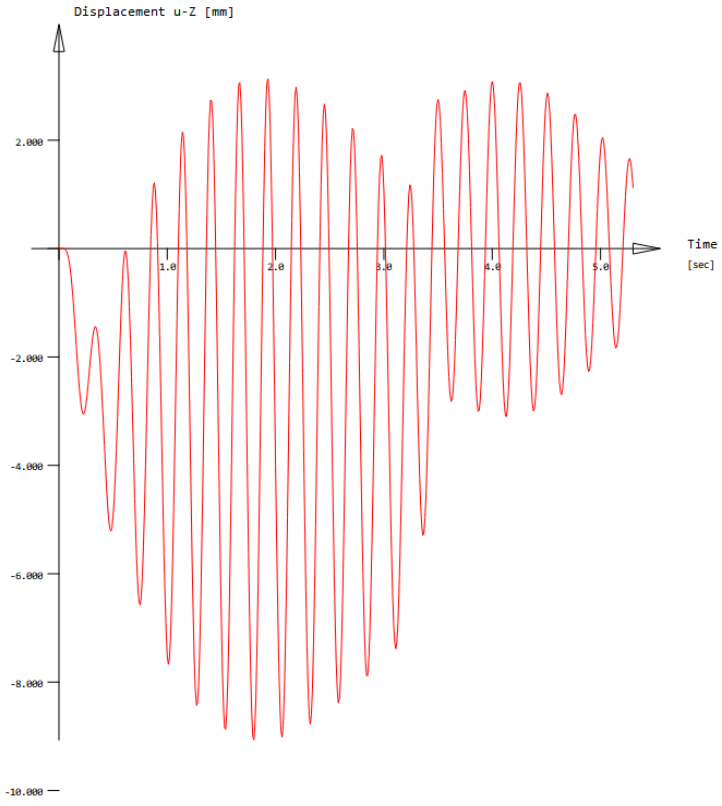

Figure 3.1-11: Maximum deformation 28m span.

3.1.4.3 26m SPAN

Analysis performed for RRTS Bogie Length – 21.34m

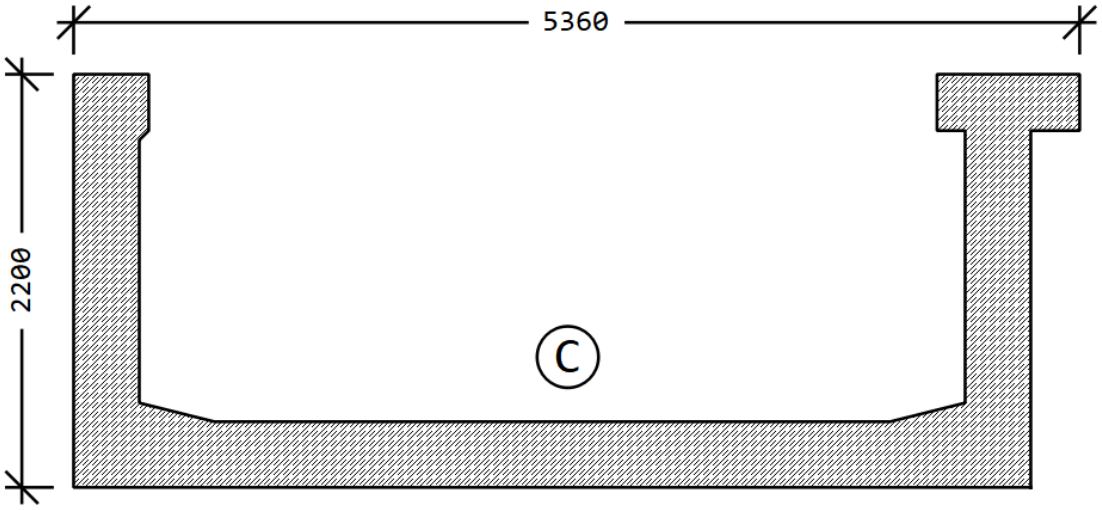

Figure 3.1-12: Cross Section-2.2m

Cross Section Properties:

Static properties of cross section

SNo	Mat MRf	A[m2] It[m4]	Ay[m2] Az[m2] Ayz[m2]	Iy[m4] Iz[m4] Iyz[m4]	yc[mm] zc[mm]	ysc[mm] zsc[mm]	E[N/mm2] G[N/mm2]	g[kg/m]	I-1[m4] I-2[m4] α[°]
1	10	3.2593E+00	1.513E+00	1.566E+00	0.0	-125.6	35000	8148.1	1.219E+01
	20[1]	1.417E-01	9.988E-01	1.218E+01	-694.7	575.4	15217	(BEAM)	1.553E+00
				3.655E-01					-88.03
= U-Girder									

[1] No valid reinforcements are defined

SNo	section number	yc[mm],zc[mm]	ordinate of elastic centroid
Mat	material number	ysc[mm],zsc[mm]	ordinate of shear centre
A[m2]	sectional area	E[N/mm2]	Young's modulus
Ay[m2],Az[m2],Ayz[m2]	transverse shear deformation area	g[kg/m]	mass per length
Iy[m4],Iz[m4],Iyz[m4]	bending moment of inertia		
I-1[m4],I-2[m4],α[°]	principal moments of inertia and angle of the principal axes		
MRf	reinforcement material number		
It[m4]	torsional moment of inertia		
G[N/mm2]	Shear modulus		

Acceleration:

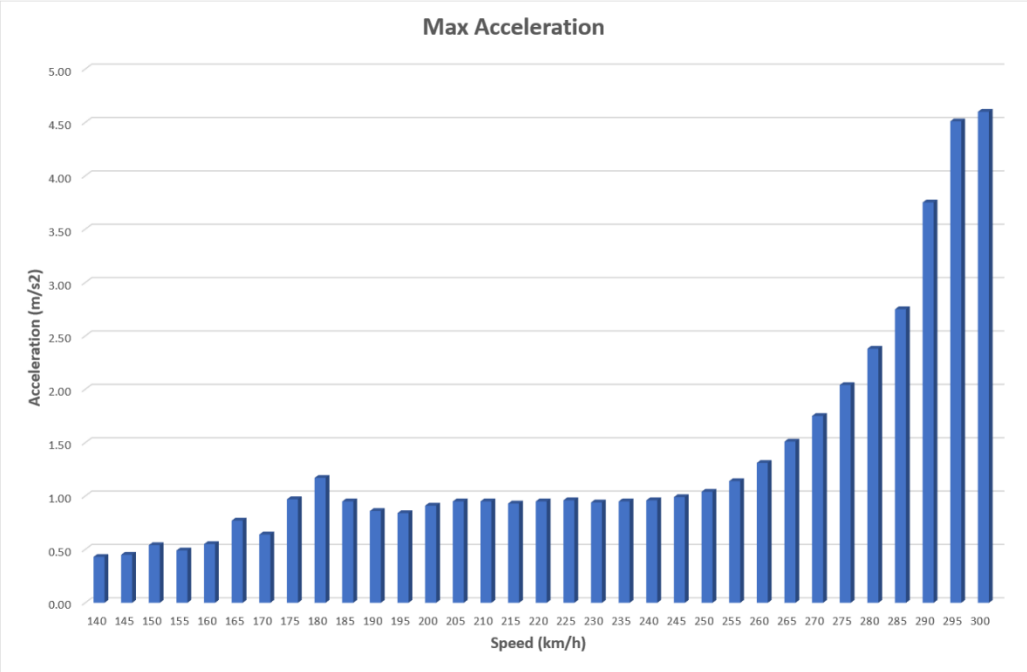

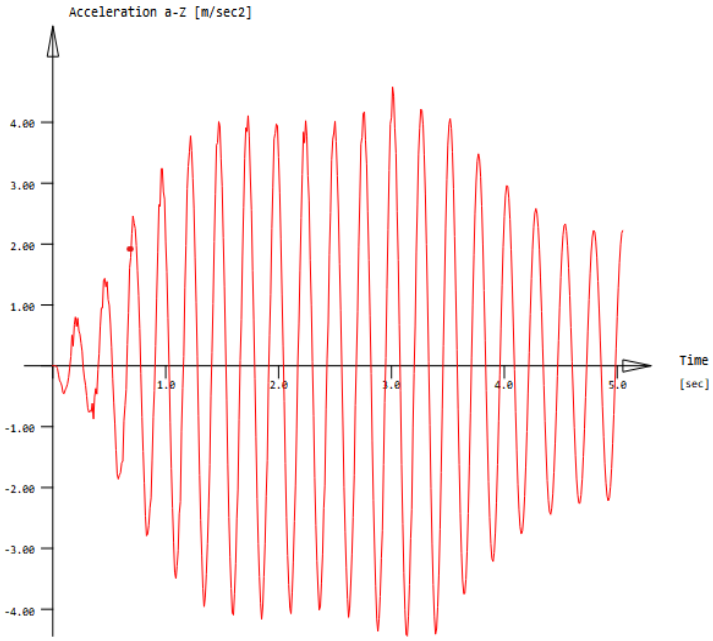

Figure 3.1-13: Maximum acceleration 26m span.

Deformation:

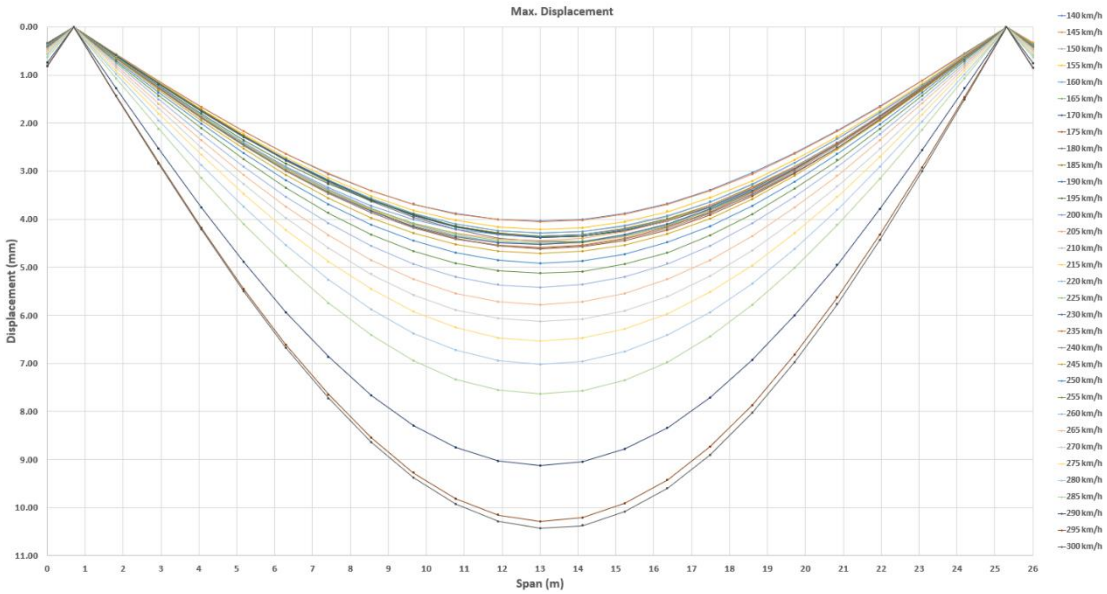

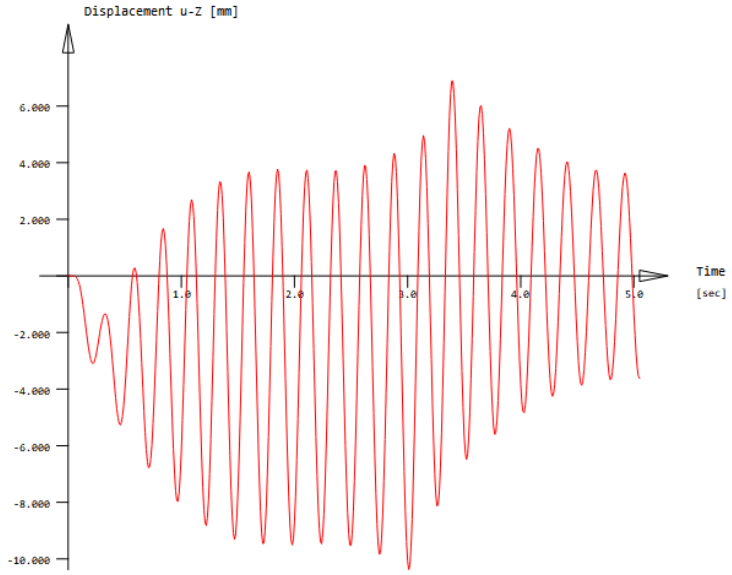

Figure 3.1-14: Maximum deformation 26m span.

Analysis performed for RRTS Bogie Length – 22.34m

Acceleration:

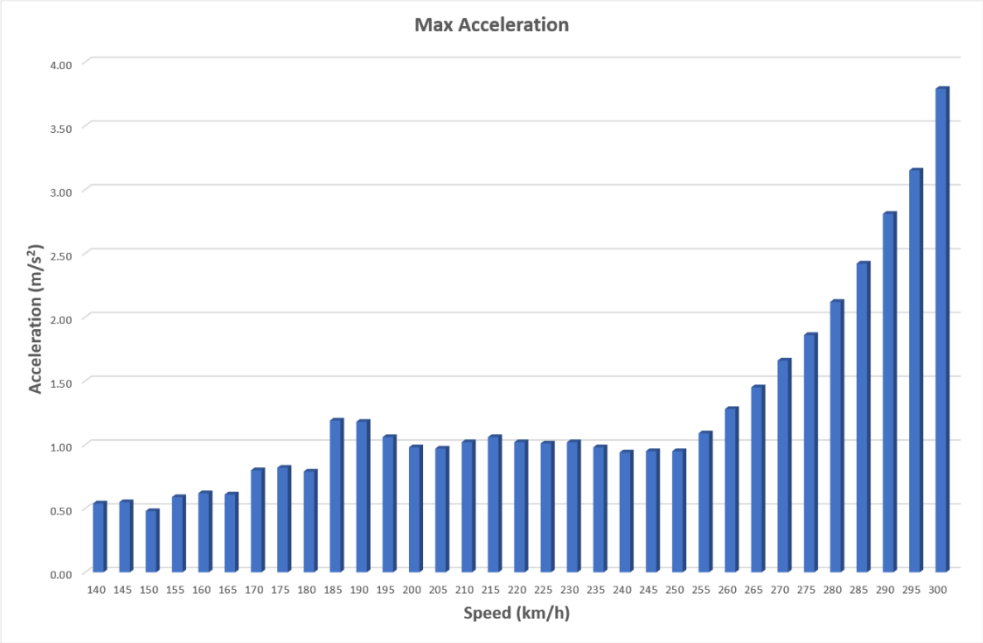

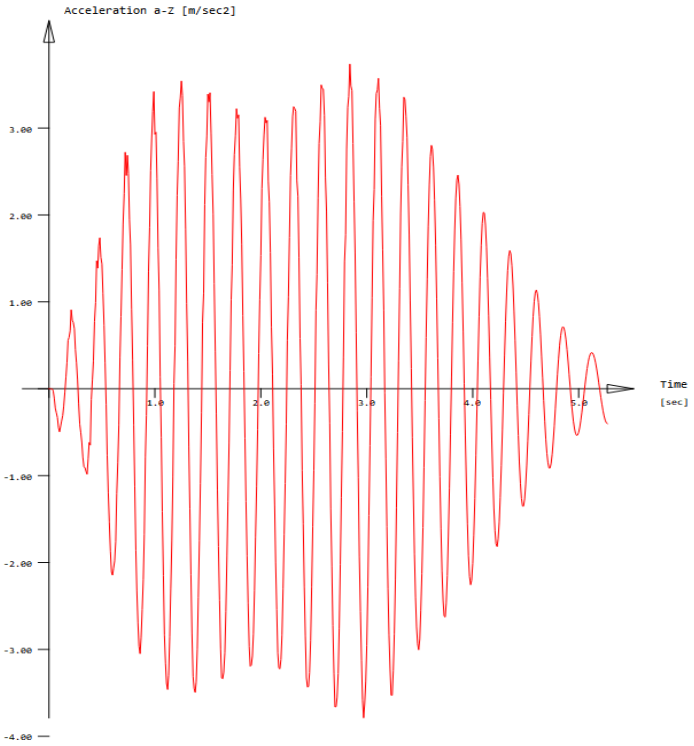

Figure 3.1-15: Maximum acceleration 26m span.

Deformation:

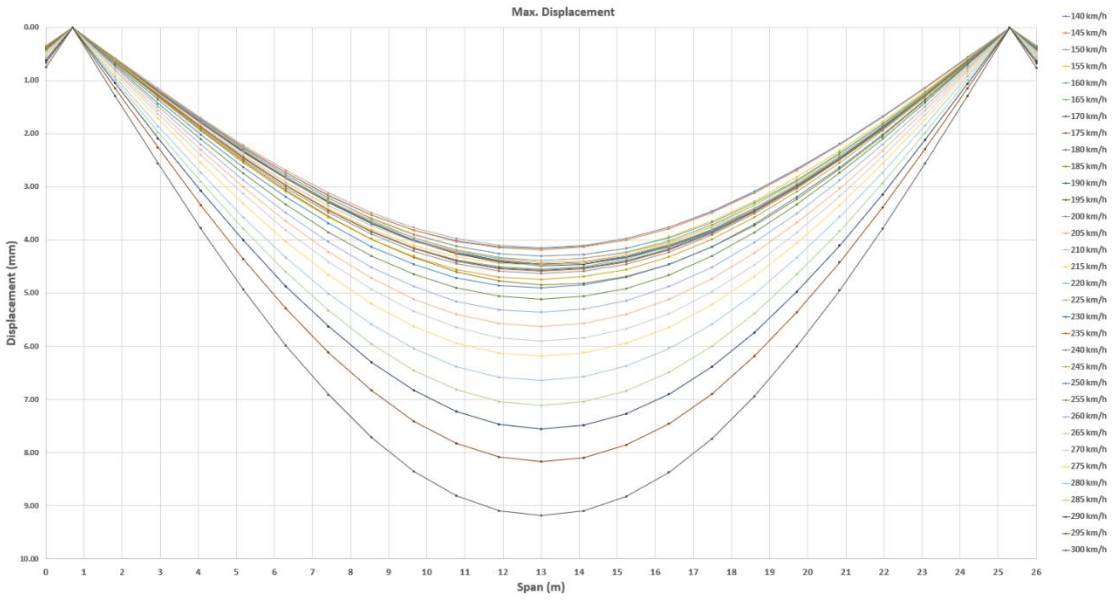

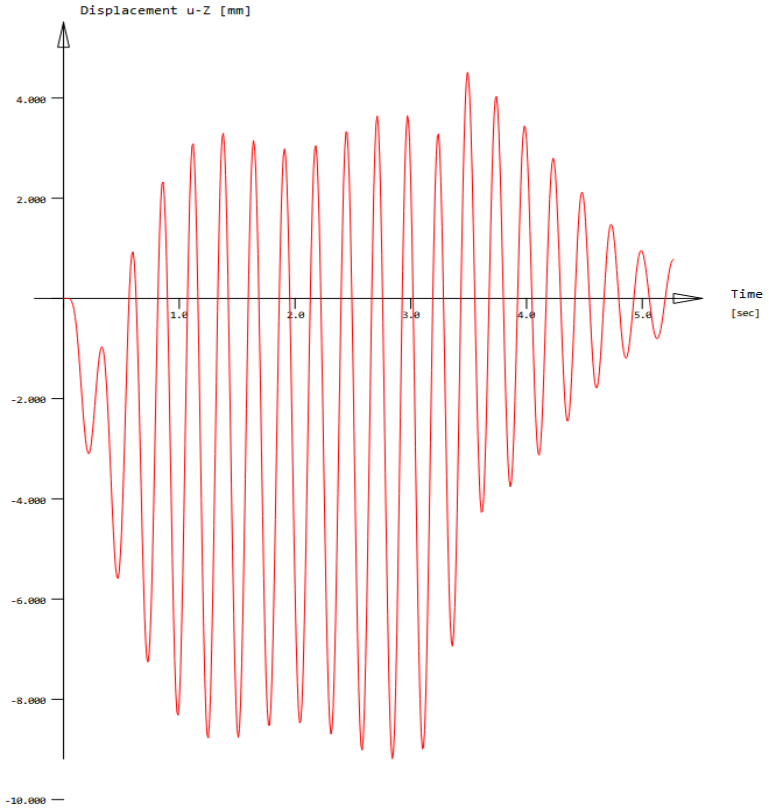

Figure 3.1-16: Maximum deformation 26m span.

3.1.4.4 23m SPAN

Analysis performed for RRTS Bogie Length – 21.34m

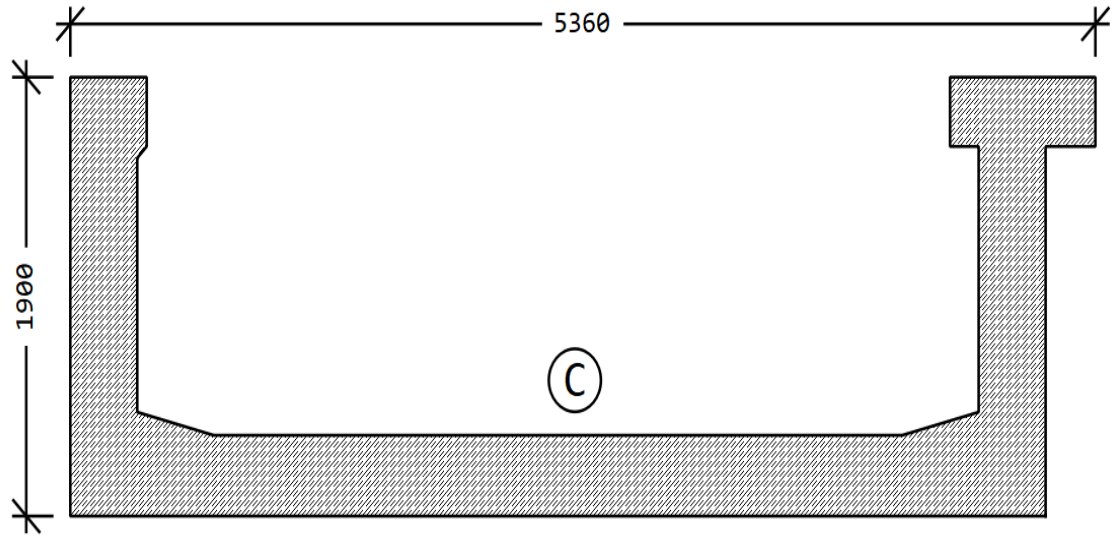

Figure 3.1-17: Cross Section-1.90m

Cross Section Properties:

Static properties of cross section

SNo	Mat	A[m2]	Ay[m2]	Iy[m4]	yc[mm]	ysc[mm]	E[N/mm2]	g[kg/m]	I-1[m4]
	MRf	It[m4]	Az[m2]	Iz[m4]	zc[mm]	zsc[mm]	G[N/mm2]		I-2[m4]
			Ayz[m2]	Iyz[m4]					α[°]
1	10	3.0493E+00	1.549E+00	1.043E+00	-5.7	-147.6	35000	7623.1	1.100E+01
	20[1]	1.332E-01	8.164E-01	1.099E+01	-587.6	437.4	15217	(BEAM)	1.033E+00
				3.135E-01					-88.20
= U-Girder									

[1] No valid reinforcements are defined

SNo	section number	yc[mm],zc[mm]	ordinate of elastic centroid
Mat	material number	ysc[mm],zsc[mm]	ordinate of shear centre
A[m2]	sectional area	E[N/mm2]	Young's modulus
Ay[m2],Az[m2],Ayz[m2]	transverse shear deformation area	g[kg/m]	mass per length
Iy[m4],Iz[m4],Iyz[m4]	bending moment of inertia		
I-1[m4],I-2[m4],α[°]	principal moments of inertia and angle of the principal axes		
MRf	reinforcement material number		
It[m4]	torsional moment of inertia		
G[N/mm2]	Shear modulus		

Acceleration:

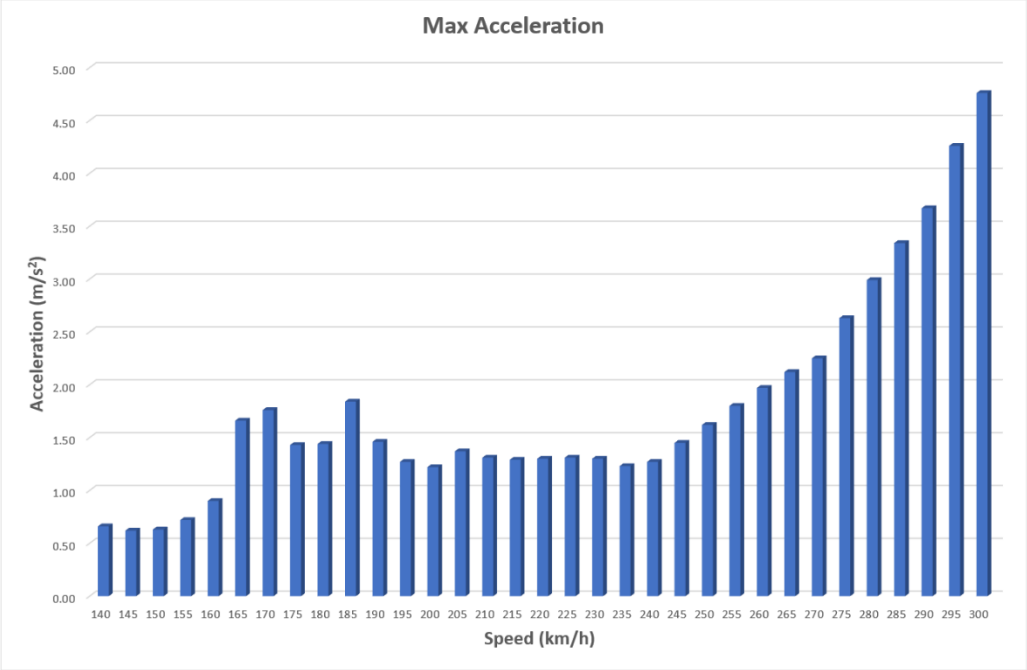

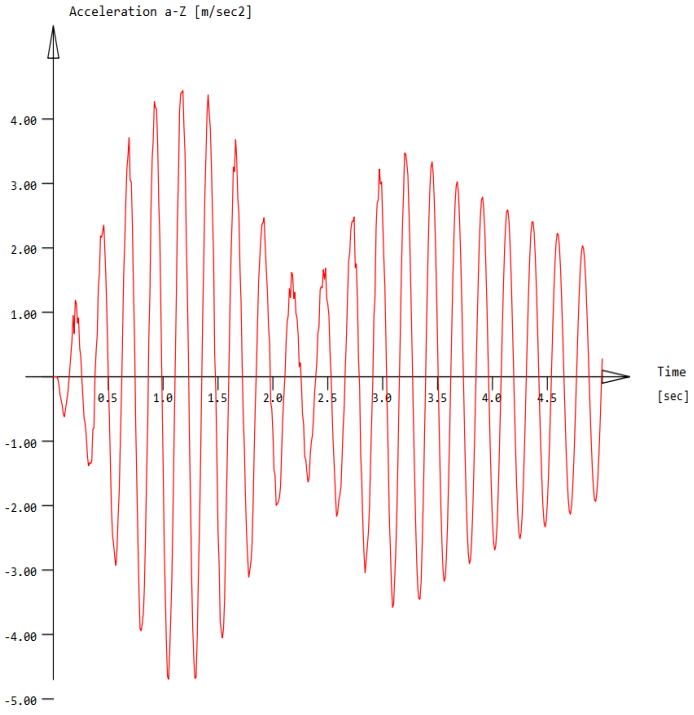

Figure 3.1-18: Maximum acceleration 23m span.

Deformation:

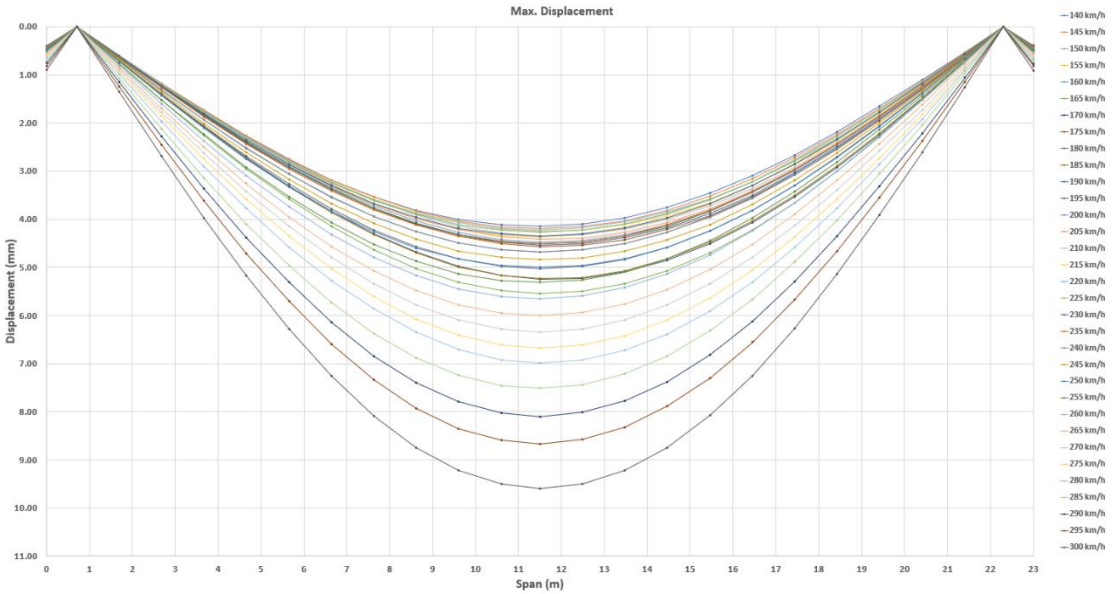

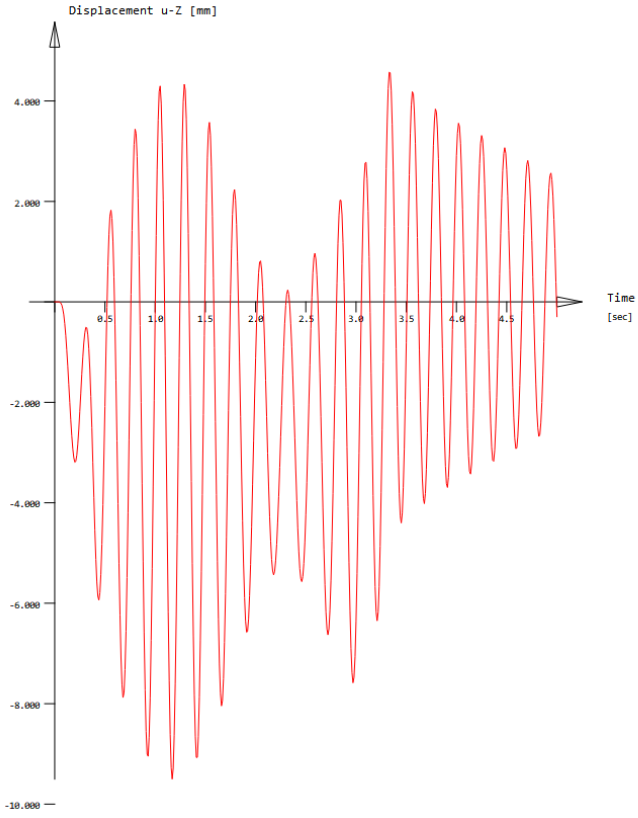

Figure 3.1-19: Maximum deformation 23m span.

Analysis performed for RRTS Bogie Length – 22.34m

Acceleration:

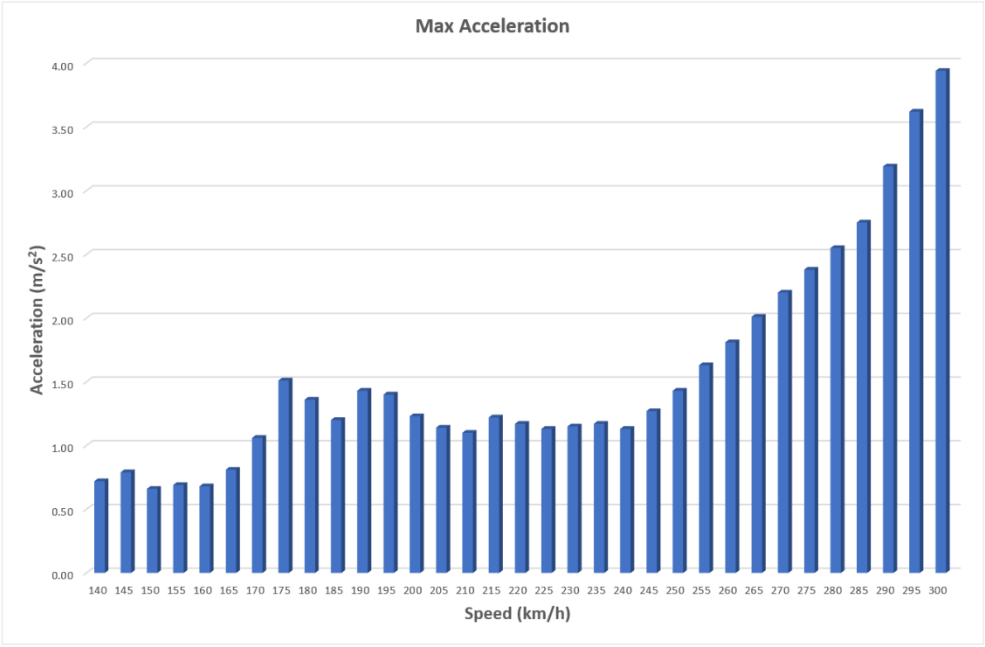

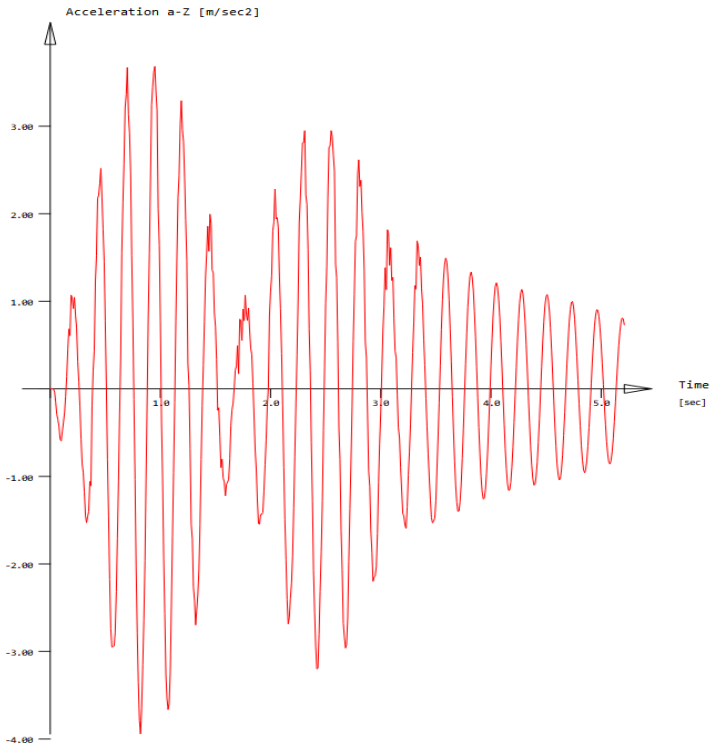

Figure 3.1-20: Maximum acceleration 23m span.

Deformation:

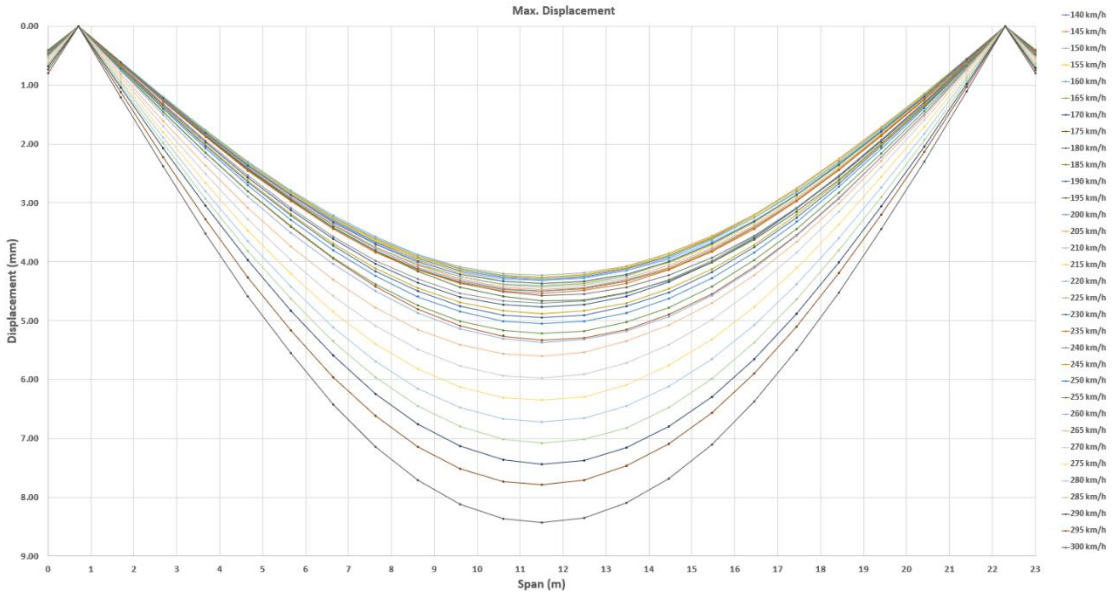

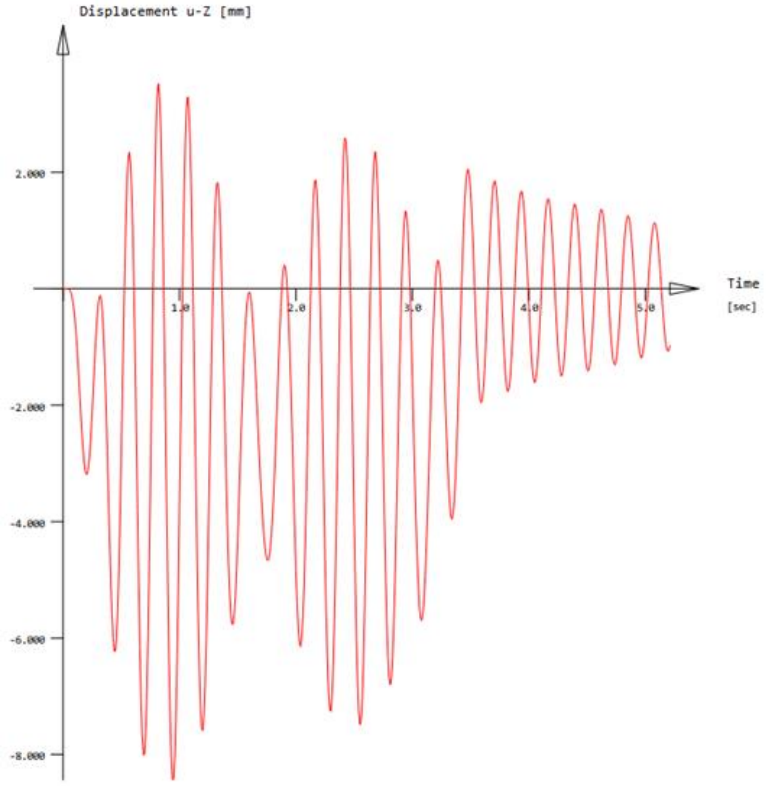

Figure 3.1-21: Maximum deformation 23m span.

3.1.4.5 20m SPAN

Analysis performed for RRTS Bogie Length – 21.34m

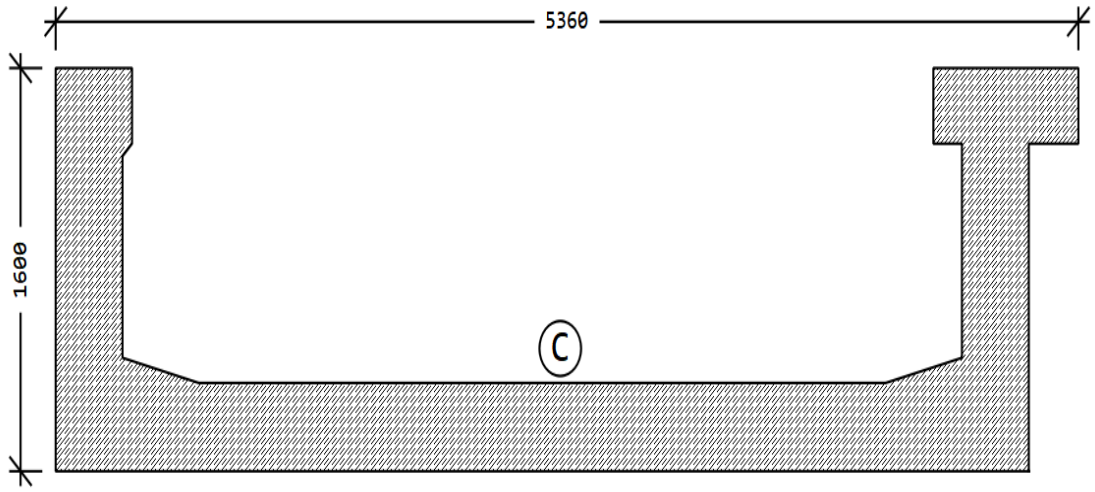

Figure 3.1-22: Cross Section-1.60m

Cross Section Properties:

Static properties of cross section

SNo	Mat	A[m2]	Ay[m2]	Iy[m4]	yc[mm]	ysc[mm]	E[N/mm2]	g[kg/m]	I-1[m4]
	MRf	It[m4]	Az[m2]	Iz[m4]	zc[mm]	zsc[mm]	G[N/mm2]		I-2[m4]
			Ayz[m2]	Iyz[m4]					α[°]
1	10	2.8393E+00	1.582E+00	6.445E-01	-12.2	-174.3	35000	7098.1	9.807E+00
	20[1]	1.247E-01	6.418E-01	9.800E+00	-486.9	302.4	15217	(BEAM)	6.372E-01
				2.598E-01					-88.38

= U-Girder

[1] No valid reinforcements are defined

SNo	section number	yc[mm],zc[mm]	ordinate of elastic centroid
Mat	material number	ysc[mm],zsc[mm]	ordinate of shear centre
A[m2]	sectional area	E[N/mm2]	Young's modulus
Ay[m2],Az[m2],Ayz[m2]	transverse shear deformation area	g[kg/m]	mass per length
Iy[m4],Iz[m4],Iyz[m4]	bending moment of inertia		
I-1[m4],I-2[m4],α[°]	principal moments of inertia and angle of the principal axes		
MRf	reinforcement material number		
It[m4]	torsional moment of inertia		
G[N/mm2]	Shear modulus		

Acceleration:

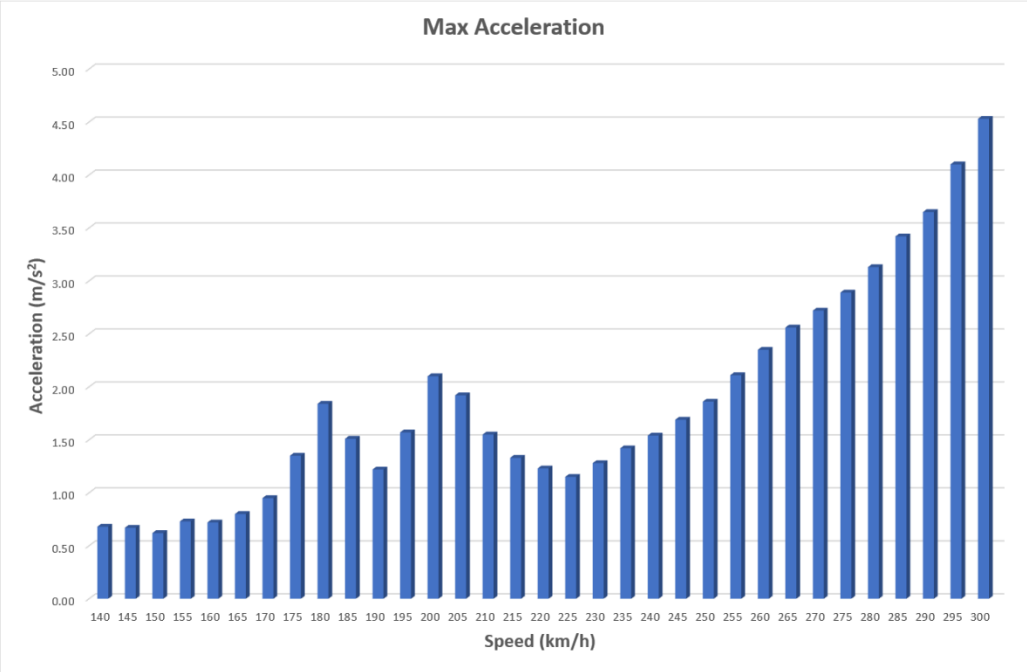

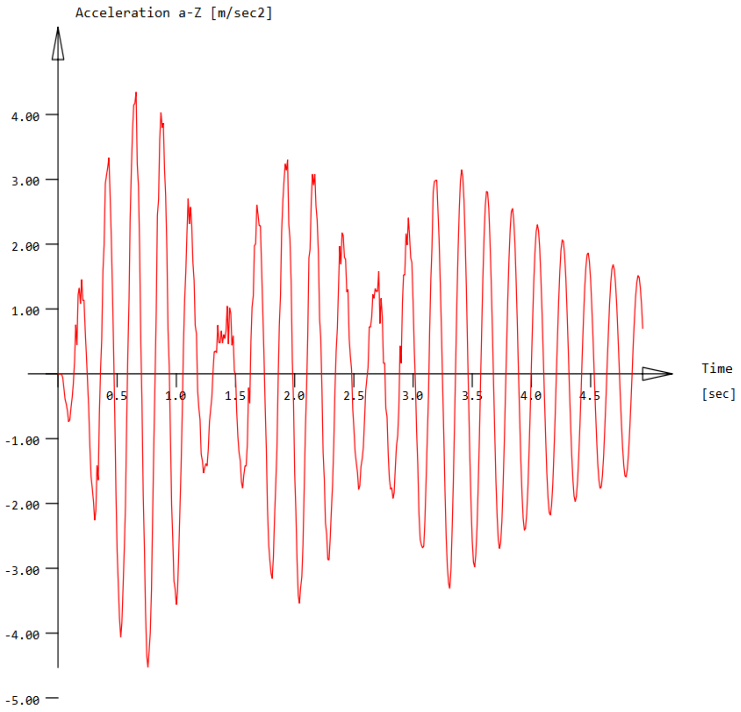

Figure 3.1-23: Maximum acceleration 20m span.

Deformation:

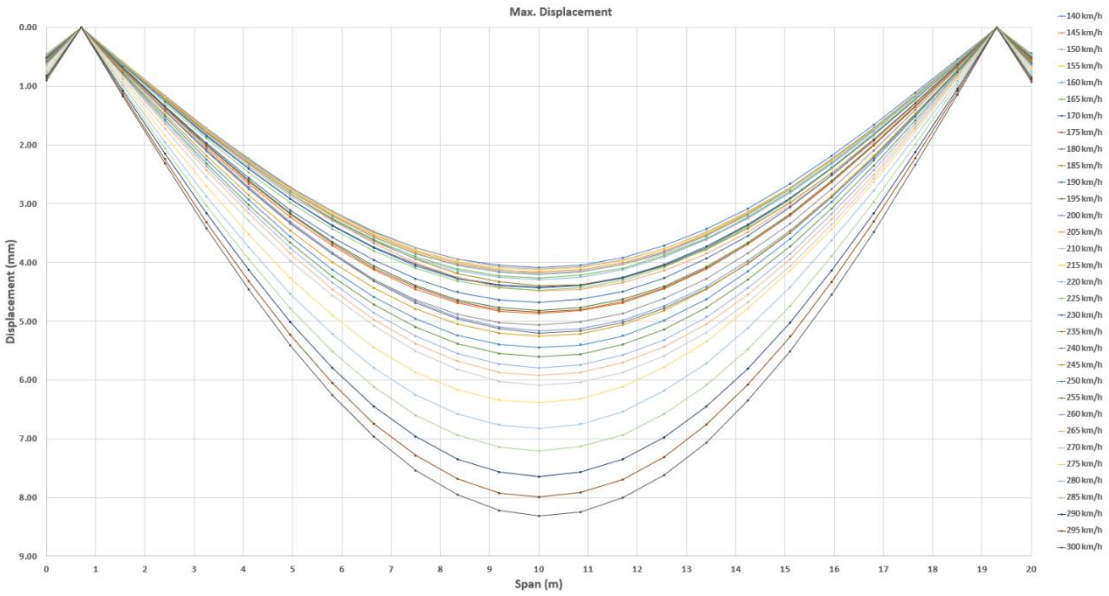

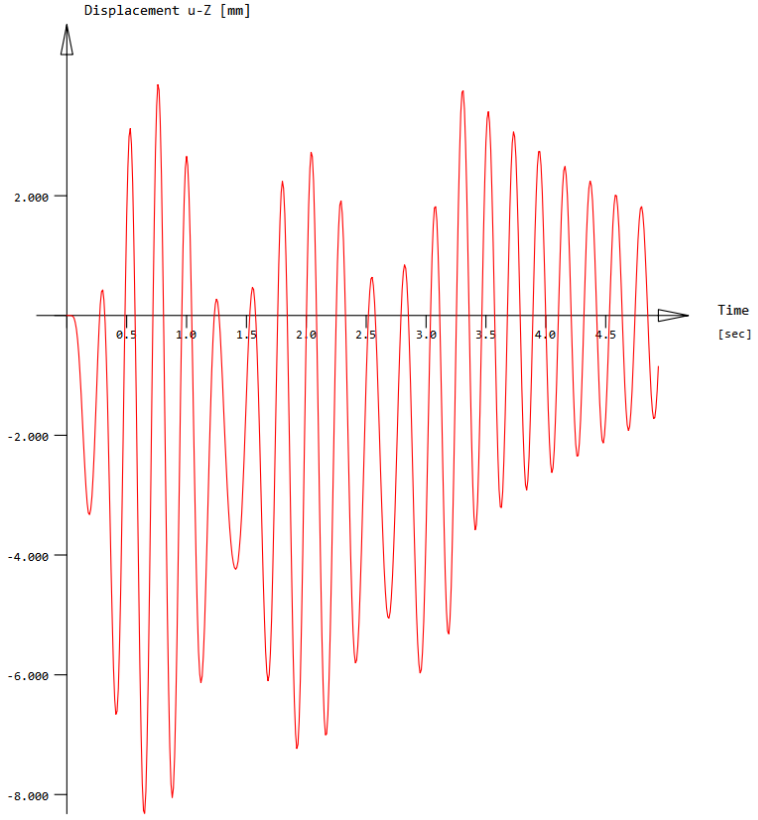

Figure 3.1-24: Maximum deformation 20m span.

Analysis performed for RRTS Bogie Length – 22.34m

Acceleration:

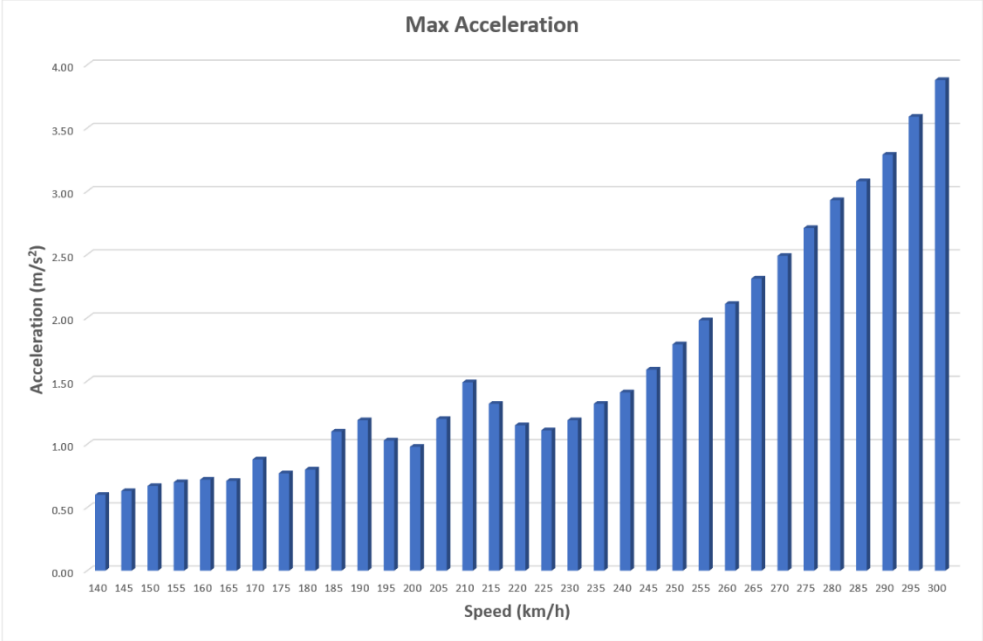

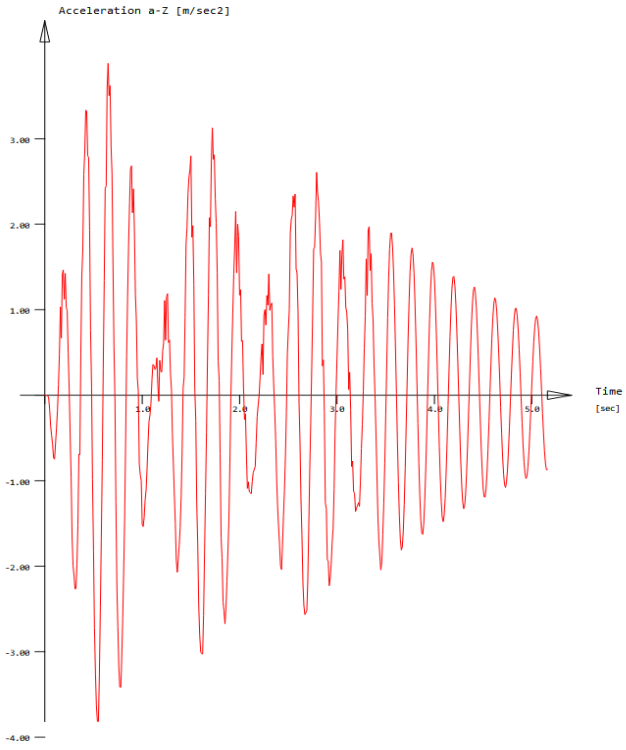

Figure 3.1-25: Maximum acceleration 20m span.

Deformation:

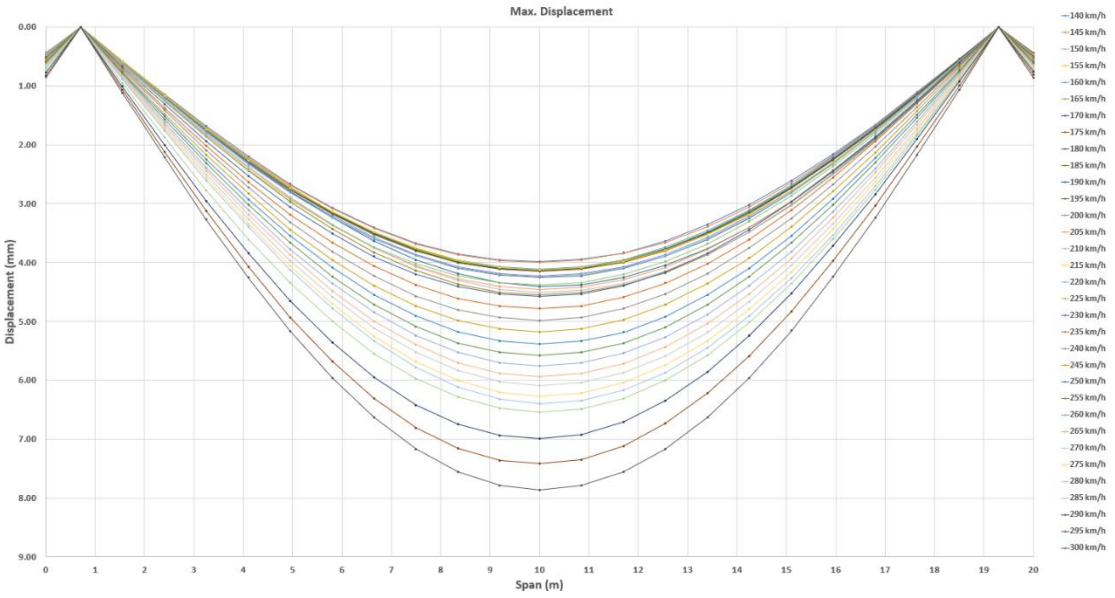

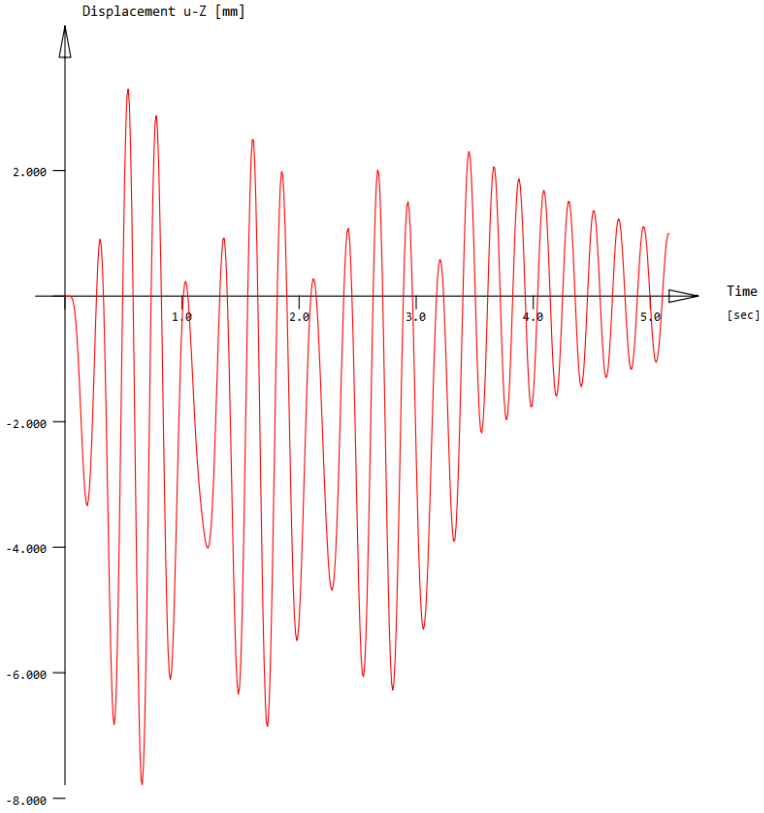

Figure 3.1-26: Maximum deformation 20m span.

3.1.5. ANALYSIS: BOX GIRDER

3.1.5.1 28m SPAN

Analysis performed for RRTS Bogie Length – 21.34m

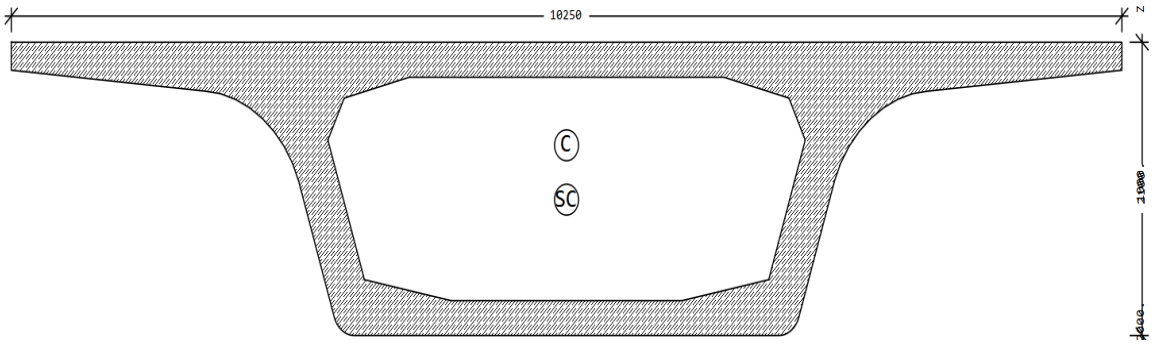

Figure 3.1-27: Cross Section-2.1m

Cross Section Properties:

Static properties of cross section

SNo	Mat	A[m2]	Ay[m2]	Iy[m4]	yc[mm]	ysc[mm]	E[N/mm2]	g[kg/m]	I-1[m4]
	MRf	It[m4]	Az[m2]	Iz[m4]	zc[mm]	zsc[mm]	G[N/mm2]		I-2[m4]
			Ayz[m2]	Iyz[m4]					α[°]
2	10	5.5699E+00	3.775E+00	3.191E+00	0.0	0.0	36283	13924.9	3.508E+01
	20[1]	7.031E+00	1.099E+00	3.508E+01	738.0	1127.0	15118	(BEAM)	3.191E+00
				-8.693E-07					90.00

= Box Mid section

[1] No valid reinforcements are defined

SNo	section number	yc[mm],zc[mm]	ordinate of elastic centroid
Mat	material number	ysc[mm],zsc[mm]	ordinate of shear centre
A[m2]	sectional area	E[N/mm2]	Young's modulus
Ay[m2],Az[m2],Ayz[m2]	transverse shear deformation area	g[kg/m]	mass per length
Iy[m4],Iz[m4],Iyz[m4]	bending moment of inertia		
I-1[m4],I-2[m4],α[°]	principal moments of inertia and angle of the principal axes		
MRf	reinforcement material number		
It[m4]	torsional moment of inertia		
G[N/mm2]	Shear modulus		

Acceleration:

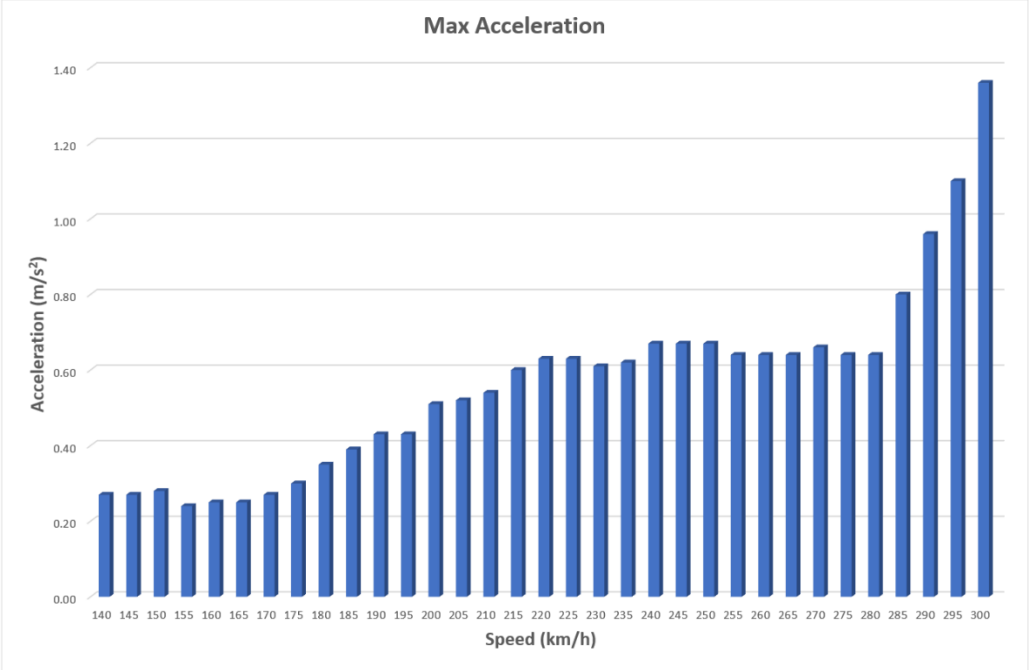

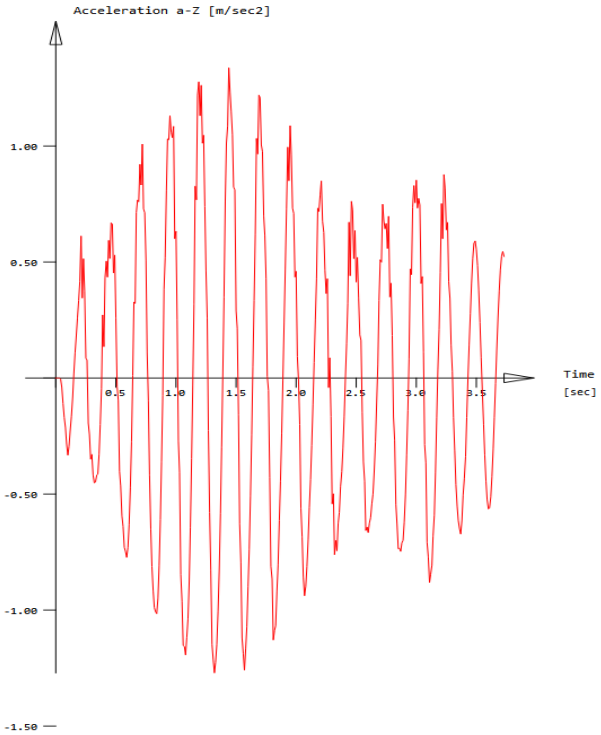

Figure 3.1-28: Maximum acceleration 28m span.

Deformation:

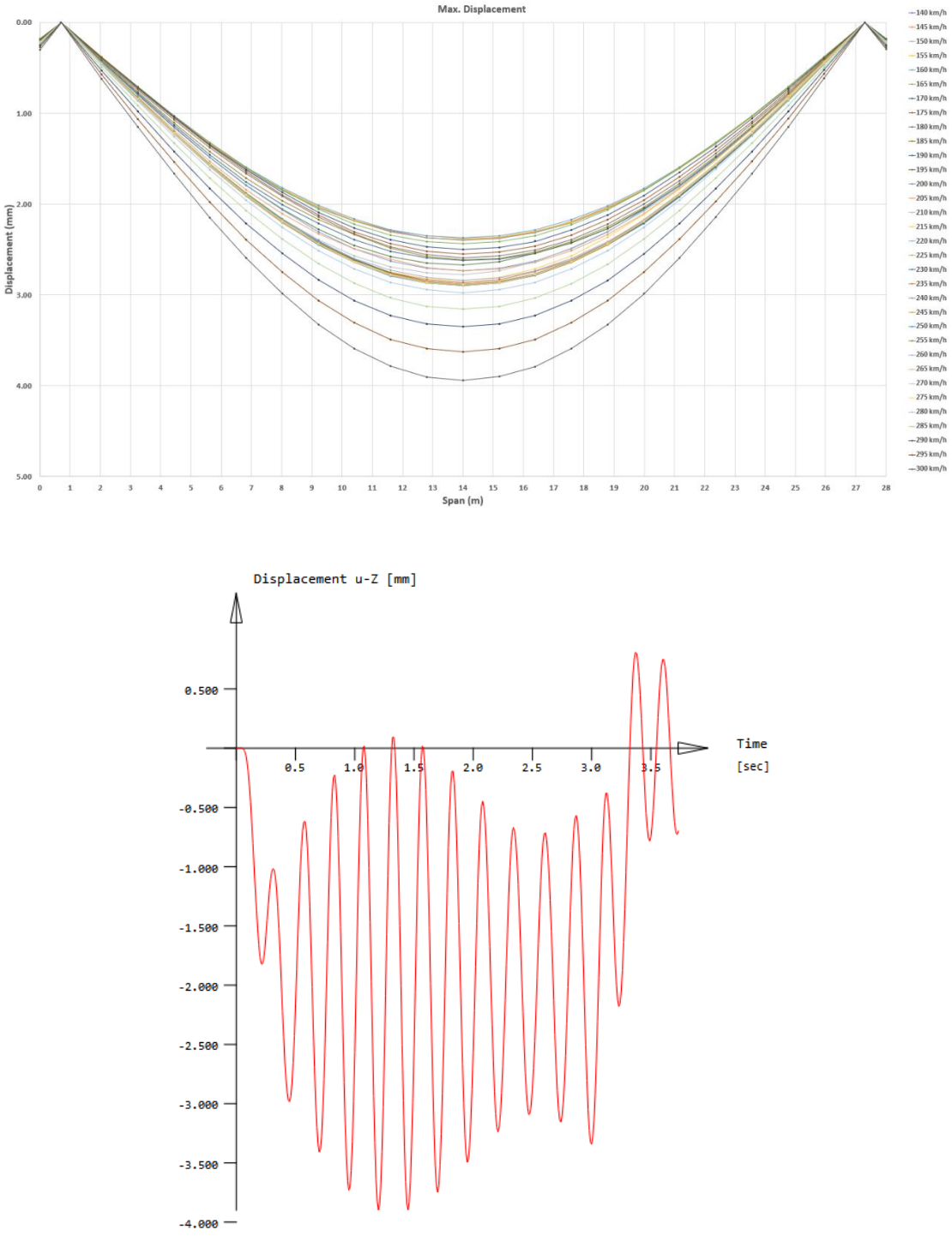

Figure 3.1-29: Maximum deformation 28m span.

Analysis performed for RRTS Bogie Length – 22.34m

Acceleration:

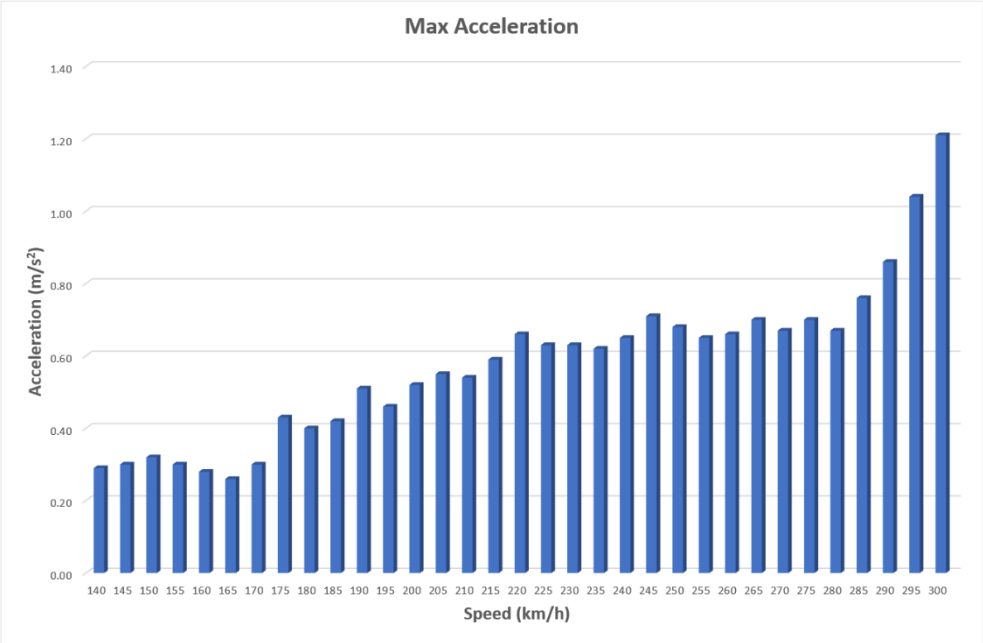

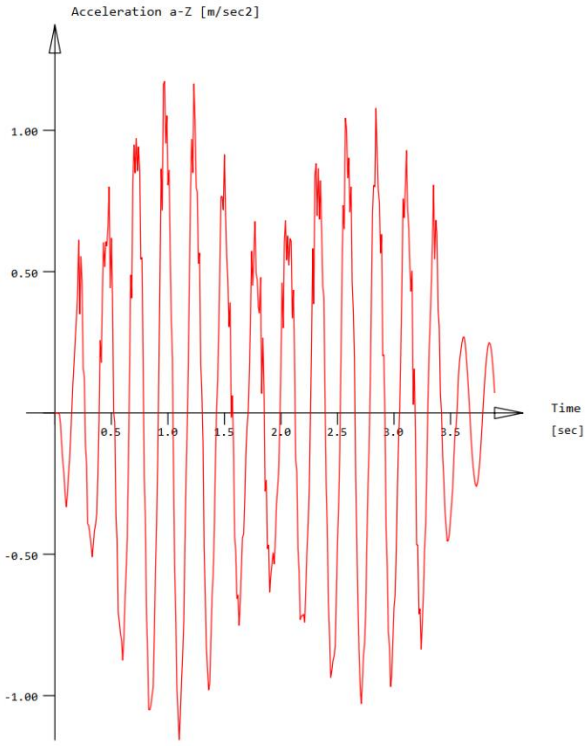

Figure 3.1-30: Maximum acceleration 28m span.

Deformation:

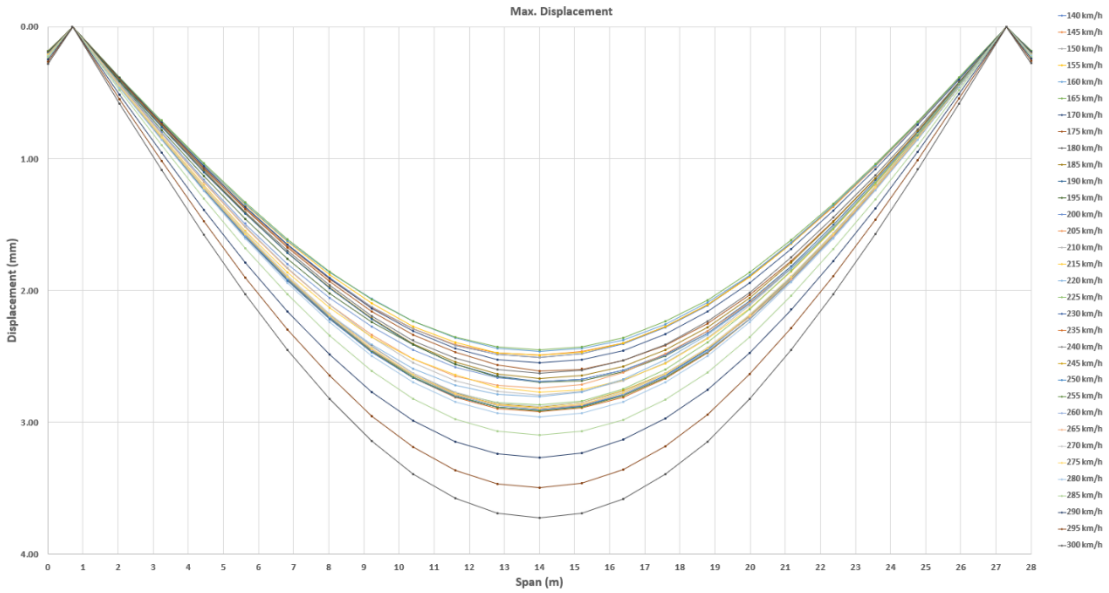

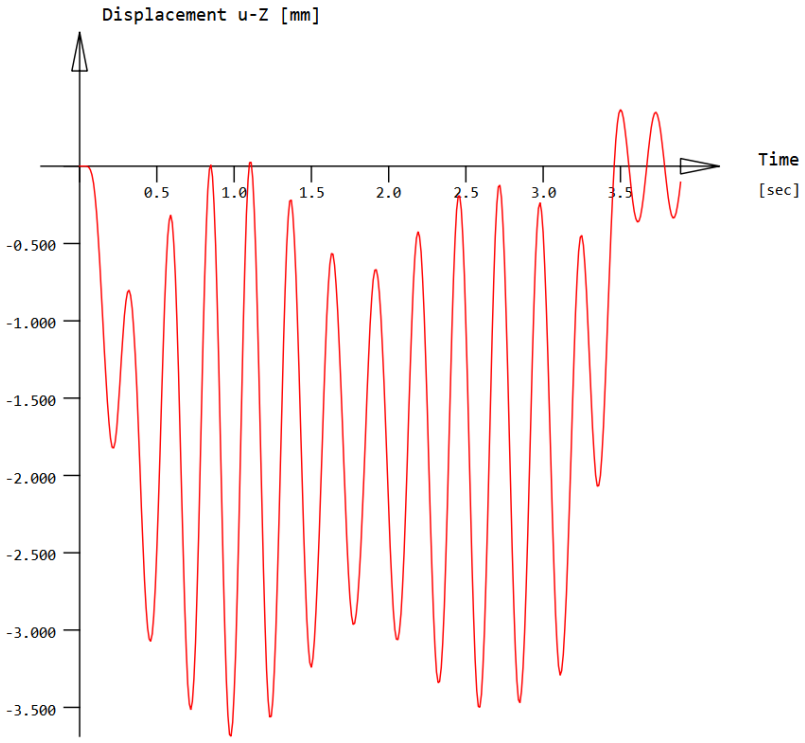

Figure 3.1-31: Maximum deformation 28m span.

3.1.5.1 26m SPAN

Analysis performed for RRTS Bogie Length – 21.34m

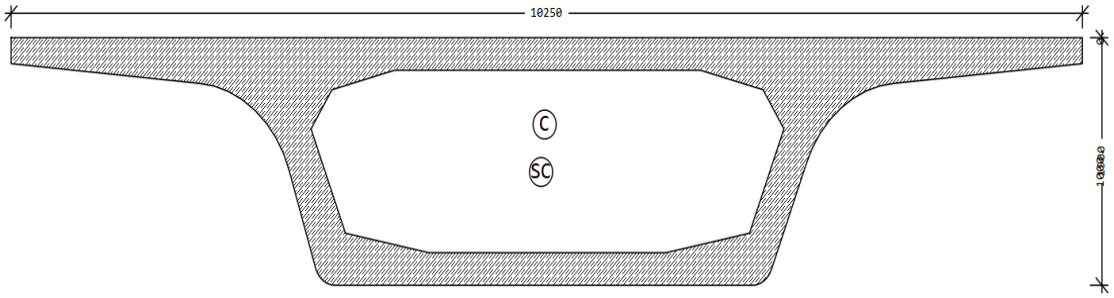

Figure 3.1-32: Cross Section-1.9m

Cross Section Properties:

Static properties of cross section

SNo	Mat	A[m2]	Ay[m2]	Iy[m4]	yc[mm]	ysc[mm]	E[N/mm2]	g[kg/m]	I-1[m4]
	MRf	It[m4]	Az[m2]	Iz[m4]	zc[mm]	zsc[mm]	G[N/mm2]		I-2[m4]
			Ayz[m2]	Iyz[m4]					α[°]
2	10	5.3547E+00	3.799E+00	2.493E+00	-20.0	-54.2	36283	13386.9	3.417E+01
	20[1]	5.769E+00	8.792E-01	3.417E+01	666.7	1030.7	15118	(BEAM)	2.493E+00
				-7.214E-02					89.87

= Box Mid section

[1] No valid reinforcements are defined

SNo	section number	yc[mm],zc[mm]	ordinate of elastic centroid
Mat	material number	ysc[mm],zsc[mm]	ordinate of shear centre
A[m2]	sectional area	E[N/mm2]	Young's modulus
Ay[m2],Az[m2],Ayz[m2]	transverse shear deformation area	g[kg/m]	mass per length
Iy[m4],Iz[m4],Iyz[m4]	bending moment of inertia		
I-1[m4],I-2[m4],α[°]	principal moments of inertia and angle of the principal axes		
MRf	reinforcement material number		
It[m4]	torsional moment of inertia		
G[N/mm2]	Shear modulus		

Acceleration:

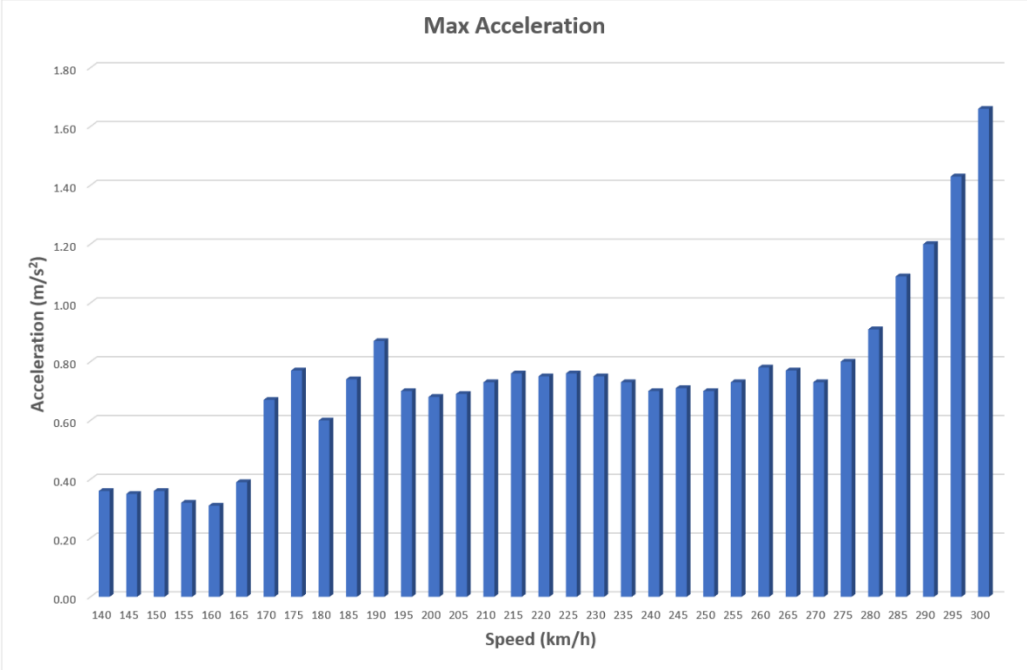

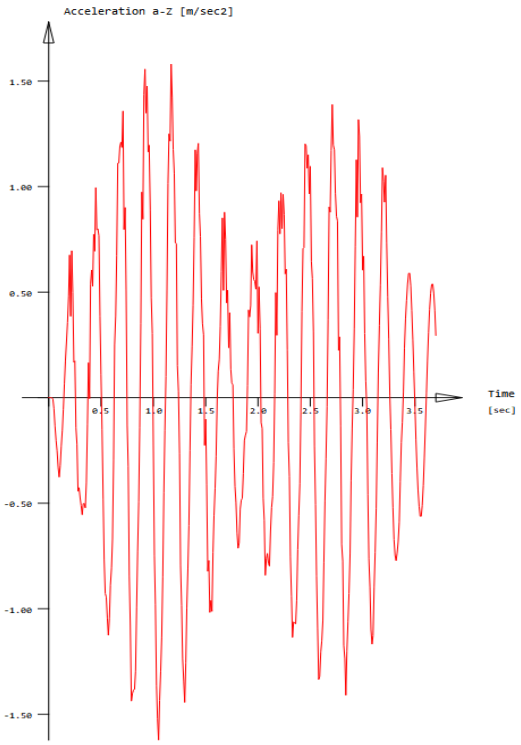

Figure 3.1-33: Maximum acceleration 26m span.

Deformation:

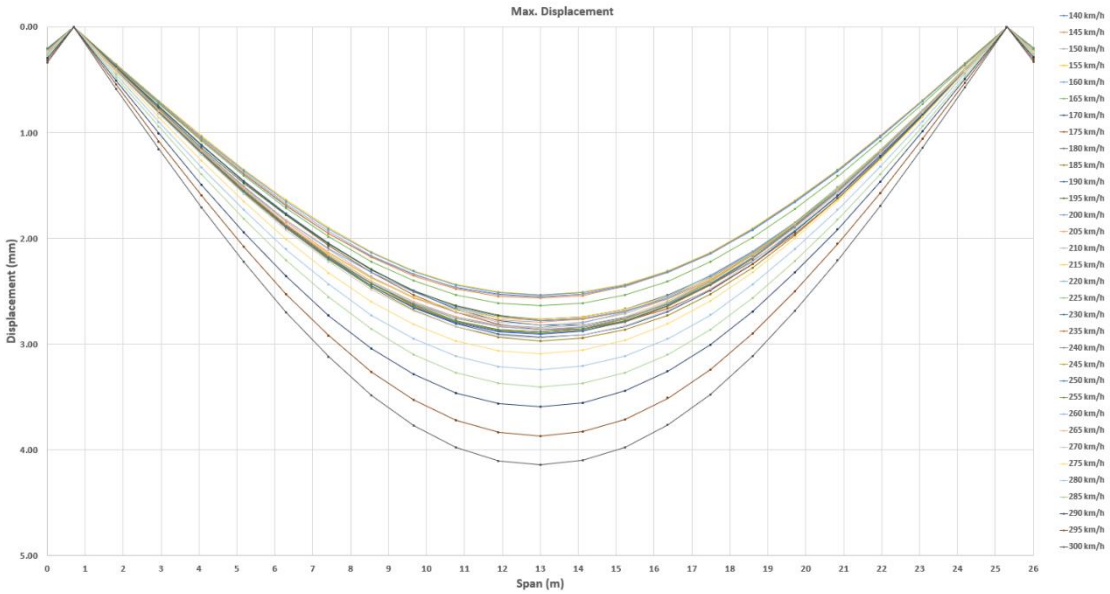

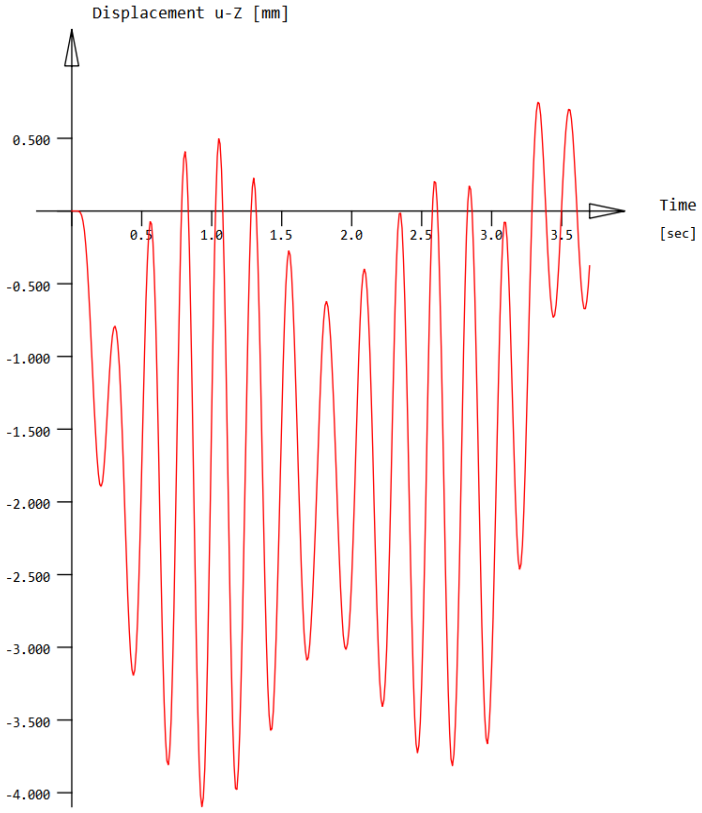

Figure 3.1-34: Maximum deformation 26m span.

Analysis performed for RRTS Bogie Length – 22.34m

Acceleration:

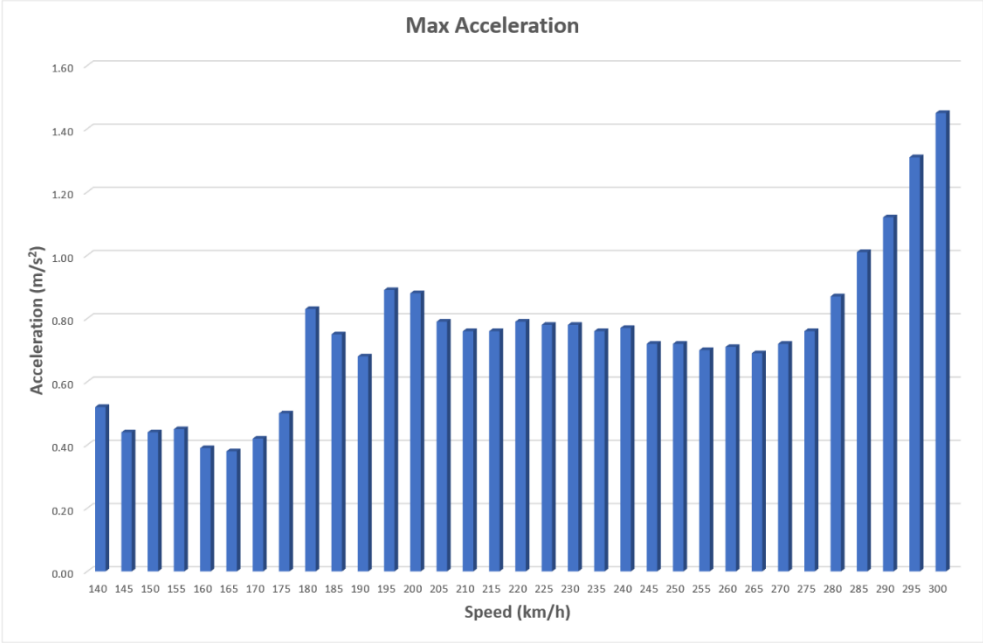

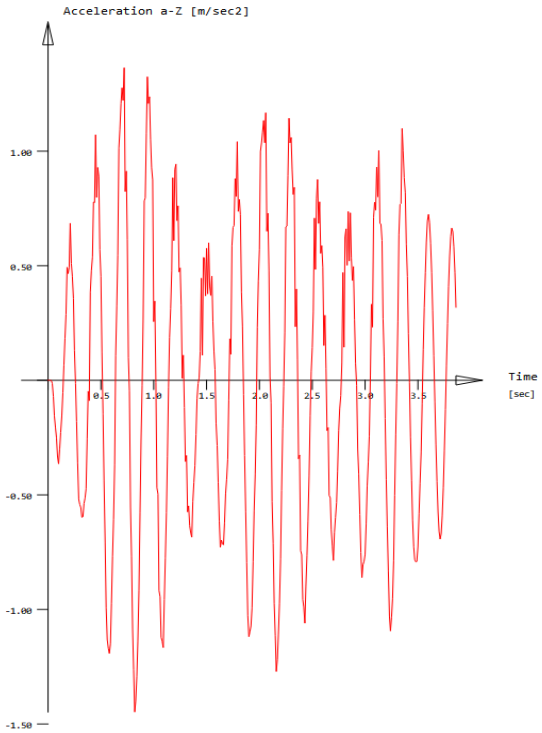

Figure 3.1-35: Maximum acceleration 26m span.

Deformation:

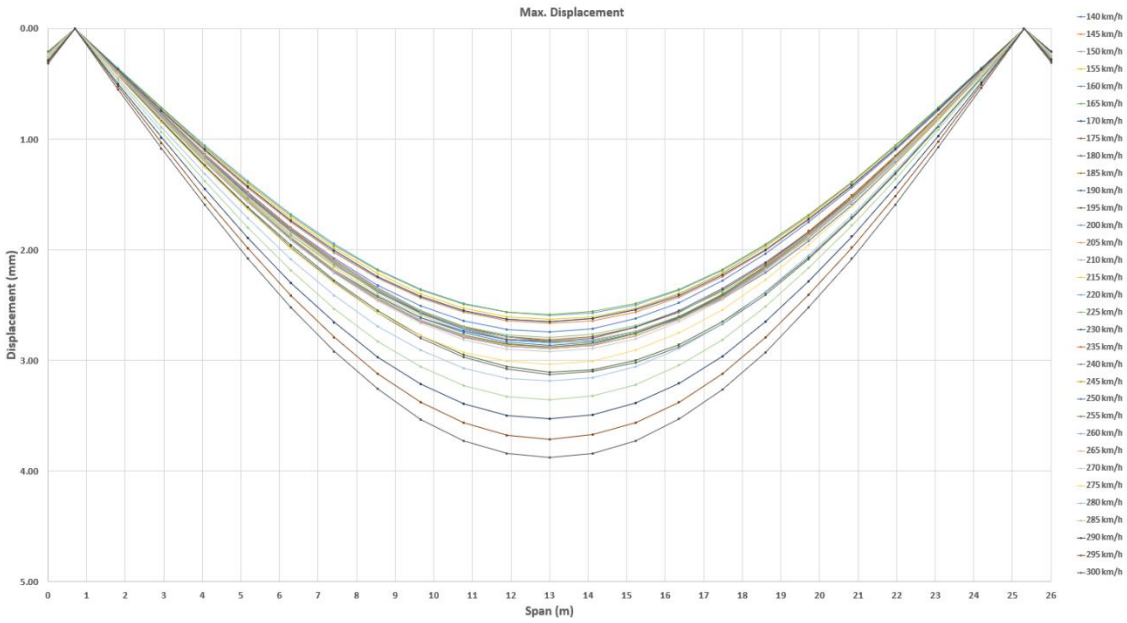

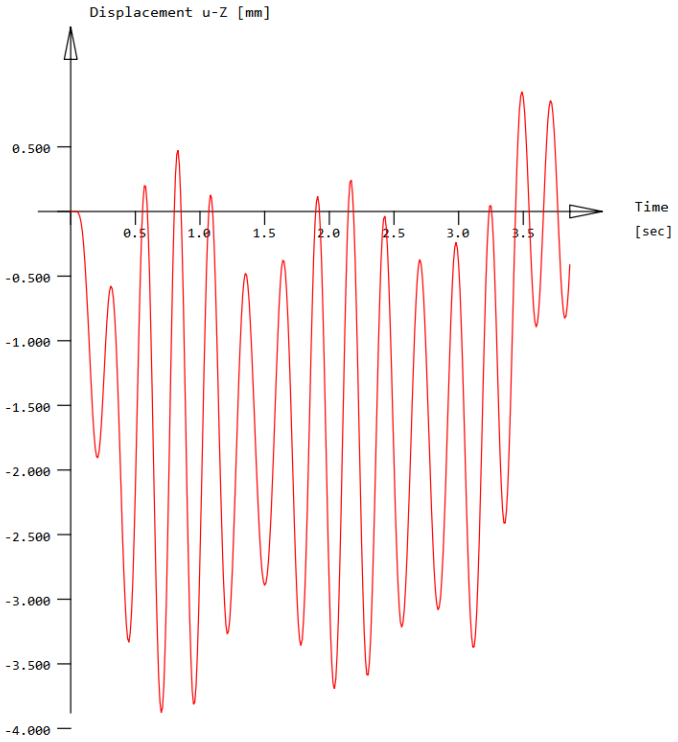

Figure 3.1-36: Maximum deformation 26m span.

3.1.5.2 23m SPAN

Analysis performed for RRTS Bogie Length – 21.34m

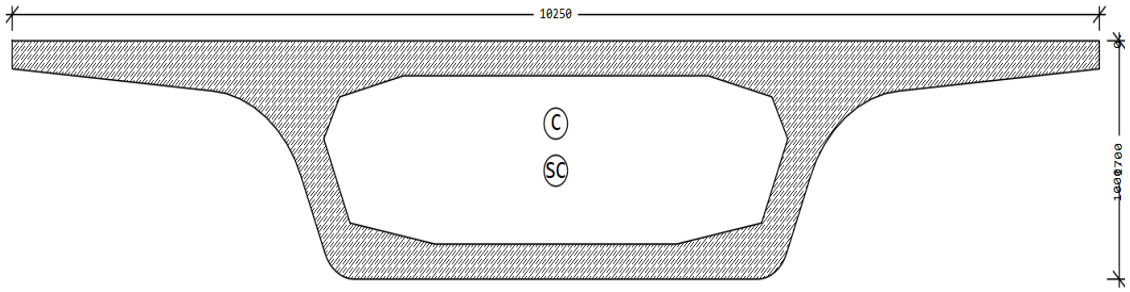

Figure 3.1-37: Cross Section-1.7m

Cross Section Properties:

Static properties of cross section

SNo	Mat	A[m2]	Ay[m2]	Iy[m4]	yc[mm]	ysc[mm]	E[N/mm2]	g[kg/m]	I-1[m4]
	MRf	It[m4]	Az[m2]	Iz[m4]	zc[mm]	zsc[mm]	G[N/mm2]		I-2[m4]
			Ayz[m2]	Iyz[m4]					α[°]
2	10	5.1628E+00	3.810E+00	1.855E+00	0.0	0.0	36283	12907.0	3.296E+01
	20[1]	4.465E+00	7.255E-01	3.296E+01	590.7	926.8	15118	(BEAM)	1.855E+00
				-1.273E-06					90.00

= Box Mid section

[1] No valid reinforcements are defined

SNo	section number	yc[mm],zc[mm]	ordinate of elastic centroid
Mat	material number	ysc[mm],zsc[mm]	ordinate of shear centre
A[m2]	sectional area	E[N/mm2]	Young's modulus
Ay[m2],Az[m2],Ayz[m2]	transverse shear deformation area	g[kg/m]	mass per length
Iy[m4],Iz[m4],Iyz[m4]	bending moment of inertia		
I-1[m4],I-2[m4],α[°]	principal moments of inertia and angle of the principal axes		
MRf	reinforcement material number		
It[m4]	torsional moment of inertia		
G[N/mm2]	Shear modulus		

Acceleration:

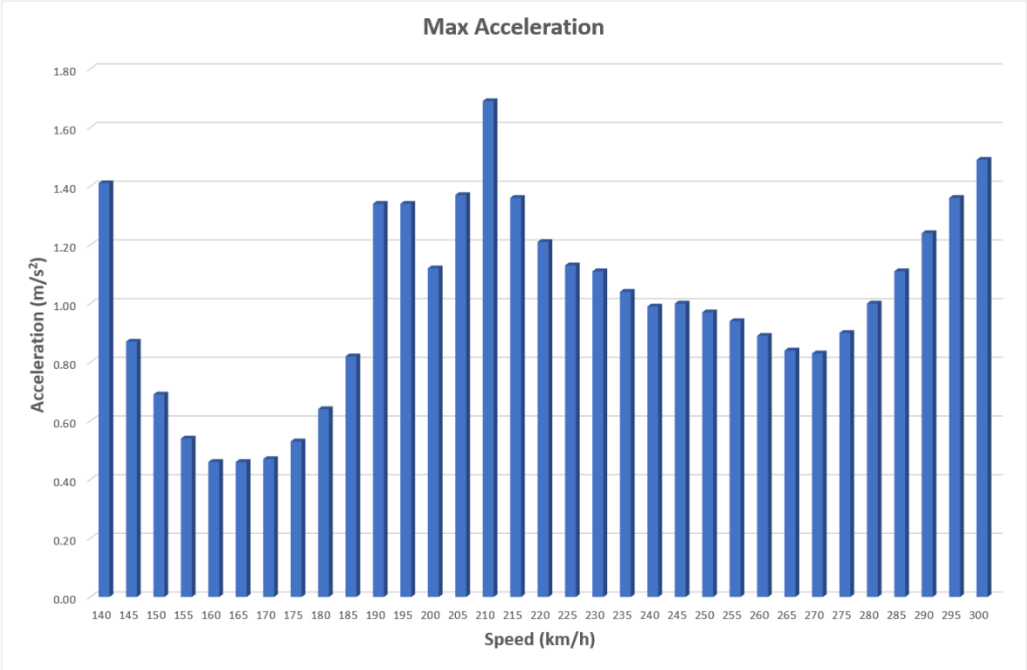

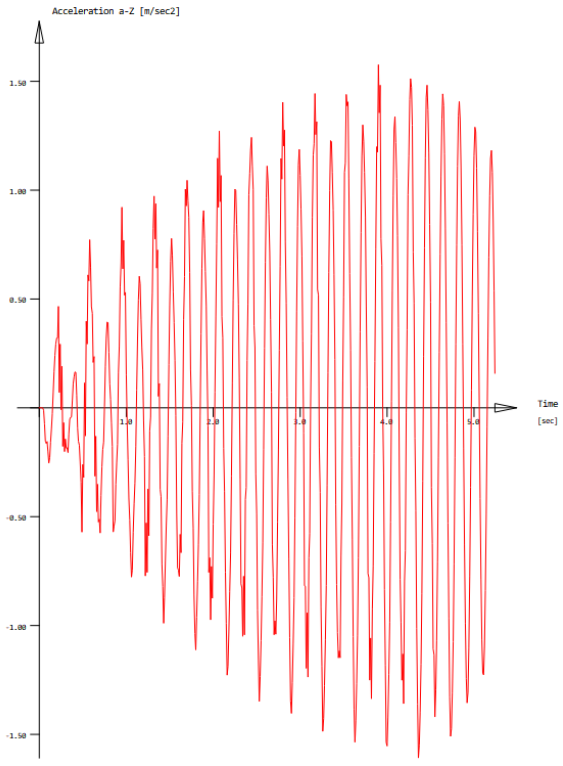

Figure 3.1-38: Maximum acceleration 23m span.

Deformation:

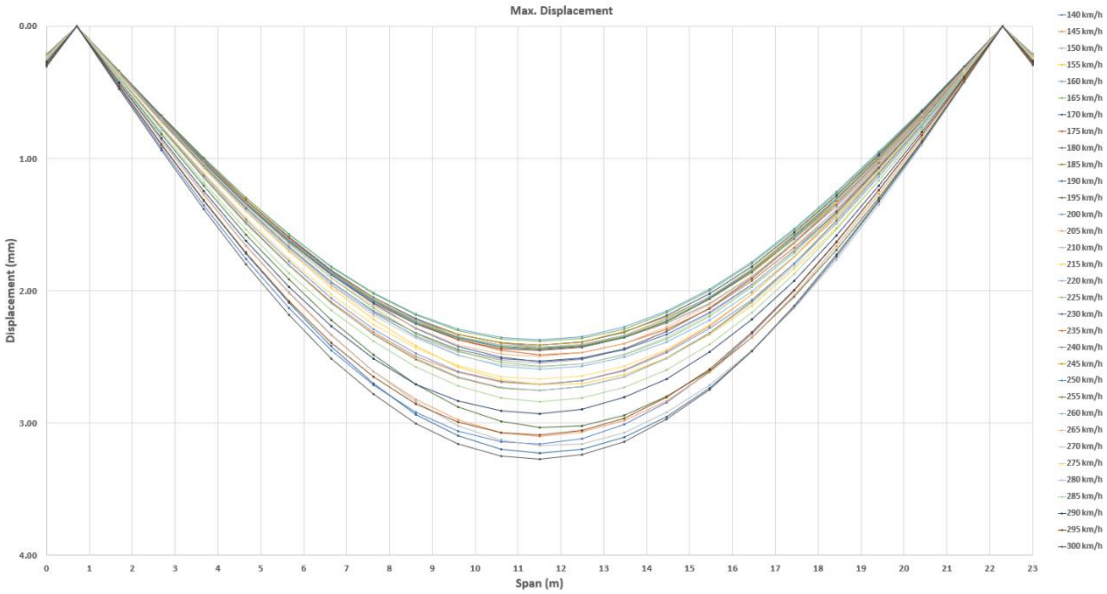

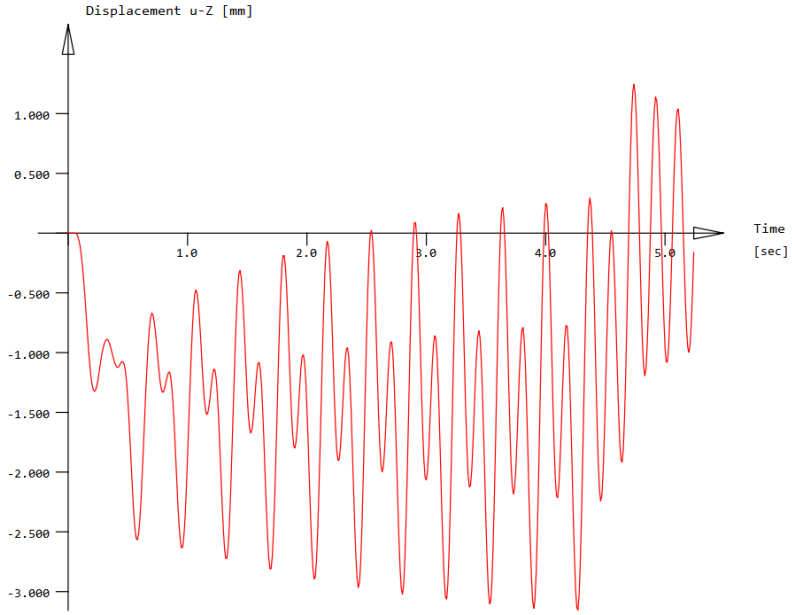

Figure 3.1-39: Maximum deformation 23m span.

Analysis performed for RRTS Bogie Length – 22.34m

Acceleration:

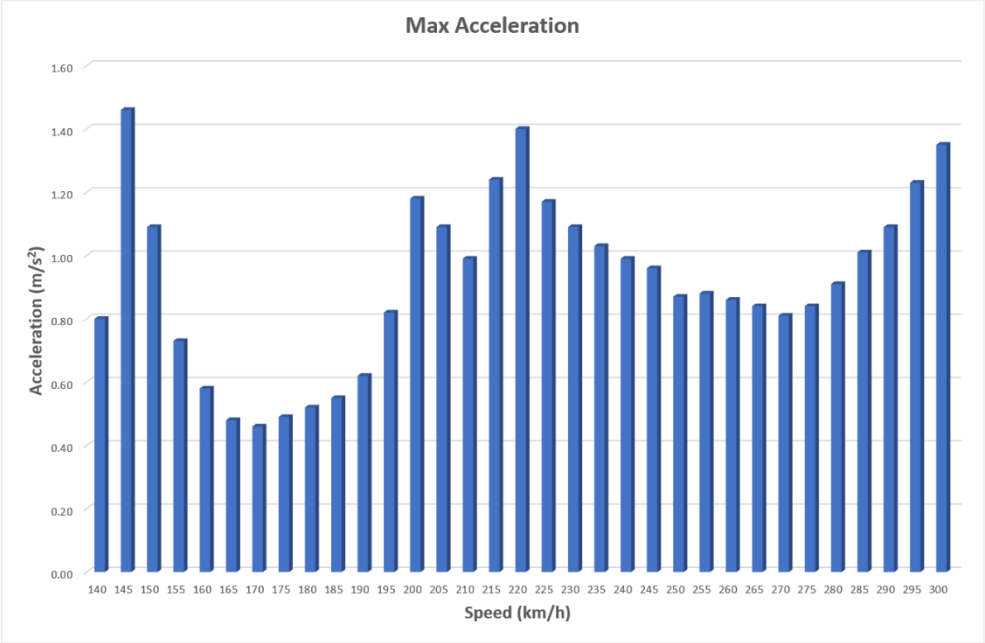

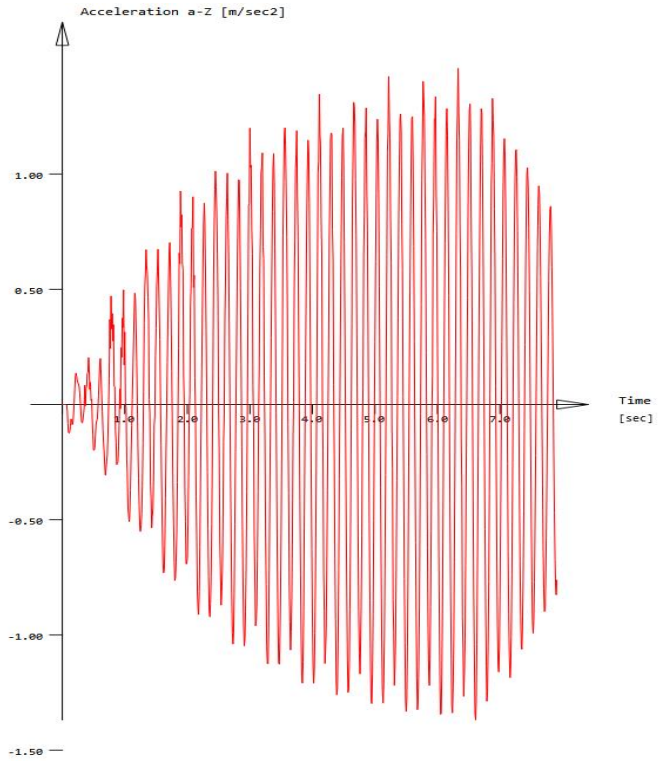

Figure 3.1-40: Maximum acceleration 23m span.

Deformation:

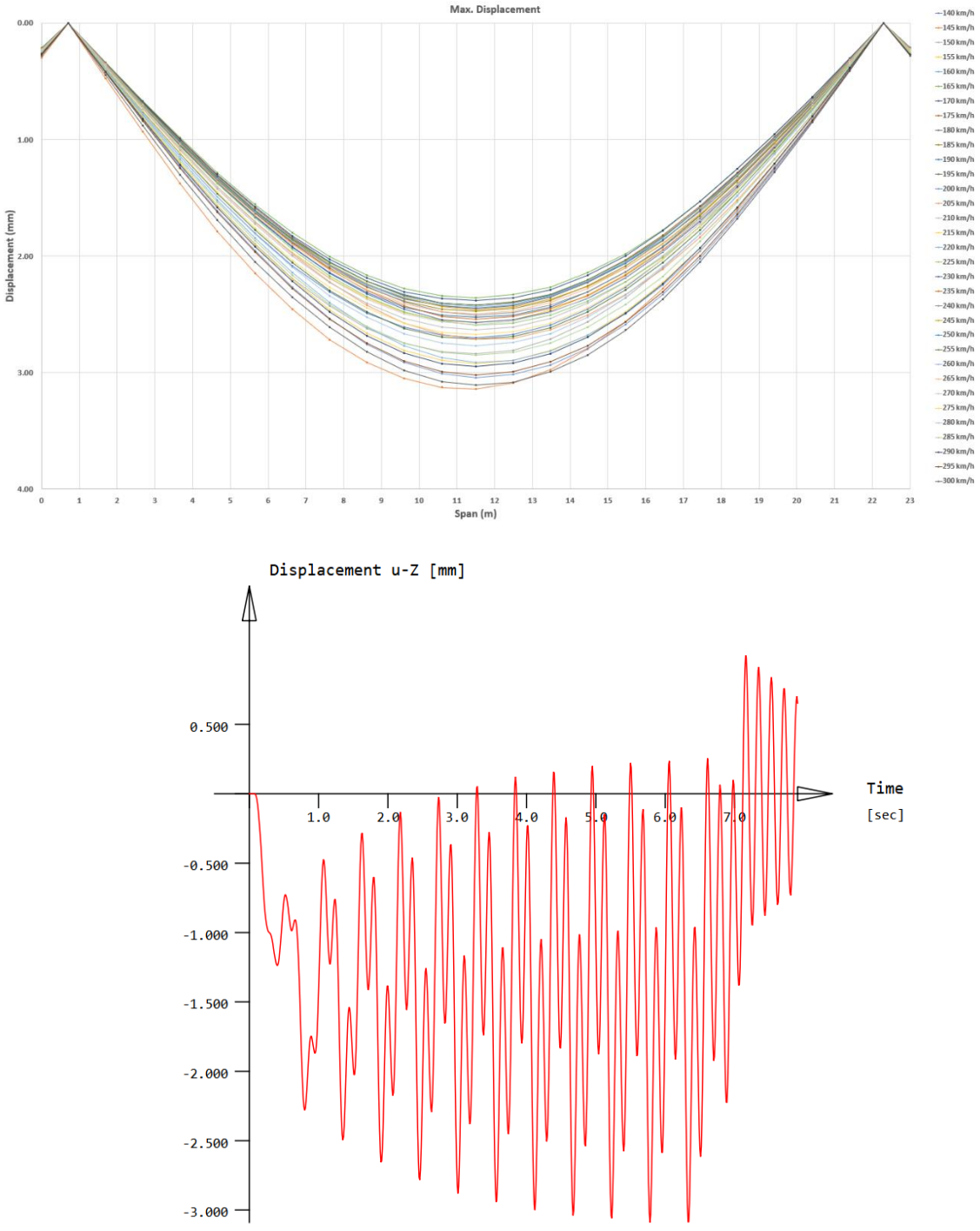

Figure 3.1-41: Maximum deformation 23m span.

3.1.5.3 20m SPAN

Analysis performed for RRTS Bogie Length – 21.34m

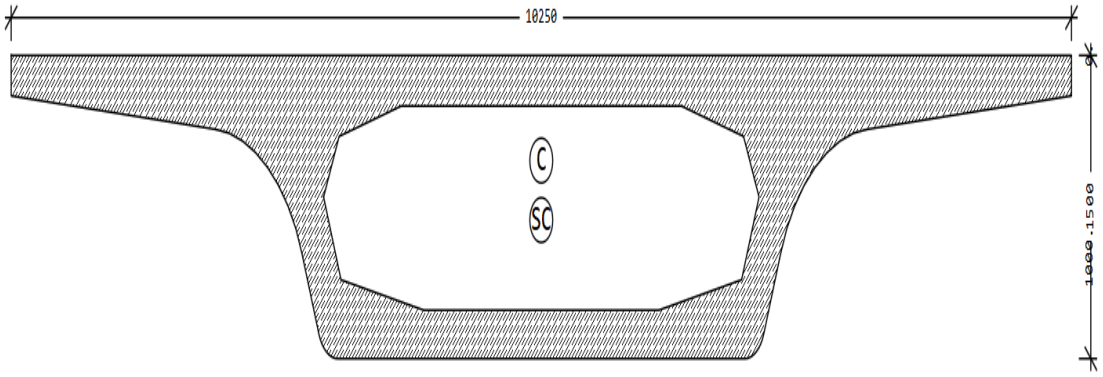

Figure 3.1-42: Cross Section-1.5m

Cross Section Properties:

Static properties of cross section

SNo	Mat MRf	A[m2] It[m4]	Ay[m2] Az[m2] Ayz[m2]	Iy[m4] Iz[m4] Iyz[m4]	yc[mm] zc[mm]	ysc[mm] zsc[mm]	E[N/mm2] G[N/mm2]	g[kg/m]	I-1[m4] I-2[m4] α[°]
2	10	5.0302E+00	3.811E+00	1.341E+00	0.0	0.0	36283	12575.5	3.218E+01
	20[1]	3.366E+00	6.173E-01	3.218E+01	520.0	814.6	15118	(BEAM)	1.341E+00
				-4.312E-07					90.00
= Box Mid section									

[1] No valid reinforcements are defined

SNo	section number	yc[mm],zc[mm]	ordinate of elastic centroid
Mat	material number	ysc[mm],zsc[mm]	ordinate of shear centre
A[m2]	sectional area	E[N/mm2]	Young's modulus
Ay[m2],Az[m2],Ayz[m2]	transverse shear deformation area	g[kg/m]	mass per length
Iy[m4],Iz[m4],Iyz[m4]	bending moment of inertia		
I-1[m4],I-2[m4],α[°]	principal moments of inertia and angle of the principal axes		
MRf	reinforcement material number		
It[m4]	torsional moment of inertia		
G[N/mm2]	Shear modulus		

Acceleration:

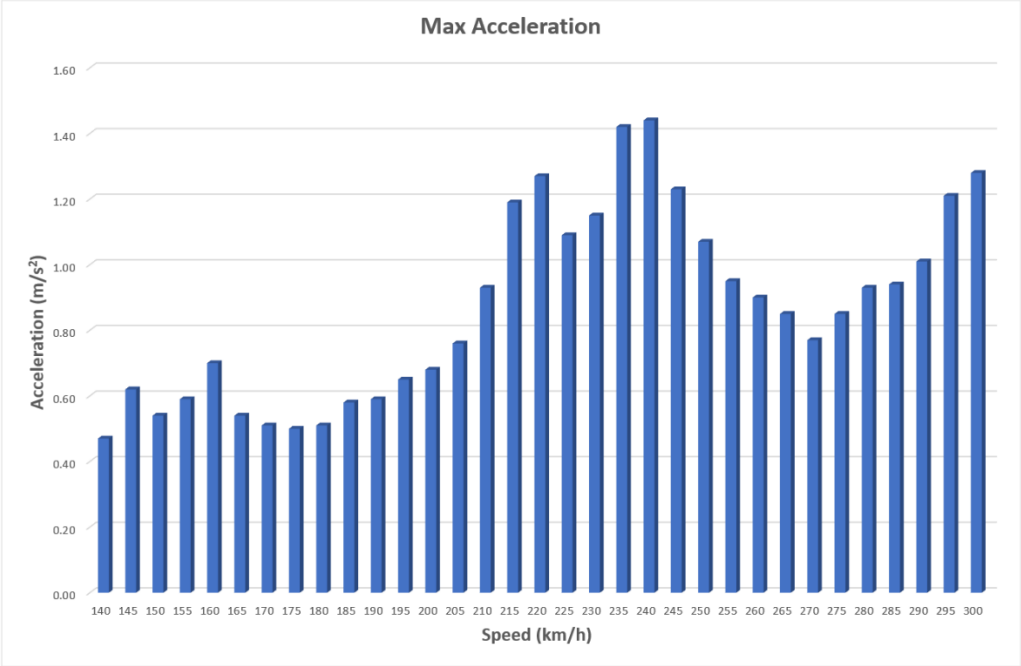

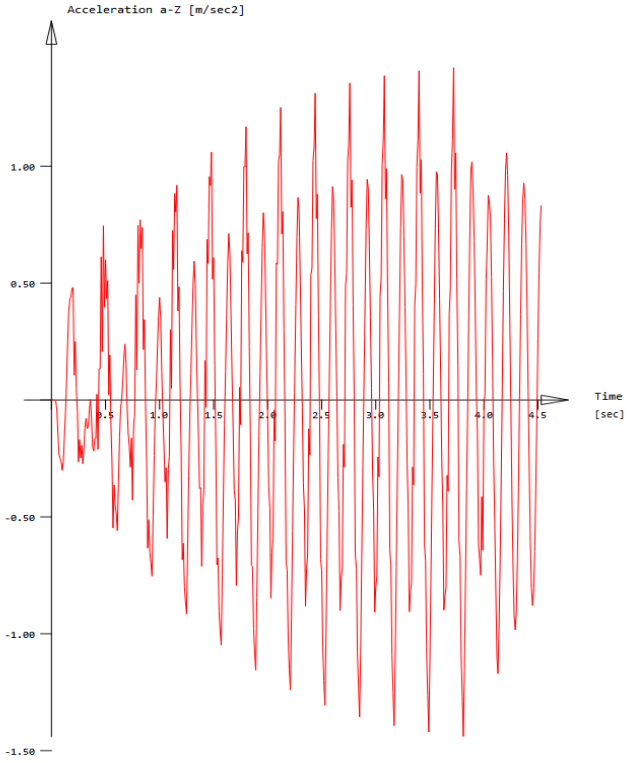

Figure 3.1-43: Maximum acceleration 20m span.

Deformation:

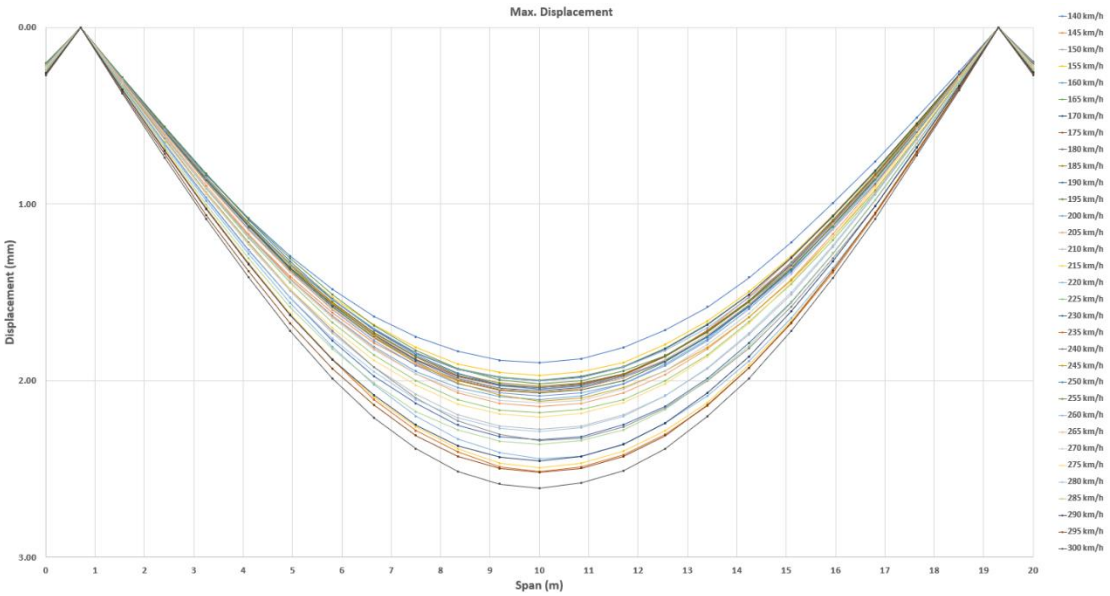

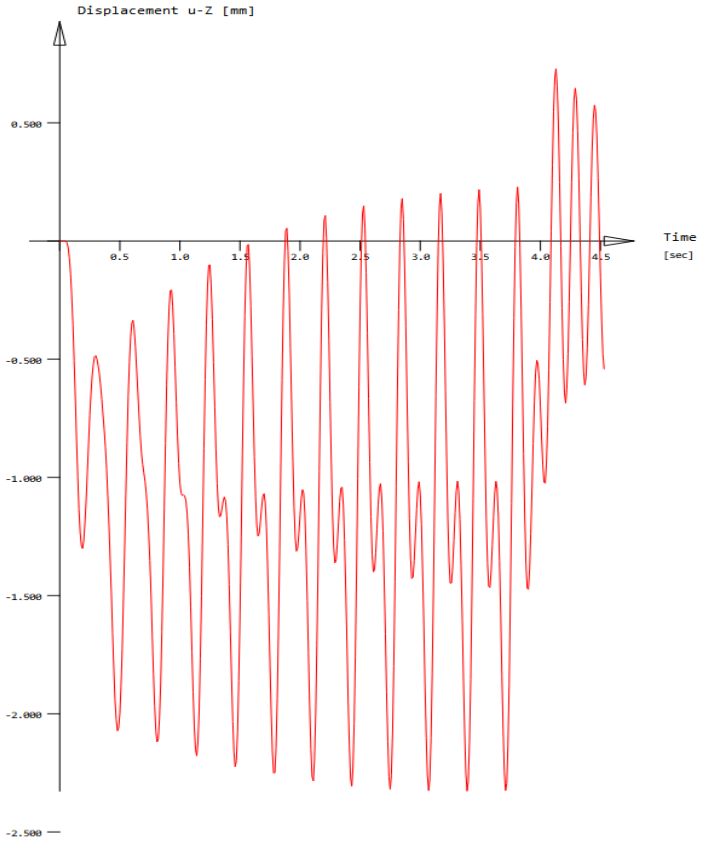

Figure 3.1-44: Maximum deformation 20m span.

Analysis performed for RRTS Bogie Length – 22.34m

Acceleration:

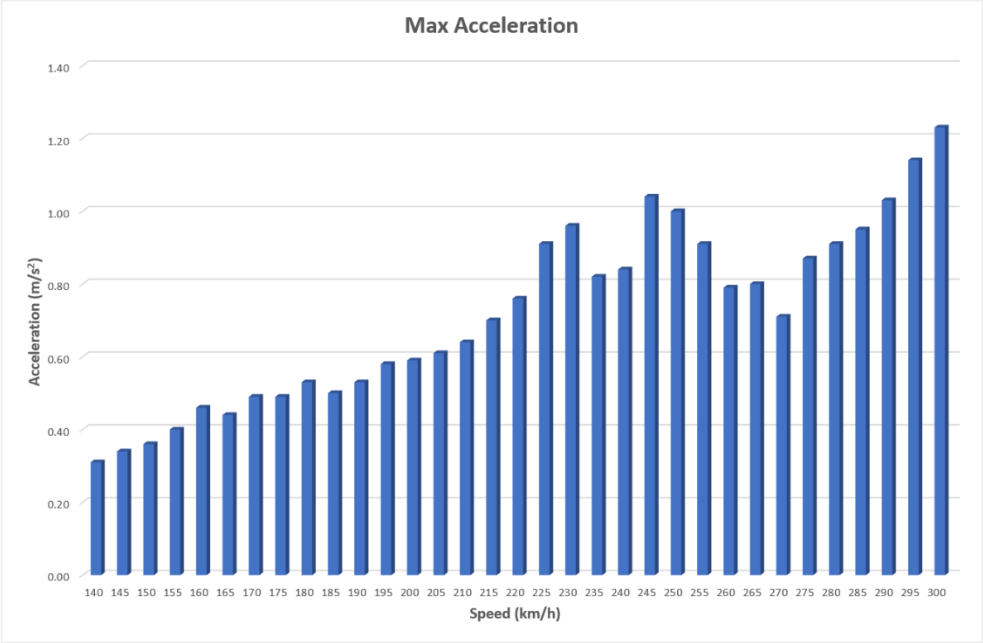

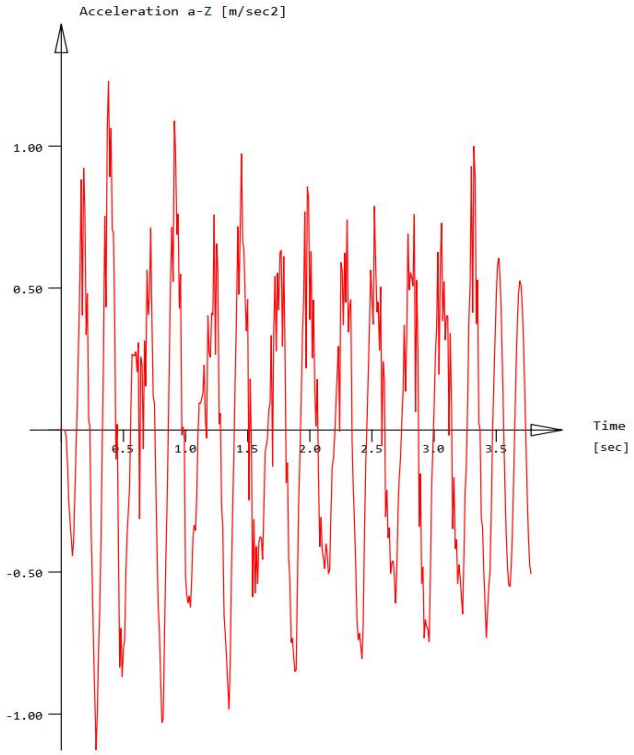

Figure 3.1-45: Maximum acceleration 20m span.

Deformation:

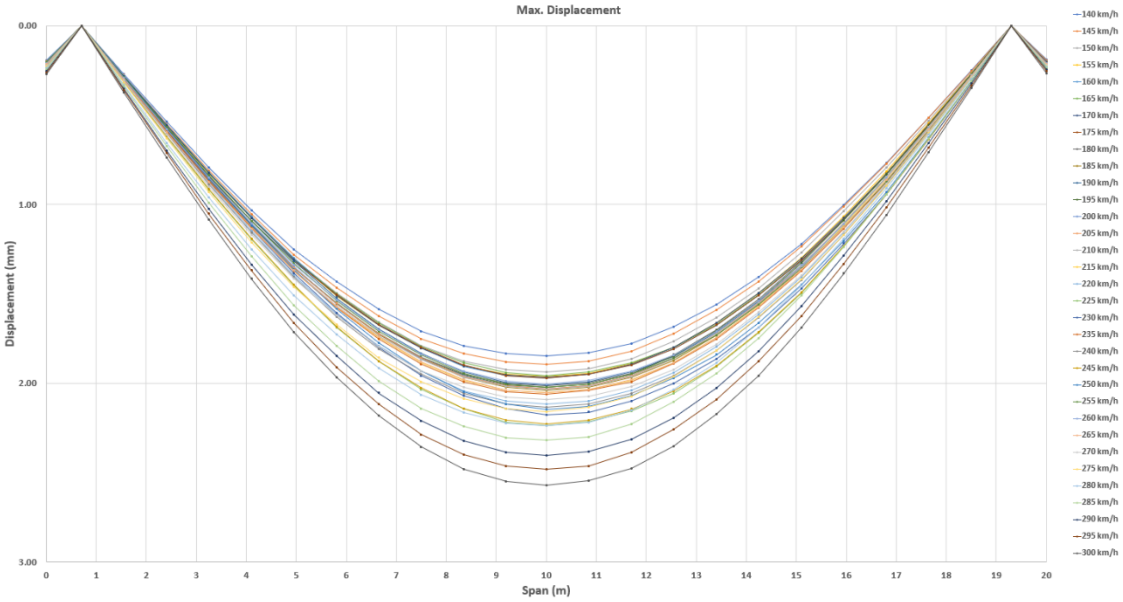

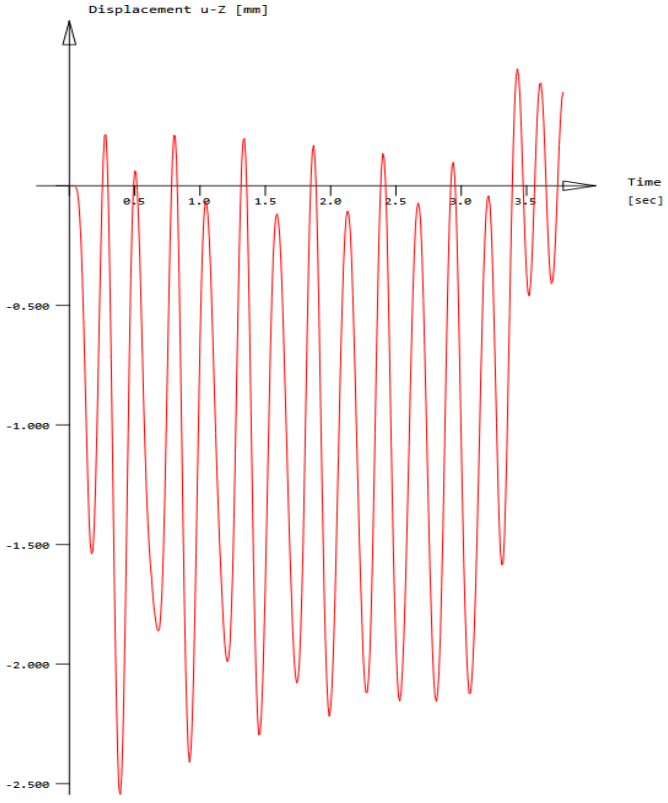

Figure 3.1-46: Maximum deformation 20m span.

3.2. FINDING & DISCUSSION

This section provides the key findings derived from the comparative study of U-Girder and Box Girder superstructure under high-speed loading of regional rapid transit system (RRTS) in India. This study investigates the structural behavior, dynamic response, economic considerations, and construction benefits of both superstructures in the context of high-speed rail infrastructure.

The analysis encompasses various aspects such as maximum acceleration and deflection under different speed and span configuration and checking the feasibility of section under high-speed loading.

The summarized table below highlights the core findings, offering a clear and concise comparison of the performance metrics and economic implication.

Description		Live Load Length	Acceleration (m/s^2)	Acceptable Limit	Deflection (mm)	Acceptable Limit
U-Girder	28m Span	21.34	4.36	5 m/s^2	9.8	27.14
		22.34	3.63	5 m/s^2	9.07	27.14
	26m Span	21.34	4.6	5 m/s^2	10.44	25.10
		22.34	3.79	5 m/s^2	9.19	25.10
	23m Span	21.34	4.76	5 m/s^2	9.59	22.04
		22.34	3.94	5 m/s^2	8.43	22.04
	20m Span	21.34	4.53	5 m/s^2	8.32	18.98
		22.34	3.88	5 m/s^2	7.86	18.98

Table 3.2-1: Summary of results-U-Girder

Description		Live Load Length	Acceleration (m/s^2)	Acceptable Limit	Deflection (mm)	Acceptable Limit
Box Girder	28m Span	21.34	1.36	5 m/s^2	3.94	27.14
		22.34	1.21	5 m/s^2	3.73	27.14
	26m Span	21.34	1.66	5 m/s^2	4.14	25.10
		22.34	1.45	5 m/s^2	3.88	25.10
	23m Span	21.34	1.69	5 m/s^2	3.27	22.04
		22.34	1.46	5 m/s^2	3.14	22.04
	20m Span	21.34	1.44	5 m/s^2	2.61	18.98
		22.34	1.23	5 m/s^2	2.57	18.98

Table 3.2-2: Summary of results-Box Girder

Through a detailed and systematic presentation of the results summarized above, the following insights can be drawn:

i. The U-Girder tends to exhibit higher deflection due to their lower torsional rigidity, whereas the Box Girder demonstrates higher torsional rigidity causing reduced deflection, enhancing their suitability for longer spans and higher load.
ii. When subjected to high-speed train loads, Box Girder shows lower vertical acceleration and lateral vibration resistance compared to U-Girders.
iii. This is attributed to the closed cross-section of Box Girder, which provides greater stiffness and stability. Both Girder types, however, maintain acceptable levels of vertical displacement and acceleration as per BS EN 1991-2: 2003 and BS EN 1990.

iv. U-Girder is more susceptible to increased vibration and deflection at higher speed, as it can be seen in figure 3.1-5, there is a steep rise in acceleration the train speed exceeds 250 km/h.

Span	U-Girder		Box Girder	
	Cross Section area (m^2)	Depth (m)	Cross Section area (m^2)	Depth (m)
28m	3.40	2.45	5.60	2.10
26m	3.26	2.20	5.35	1.90
23m	3.05	1.90	5.16	1.70
20m	2.84	1.60	5.03	1.50

Table 3.2-3: Concrete required for both superstructure.

v. The U-Girder consistently have smaller cross-sectional area and volumes compared to Box Girders for all span lengths, however as the span increases, both U-Girder and Box Girder volume increases, but the volume of increase is more significant for Box Girder due to their larger cross-sectional area.

vi. U-Girder requires less concrete volume compared to Box Girder, resulting in potential cost savings and reduced environmental impact.

vii. Despite the smaller volumes, U-Girder maintain sufficient structural integrity and load carrying capacity.

viii. U-Girder offers a more efficient use of concrete, making them a cost-effective option for bridge construction projects where minimizing material usage, faster construction leading to lower labor and equipment costs.

ix. Based on the results presented above, it can be inferred that the U-girder demonstrates satisfactory performance with both acceleration and deflection remaining within the acceptable limits as well as helps in reducing overall carbon footprint. This suggest that the U-girders are suitable for high-speed loading applications.

The factors such as Material usage, transportation, construction process can have impact on the total cost of the projects and even on carbon emission which needs to be minimized as much as possible.

U-Girder typically require less concrete compared to Box Girder due to their simpler cross-sectional shape. This means fewer raw materials are needed for production, resulting in reduced carbon emissions associated with the extraction and processing of materials.

Constructing a Box Girder involves complex formwork and casting process as well as longer curing times for the larger volume of concrete when compared to U-Girder, construction of which is generally simpler and faster.

The Shorter construction time required in U-Girder causes reduced energy consumption, and lower emissions from construction equipment and machinery. Since being lighter and smaller in size are relatively easier to transport, resulting in lower fuel consumption and emission during transportation compared to heavier Box Girder.

The other advantages of U-Girder when compared to Box Girder are listed below:

i. **Reducing the longitudinal profile of the Rail line.**

   The alignment of the rail line on the viaducts is largely influenced by the necessary clearance for the road traffic beneath the deck. This clearance, combined with the distance between the bottom of the deck and the rail level, determines the height at which the rail is positioned.

   For a Box Girder section, the deck depth ranges from 1.5m to 2.1m. In contrast, a U-shaped section's structural depth beneath the track matches the thickness of the bottom slab. As a result, the rail level of the project can be lowered by approximately 1m to 1.8m

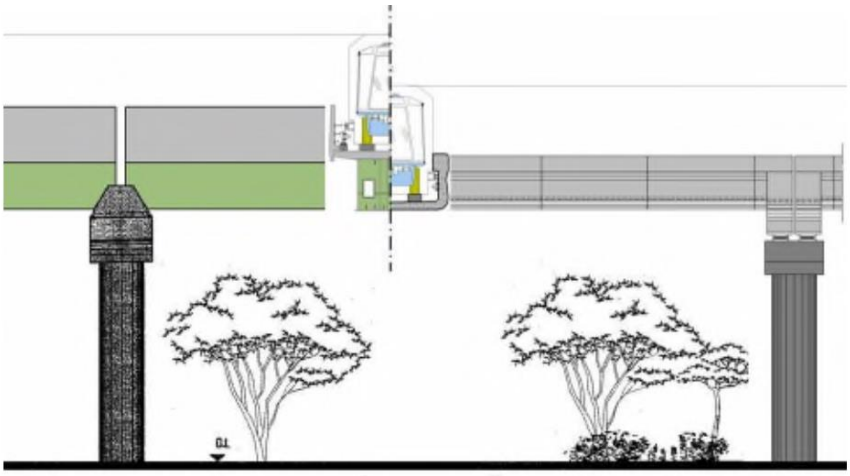

Figure 3.2-1: Comparison of Rail Profile

By lowering the profile, it has several implications, such as the horizontal forces applied are also reduced, leading to decreased bending moment on piers and foundations. As a result, there is a reduction in quantity and cost of the structural element.

Moreover, lowering the profile also has a profound impact on the amount of earthwork required in the project. This reduction in earthwork not only brings down the project cost through direct savings on excavation, transportation and disposal but also simplifies the construction process and reduces the environmental footprint.

ii. Lowering the station level.

As a result of the aforementioned reduction in the longitudinal profile of the line, there is a corresponding decrease in the elevation of the stations. This reduction is elevation leads to cost savings as it decreases the impact of the wind and seismic forces on the pier and foundation, enhancing stability and safety.

This has direct impact on the accessibility and convenience of passengers as they less height to climb from road level to platform level, especially for elderly and disabled passengers.

Moreover, lower station level may reduce both the initial investment and long-term maintenance costs for escalators.

CHAPTER 4: CONCLUSION & FUTURE SCOPE

4.1. CONCLUSION

Based on the comparative study conducted on U-Girder and Box Girder superstructures under high-speed loading for regional rapid transit system (RRTS) in India, the following conclusion can be drawn:

1) It is evident that both the U-Girder and Box Girder demonstrate the capacity to withstand high speed train loading.
2) U-Girder exhibits higher deflection due to lower torsional rigidity, whereas Box Girder demonstrate greater torsional rigidity resulting in reduced deflection. However, both types of superstructures maintain acceptable levels of acceleration and deflection under high-speed loading conditions.
3) U-Girder require less concrete compared to Box Girder, leading to potential cost savings and reduced environmental impact. Despite smaller cross-sectional area, U-Girder maintains sufficient structural integrity and load carrying capacity, making them a cost-effective option for the bridge construction projects.
4) Moreover, considering the carbon footprints U-Girder offer distinct advantages over Box Girders. Their simpler cross-sectional shape requires fewer raw material for production, leading to reduced carbon emissions associated with material extraction and processing. Furthermore, the construction process for U-Girder is generally simpler and faster, resulting in lower energy consumption and emissions from construction equipment and machinery. Additionally, U-Girder are lighter and smaller in size, making them easier to transport and further reducing fuel consumption and emissions during transportation.
5) In light of these findings, U-Girder present a compelling option for bridge/viaduct construction projects where minimizing material usage, reducing environmental impact and optimizing cost efficiency are paramount.

4.2. FUTURE SCOPE

The findings presented in this thesis offer valuable insights and lays the foundation for future research and application.

This thesis can be further extended to analyze and understand the behavior of U-Girder for continuous span configuration. It can be further extended to understand the behavior of U-girder using shell modelling to understand the lateral distribution as well as a comprehensive life cycle assessments can be performed to evaluate the environmental impact of the bridge construction projects involving U-Gider and Box Girders. This would involve assessing the environmental footprint throughout the entire life cycle of the bridge including the end-of-life disposal.

REFERENCES

1) Xia, H., et al. (2003). Dynamic analysis of high-speed railway bridge under articulated trains. *Engineering Structures*, 81(26-27), 2467-2478.
2) Shaikh, M.F., & Nallasivam, K.J.A. (2023). Dynamic response of a box-girder bridge using the finite element technique. *Journal of Civil Engineering*, 1-14.
3) Al-Ghabsha, A.T.S., & Mahmood, M.N.J.A.-R.E. (2006). Dynamic analysis of bridges subjected to moving vehicles. *Journal of Engineering Analysis with Boundary Elements*, 14, 34-50.
4) Oh, S.-T., et al. (2011). Dynamic analysis of a wheel force for a running high-speed vehicle on railway PSC box girder bridge. *Structural Engineering International*, 11(4), 31-40.
5) König, P., et al. (2021). Dynamic analysis of railway bridges exposed to high-speed trains considering the vehicle–track–bridge–soil interaction. *Engineering Structures*, 232, 4583-4608.
6) GOICOLEA, J.M., et al. (2008). Dynamic loads in new engineering codes for railway bridges in Europe and Spain. In *Bridges for High-Speed Railways: Revised Papers from the Workshop, Porto, Portugal, 3-4 June 2004*. CRC Press.
7) Björklund, L. (2005). Dynamic analysis of a railway bridge subjected to high-speed trains. *Structural Engineering and Mechanics*, 20(2), 193-210.
8) Habibunnisa, S., et al. (2019). Dynamic analysis of horizontally curved bridges. *Journal of Civil Engineering and Management*, 8(9), 953-959.
9) Dutoit, D., et al. (2008). 150 km of U Shape prestressed concrete decks for LRT viaducts. In *17th Congress of IABSE: Creating and Renewing Urban Structures*. International Association for Bridge and Structural Engineering.
10) MP, P.K., & Shilpa, B. (2016). Dynamic analysis of box girder bridges. *Journal of Structural Engineering*, 42(3), 191-2009
11) Xie, H., Yan, B., & Huang, J. (2020). Vertical dynamic analysis of ballastless tracks on train-track-bridge system. *MATEC Web of Conferences*, 304, 04004.
12) Goicolea, J., et al. (2002). New dynamic analysis methods for railway bridges in codes IAPF and Eurocode 1. *Journal of Structural Engineering*, 128(1), 1-43.

13) Erduran, E., et al. (2022). Parametric analysis of the dynamic response of railway bridges due to vibrations induced by heavy-haul trains. *Journal of Structural Engineering*, 1-14.

14) Verma, V., et al. (2021). Modal analysis of a thin-walled box-girder bridge and railway track using finite element framework. *International Journal of Structural Stability and Dynamics*, 4(4), 64-83.

15) Qassim, H.J., & Mohamad-Ali, A.A. (2020). Dynamic analysis of composite multi I-girders bridge using finite element method. *IOP Conference Series: Materials Science and Engineering*, 745(1), 012009.

16) Raju, V., & Menon, D. (2014). Longitudinal analysis of concrete U-girder bridge decks. *Proceedings of the Institution of Civil Engineers - Bridge Engineering*, 167(3), 139-156.

17) Koç, M.A., et al. (2022). Dynamic analysis of high-speed train moving on perforated Timoshenko and Euler–Bernoulli beams. *Journal of Vibration and Control*, 18(4), 893-917.